DEHGHANIAN, CHANGIZ

THE ELECTROCHEMICAL BEHAVIOR OF STEEL IN SALT-CONTAMINATED CONCRETE

The University of Oklahoma PH.D. 1980

THE UNIVERSITY OF OKLAHOMA

GRADUATE COLLEGE

THE ELECTROCHEMICAL BEHAVIOR OF STEEL IN SALT-CONTAMINATED CONCRETE

A DISSERTATION

SUBMITTED TO THE GRADUATE FACULTY

in partial fulfillment of the requirements for the

degree of

DOCTOR OF PHILOSOPHY

By

CHANGIZ DEHGHANIAN

Norman, Oklahoma

1980

THE ELECTROCHEMICAL BEHAVIOR OF STEEL IN

SALT-CONTAMINATED CONCRETE

APPROVED BY

DISSERTATION COMMITTEE

ACKNOWLEDGMENTS

The author would like to thank all the committee members for serving on his Doctoral Committee. He especially wishes to express deep appreciation to Dr. Carl E. Locke, chairman of the committee, for his sustained interest, valuable advice, and generous assistance in guiding this study to completion. It has been my pleasure to work with Professor Locke for his knowledge, experience, and insight, and I have benefited greatly in learning and working on various projects.

This research was funded by the National Science Foundation. The assistance and support tendered by this organization to this research is gratefully acknowledged.

I also would like to express my deepest appreciation to my parents and my family for their encouragement and affection during the course of this study.

Thanks to K. Hudson for machine shop work and to Mrs. Rose Benda for which the readability and the appearance of the manuscript have been greatly enhanced by her diligent typing efforts.

ABSTRACT

Corrosion of reinforcing steel in concrete is a problem because of the presence of chloride ions at the steel-concrete interface. The chloride ion may be introduced into the concrete in two ways: (1) as a contaminant in the mix and (2) from external sources such as deicing salts or sea water. Therefore, for better protection of steel in concrete, an understanding of the electrochemistry of steel in concrete is of prime importance.

In this study, the anodic and cathodic polarization curves were obtained for steel in concrete samples of Types I and V Portland cement with various salt contents, exposed to the dry conditions of the laboratory and also to distilled water for 90 to 170 days. Significant differences were found in the electrochemical behavior of steel in Types I and V Portland cement. Type V Portland cement concrete provides better protection for the embedded steel, compared to Type I, when the samples were exposed to corrosive conditions, as in salt solutions.

The change in the moisture content of the concrete also had a significant effect on potential and current requirements.

The anodic and cathodic polarization of steel in Types I and V Portland cement concrete samples with no salt content, exposed to solutions with various salt concentrations, were also performed. It was found that the diffusion of chloride ions into concrete increased as the salt con-

centration of the solutions increased. The penetration of salt also increased as exposure time to the salt solution increased.

A solid Mo/MoO_3 electrode embedded adjacent to steel was used in all concrete slabs. The potential measurement was made with respect to this electrode, in order to reduce the IR drop associated with concrete.

It was also found that the high Tafel slope for the polarization curves in concrete was not mainly due to the IR drop but rather to the diffusion problem.

Most off-shore pipelines are cathodically protected. These lines have a Portland cement concrete layer on the outside to provide negative buoyancy. This concrete layer contains a steel wire reinforcing mesh. In this study, the effect of a wire mesh on current and potential measurement was also investigated in two different environments: (1) in a saturated $Ca(OH)_2$ solution and (2) the concrete slabs. Wire meshes with different hole sizes were used. It was found that the wire mesh had no effect on current and potential distribution. However, the potential of the wire mesh was shifted by the passage of current resulting from the potential gradient caused by the IR drop in the electric field between anode and cathode.

TABLE OF CONTENTS

LIST OF TABLES

LIST OF FIGURES

CHAPTER 1

INTRODUCTION

Concrete normally provides a high degree protection against corrosion to embedded steel, because steel in concrete is polarized anodically and a thin protective film of gamma iron oxide ($\gamma - Fe_2O_3$) is formed on the steel surface. This passive film will be maintained on the steel surface when the pH in the environment around the steel remains in the range of 12.5 - 12.8 [1]. However, chloride ions can disrupt this passive film and the steel will corrode. The corrosion products formed have a volume twice that of the parent metal, which causes the concrete to crack because of low tensile strength. The corrosive chemicals can then find easy access to the steel surface through these cracks and intensify corrosion. Thus, in order to reduce this corrosion, many investigators have considered the influence of variables such as cement type [2], concrete mix design [3,4], and chloride concentration [3,5,6].

Little work has been done on the electrochemistry of the steel in concrete. The problem of steel corrosion in concrete has received more attention in recent years because of its impact on bridge deck deterioration. The corrosion of steel in bridge decks has intensified because of a drastic increase in the use of deicing salt. It has been reported that the cost of reparing bridge decks in the U.S. in 1975 was $200 million [7].

As mentioned, one of the important variables affecting the cor-

rosion of steel in concrete is chloride. Chloride may be introduced into the concrete-steel interface by the intrusion of sea water or the use of deicing salts, or it may be included in the concrete mix.

The intrusion of chloride ions through the concrete cover is an important parameter affecting the time it takes for the reinforcing steel to corrode. These chloride ions can penetrate through the mass of concrete and build up to levels sufficient to induce corrosion.

The present investigation was an initial attempt to determine the impact of factors such as salt (mixed or diffused in cured concrete), type of cement, and moisture on the corrosion of steel in concrete. The effects of these factors were evaluated by electrochemical techniques, such as anodic and cathodic polarization.

Most off-shore pipelines are cathodically protected. These pipelines are coated with a layer of Portland cement concrete on the outside to provide a negative buoyancy. This concrete layer contains a steel wire reinforcing mesh and the pipeline potential is controlled by an external $Cu/CuSO_4$ electrode. Therefore, the existance of the wire mesh may shield the current and cause a problem on current and potential distribution. A series of experiments were conducted to determine the extent of this problem when the wire mesh is connected and disconnected to the steel plate.

The magnitude and the possibility of the IR drop in the potential measurements were also evaluated.

CHAPTER II

THEORETICAL BACKGROUND

Concrete Properties

2.1 Physical Properties

In order to investigate the corrosion of steel in concrete properly, engineers should know some factors about concrete's properties.

Concrete consists of sand, gravel or an aggregate, mixed with cement and water. Cement is a mixture of complex calcium silicates and aluminates (this will be fully discussed in the next section: Chemistry of Concrete) which hydrate with water to form a solid mass. The physical properties of this mass have been the subject of many studies, Scott's [8] and Power and Brownyard's [4] being two of the most complete.

One of the most important properties of concrete is the void created in paste hydration. These voids will be filled with air and water, which contain elements capable of attacking the reinforcing.

2.1.1 Aggregate. Aggregate is one of the factors which influences the physical properties of concrete. Aggregate is not fully inert and its physical, thermal, and sometimes its chemical properties influence the performance of concrete. All aggregate particles originally formed a part of a larger mass, which may have been fragmented by a natural process of weathering and abrasion or by crushing. Many of the aggregate's

properties depend entirely on those of the parent rock: chemistry; mineral composition; specific gravity; strength; petrographic description; hardness; physical and chemical solubility of pore structure. On the other hand, some properties are associated with the aggregate but absent in the parent rock: particle shape and size; absorption; surface texture. All of these properties may have a considerable influence on the quality of the concrete, either in a fresh or hardened state.

2.1.2 Hydration and Capillary Pores. Hydration is another factor which affects physical properties of concrete, therefore, knowledge of cement gel is important.

Hydrates of various compounds in the hardened paste are referred to as gel. Crystals of $Ca(OH)_2$; unhydrated cement, some minor compounds, and the water-filled spaces in the fresh paste are in the hardened paste. The voids in the paste are called gel pores.

The capillary pores are that region of the gross volume not filled by hydration products during hydration. The capillary porosity of the hardened paste is dependent on both the water-cement ratio of the mix and the degree of hydration.

The volume of this capillary system decreases with the progress of hydration, because the hydration products occupy a volume twice that of the original phase (cement).

It is believed that at water/cement ratio greater than 0.38, the volume of gel is not enough to fill all the capillary pore spaces. Therefore, some remain empty even after the completion of the hydration process. The shapes and sizes of these capillary pores are different, and it is thought that there is an interconnected system randomly

distributed throughout the cement paste [10]. The permeability of the hardened concrete is affected by these interconnected capillary pores. A suitable water/cement ratio and a long period of moist curing reduce the continuous capillaries significantly. For water/cement ratios above 0.7, even complete hydration would not produce enough gel to block all the capaillaries. Eliminating the continuous capillaries is so important that it is one condition of a "good" concrete.

2.1.3 Cement Gel. Cement gel is defined as the cohesive mass of hydrated cement in its densest paste, including the gel pores. Gel pores are porous because of the large quantities of evaporable water they can hold. These gel pores are much smaller than the capillary pores.

The source of the gel's strength is not completely understood, but it may come from two kinds of cohesive bonds [11]. The first type is a physical attraction between surfaces which are separated by small gel pores (15 to 20°A). This attraction is usually referred to as van Der Waal's forces. The second type of cohesion is a chemical bond.

The relative importance of these physical and chemical bonds cannot be estimated, but both undoubtedly contribute to the very considerable strength of the hardened paste.

2.1.4 Resistivity. Porous nature of concrete and the work of Hausman [12] and British paper [13], indicates that concrete is highly resistant to the passage of current. The work of Hammon and Robson [14] shows that the electrical resistivity of concrete is highly dependent on moisture content. They found that moist concrete is an electrolyte having a resistivity of the order of 10^4 ohm-cm, a value which is in the range of semi-conductors. On the other hand, another investigation

[15] has shown that oven-dried concrete at 105°C has a resistivity of the order of 10^{11} ohm-cm.

The significant increase in the resistivity of concrete because of a reduction of water probably indicates that the current is conducted through moist concrete by ions in the evaporable water. Therefore, the resistivity of moist concrete will drop significantly because of the increase in water and ions present.

Other studies indicate that the electrical resistivity of concrete increases with age and with a reduction in the water/cement ratio [16].

Locke and Dauda [17] and Hsu [18] found that the resistivity of concrete increased to 10^{10} ohm-cm after 24 hours of drying in the oven. They also found that the resistivity dropped to 10^{4} ohm-cm after the concrete was soaked in water for 24 days (moisture content 6.1%). The resistivity rose to $10^{6} - 10^{7}$ ohm-cm, however, when the concrete slabs were stored in the laboratory at room temperature (moisture content 1.1%). Similar results have been found by the other investigators [19,20].

2.2 Chemistry

2.2.1 Chemical Composition of Portland Cement. Knowledge of the common chemical constituents of cement is important to understanding its nature and behavior. Portland cement is mainly composed of lime, silica, alumina and iron oxide. These compounds interact in the kiln to form a series of more complex products. These are listed in Table 1, with their symbols.

Table 1

Main Compounds in Portland Cement

Name of Compound	Oxide Composition	Abbreviation
Tricalcium Silicate	$3\ CaO \cdot SiO_2$	C_3S
Dicalcium Silicate	$2\ CaO \cdot SiO_2$	C_2S
Tricalcium Aluminate	$3\ CaO \cdot Al_2O_3$	C_3A
Tetracalcium Aluminoferrite	$4\ CaO \cdot Al_2O_3 \cdot Fe_2O_3$	C_4AF

In addition to these main compounds, minor compounds, such as MgO, TiO_2, Mn_2O_3, K_2O, and Na_2O, also exist. These usually amount to no more than a few percent of the cement's weight. However, two of these minor compounds are of interest: the oxides of sodium and potassium, Na_2O and K_2O, also known as alkalies. (Note: Other alkalies also exist in cement.) These oxides react with some aggregates, and the products cause disintegration of the concrete, as well as affecting the rate of gain of cement strength [21]. Therefore, the term "minor compounds" refers simply to their quantity and not necessarily to their importance.

The actual quantities of the compounds vary considerably from cement to cement. In fact, different types of cement are obtained by suitable proportioning of the materials.

Table 2 gives the oxide composition of a typical cement [22].

Table 2

Oxide Composition of a Typical Type I Portland Cement

Name of Oxide	Typical Oxide Composition Percent
CaO	63
SiO_2	20
Al_2O_3	6
Fe_2O_3	3
MgO	1.5
SO_3	2
K_2O	1
Na_2O	1
Others	1
Loss of Ignition	2
Insoluble Residue	0.5

2.2.2 Influence of Composition on the Characteristics of Portland Cement. Some characteristics of the principal compounds of Portland cement are given in Table 3. Knowing these characteristics allows for controlling the properties of the cement by altering the proportions of the compounds. Consider the following examples. For a cement of low heat generation, a relatively high C_2S content and low C_3S and C_3A cements are desirable. In general, the early strength of a Portland cement will be higher with higher percentages of C_2S, and if moist curing is continuous, the later age strengths, after about 6 months, will also be greater with the higher percentages of C_2S. A low C_3A cement generates less heat, develops higher ultimate strength, and exhibits greater resistance to destructive elements than a cement

containing larger amounts of this compound [23,24]. Portland cements with a high C_3A, such as type I Portland cement are used because C_3A contributes to strength developed during the first day after wetting. Thus, type I is usually suitable in general concrete construction where there is no exposure to sulphates in soils or in ground water.

Table 3

Characteristics of the Major Compounds in Portland Cement

Properties	Relative Behavior of Each Compound			
	C_3S	C_2S	C_3A	C_4AF
Rate of Reaction	Medium	Slow	Fast	Slow
Heat Liberated, per unit of Compound	Medium	Small	Large	Small
Cementing Value, per unit of Compound in				
Early Days of Hydration	Good	Poor	Good	Poor
Ultimate Days of Hydration	Good	Good	Poor	Poor

2.2.3 Heat of Hydration of Cement. Hydration of cement compounds is exothermic, up to 120 calories per gram of cement liberated. This heat of hydration, as measured, consists of the chemical heat of the reactions of hydration and the heat of adsorption of water on the surface of the gel formed by the process of hydration [25].

For the usual range of Portland cements, Borgue [26] observed that about one-half the total heat is liberated in one to three days, about three-quarters in seven days, and 83 to 91 percent in six months. Because heat depends on the chemical composition of the cement, reducing the proportions of the compounds that hydrate most rapidly (C_3A and C_3S), checks

the high rate of heat liberation in the early life of concrete.

2.2.4 The Effect of Accelerators. The accelerator is a substance added to concrete to increase the rate at which strength develops. Usually, an accelerator is used when the concrete is to be placed at low temperatures (30 to 40°F) or when urgent repair work is to be done. Calcium choride is a basic and well-tried accelerator.

Calcium chloride increases the rate of heat liberation during the first few hours after mixing. $CaCl_2$ is probably a catalyst in the reaction of C_3S and C_2S. The hydration of C_3A is delayed sometimes, but the normal process of hydration of the cement is not changed.

Addition of $CaCl_2$ does decrease the resistance of cement to sulfate attack and increases the risk of an alkali-aggregate reaction when the aggregate is reactive. On the other hand, $CaCl_2$ has been found to increase the resistance of concrete to errosion and abrasion [17].

The action of sodium chloride is similar to that of calcium chloride but of lower intensity. The effects of NaCl are also more variable and a depression in the heat of hydration with a consequent loss of strength at 7 days and later has been observed.

Corrosion of Steel in Concrete

2.3 General View of Corrosion

Knowledge of corrosion has increased rapidly over the past 20 years, but many aspects of the problem are still not completely understood. When the corrosion mechanism is subjected to a single system, the situation becomes extremely complex. Clearly the factors which influence various reactions are not independent and it is therefore no surprise to

find conflicting theories on the nature of corrosion. However, certain facts have been found by means of considerable study and investigation.

Corrosion is the deterioration or destruction of a metal by means of a chemical interaction with its environment. The reaction is electrochemical in nature. According to Evans [28], corrosion may be thought of as a transformation of the metal from the elementary to the combined condition.

The corrosion mechanism of reinforcing steel in concrete is similar to that in a basic galvanic cell but much more complicated. Therefore, a more detailed discussion of the general electrochemical mechanism is necessary.

The electrochemical mechanism is the only way a chemical reaction can take place on the surface of the reinforcing steel. For this reaction to happen, three conditions must be met: (1) a potential difference between two metallic areas must exist; (2) a conductive path must exist; (3) proper electrode reactions must take place [29]. If these conditions exist, then the steel will corrode.

2.4 Chemical Reactions

Metals high in the electromotive force series will have a greater tendency to corrode. Iron is one metal relatively high in this series and therefore, will have a substantial tendency to enter into electrolyte (solution or concrete). The area where the metal ions go into electrolyte becomes an anodic region. This ionization of the metal at the anode is usually called the first or primary stage of the corrosion reaction and may be written as the following equation [29,30]:

$$\text{Anodic reaction } Fe \rightarrow Fe^{++} + 2\bar{e} \qquad (1)$$

The anodic area of the metal contains an excess of electrons, as shown by equation (1).

In order to keep an equilibrium of electric charges, a cathodic reaction must take place. The cathodic reaction can be presented as

$$\text{(cathodic reaction)} \quad 1/2\ O_2 + H_2O + 2\bar{e} \rightarrow 2O\bar{H} \qquad (2a)$$

$$2H^+ + 2\bar{e} \rightarrow H_2 \qquad (2b)$$

These cathodic reactions, usually called secondary reactions, control the rate of corrosion for iron or structural steels. Therefore, any environmental condition affecting these reactions will likewise influence the corrosion rate.

Of these corrosion processes, the cathodic depolarization by oxygen (reaction 2a) is most important [31]. Since this reaction depends on the concentration of dissolved oxygen next to the metal, the reaction is affected by the degree of salt concentration, aeration, temperature and other factors [30]. Reaction (2b) is generally not characteristic of the corrosion of steel in concrete. However, such reactions will occur in either acid solutions or concentrated alkaline solutions.

The secondary reactions allow the primary reaction to proceed, with the accumulation of ferrous ions, Fe^{++}, in the electrolyte which, in the presence of water and oxygen, are oxidized and precipitated as rust. Two stages of oxidation may exist, depending on the availability of oxygen [28,30,32]. The first state is ferrous hydroxide, which is more soluble than the second, hydrated ferric oxide. The first is usually formed at the metal surface and is converted to hydrated ferric

oxide a little distance away from the surface where the ferric hydroxide is in contact with more oxygen. The green product of hydrated magnetite or black anhydrous magnetite may also be formed if the supply of oxygen is restricted, but these products are not common.

The structure and composition of the rust changes considerably with the conditions during its formation. This structure plays an important role in the subsequent corrosion process [30,32]. Corrosion could be retarded by the formation of a rust layer if the layer is hard, dry, and fairly adherent to the metal surface. On the other hand, if the layer is spongy and easily detachable, it will absorb oxygen and moisture from the surrounding media and therefore, will aid further activity.

Many factors influence the rate of reaction. If a process is composed of two or more reactions, as in electrochemical corrosion, the rate of the process is obtained by the rate of the slowest reactions in the special conditions [30]. Usually, the primary reaction is much faster than the secondary reactions. In addition, since the oxygen concentration of the media is the dominant influence on the secondary reactions, it is also the dominant factor in the overall corrosion rate. However, other variables are also important. If the cathode is large and consequently exposed to a greater amount of oxygen, the cell current may be strong in relation to anode size [30]. This increases the risk of attack and causes a greater penetration rate at the anode area.

The tendency of the reaction to proceed is determined by the magnitude of the electrochemical potential. Three conditions must exist to resist continued reaction [2]: (1) the supply of electrons at the metal surface must occur at a faster rate than the supply of reducible

particles from the media; (2) the corrosion product must behave as a protective coating and retard corrosion rate; and (3) the reduction reaction must be slowed down, even though adequate electrons and electrolyte particles are available at the metal-electrolyte interface. The third condition is related to electrode kinetics, a subject still not fully understood. If any of the above conditions exist, the electrode potential changes and the electrodes are said to be polarized. The increase in the slope of either the cathode or anode polarization curve reduces the local cell current and consequently the corrosion rate. On the other hand, the reduction of the slope increases the corrosion rate. This reduction in slope of the polarization curve is brought on by increasing the electrode area or introducing chemicals which aid the electrode reaction.

Variables Affecting the Corrosion of Steel in Concrete

2.5 Variables Associated with Concrete

2.5.1 Chloride and its Sources. In normal Portland cement, chloride exists in three forms [33]: (1) the free chloride ion; (2) chloride which is more or less strongly bonded with calcium silicate hydrates; (3) chloride which is combined in certain types of compounds such as the calcium aluminate chlorides, calcium ferrite chlorides, and calcium oxychloride. It is generally believed that the third type of chloride (the combined) does not further corrosion of the reinforcing process and bonded chlorides may or may not be available to cause corrosion, depending on the strength of the bonds and other factors. The free chloride ion does not attack steel in concrete. However, this ion

does provide a suitable environment for the natural conversion of iron to iron oxide [34,35].

Reinforcing steel does not corrode in uncontaminated (no chloride) Portland cement concrete because of the high pH(12 to 13) caused by soluble calcium hydroxide originally existing in the cement [36]. This high pH initially causes the formation of ferric oxide on the surface of steel, which protects it from corrosion.

However, when soluble chlorides are introduced into the concrete, this protective, high pH environment is neutralized. When sufficient chloride is present to destroy the necessary alkalinity (pH less than 10) and the normal passivity of iron [12,34,37], the natural conversion of iron to rust will occur. An increase in volume will also occur because the volume of the rust is greater than that of the parent iron.

A conflicting theory states that Cl^- attacks the passive film on the metal's surface. T. Tokuda and M.B. Ives [38] presented two mechanisms for Cl^- on the passive film. In the case of a thin film (nickel), the passive state of the film is sufficient to block any dissolution, although the metal reactivity is unchanged. However, when Cl^- is incorporated in or absorbed on the passive film, inhibition is reduced and dissolution is permitted. These findings are supported by the fact that the anodic current is increased by the addition of Cl^-, even when no pitting occurs at those regions of the surface where dissolution is permitted first.

The absorbing or penetrating ability of the aggressive cl^- ions is dependent on the nature of the passive film. When the film is thick

or stable, only the dissolution (reactivity) of the metal itself, and the inhibitive action of the passive film are in fact relevant to a discussion of the case of pitting.

Okamoto [39] has proposed that a penetration of Cl^- in the passive film may take place during anodic polarization, resulting in a "contaminated film". It has been assumed that the passive film (without Cl^-) is a hydrated oxide film with a gel-like structure. There is no doubt that chloride ions added into solution absorb on the film surface and replace water molecules as part of the $H_2O - MOH_2$ structure. This action may shift the structure of the film from one type to another. Okamoto also concluded that the resistance of the passive film to corrosion is almost completely controlled by the nature of the passive film itself, in which the bound water in the film plays an important role. This bound water may react to give various species or be replaced by the other ions from the surroundings, resulting in a disruption of the film. On the other hand, the bound water may also behave as the effective species for capturing the dissolving ions and forming resistance in the new film.

Chloride may be present in fresh concrete but it also permeates into hardened concrete from environments containing chloride.

2.5.1.1 Chloride Present in Fresh Concrete

One source of chloride in fresh concrete is calcium, which is frequently used as an accelerator for strength. Another source is seawater which is used as concrete mixing water in certain coastal areas where fresh water is not available. Salt can also be introduced by a salt-contaminated aggregate in the concrete mix.

2.5.1.2 Diffusion of Chloride into Concrete

Diffusion of chloride ions through the concrete cover is an important parameter affecting the corrosion time of reinforcing steel. Even in concrete with a low water-cement ratio, chloride ions could diffuse through the mass of concrete and build up to a level sufficient to induce corrosion.

Intrusion of chloride into concrete is a relatively slow process. These chloride ions can intrude by two basic mechanisms: capillary flow of bulk solution into under-saturated concrete and diffusion ions across a concentration gradient in saturated capillaries. What each mechanism contributes to the total amount of chloride penetrating under actual field conditions is not known. However, it seems likely that capillary forces pull the bulk solution into the surface layers, and the diffusional forces behave actively in relatively saturated concrete. Investigators [40,41] who have measured the diffusion coefficient for chloride ions in cement and concrete have found it to be in order of 10^{-8} cm^2/sec.

2.5.2 Oxygen. Oxygen is not only essential in corrosion but is primarily responsible for its progress and rate [30,32,42,43]. Oxygen behaves as a depolarizor at the cathode and consequently tends to increase the corrosion rate. Thus, this rate, in an active metal such as steel, is directly proportional to the amount of dissolved oxygen [35,44]. In fact, in aerated solutions, the effect of oxygen tends to overshadow everything else [44].

Stratfull [45] even believes that oxygen can depolarize or

reduce the effectiveness of cathodic protection by the formation of hydroxides. Therefore, less protection of steel will be made.

An unequal distribution of oxygen over the surface of the steel will set up anodic and cathodic areas [28,30,31]. Anodic areas are those with less access to oxygen and cathodic regions. Thus, a cell is set up along the steel. Therefore, the presence of oxygen in varying concentrations along the reinforcement will tend to increase the possibility of corrosion.

2.5.3 Effect of Different Types of Portland Cement. Knowledge of the compound composition of different types of Portland cement is important in understanding the effect of various types of cement on the corrosion of steel in concrete. Table 4 shows the typical compound composition.

Some investigators think that the tricalcium aluminate present in Portland cement is effective for chloride removal and can therefore, provide protection against steel corrosion. Conflicting theories are found in the literature with regard to the minimum tricalcium aluminate content necessary to prevent corrosion of reinforcing steel in concretes exposed to chlorides [47,48].

Another unanswered question concerns the protective influence of Portland cement. That is, certain Portland cement compounds or their hydration products can reduce the deleterious effects of chloride by removing it from the liquid phase which contains a considerable proportion of chloride.

However, there is evidence that differences in the composition of Portland cements do play an important role in steel corrosion

Table 4

Compound Composition of Different Types of Portland Cements [46]

Cement	Value	Compound Composition, Percent							Ignition Loss	Number of Samples
		C_3S	C_2S	C_3A	C_4AF	$CaSO_4$	Free CO	MgO		
Type I	Max.	67	31	14	12	3.4	1.5	3.8	2.3	
	Min.	42	8	5	6	2.6	0	0.7	0.6	21
	Mean	49	25	12	8	2.9	0.8	2.4	1.2	
Type II	Max.	55	39	8	16	3.4	1.8	4.4	2.0	
	Min.	37	19	4	6	2.1	0.1	1.5	0.5	28
	Mean	46	29	6	12	2.8	0.6	3.0	1.0	
Type III	Max.	70	38	17	10	4.6	4.2	4.8	2.7	
	Min.	34	0	7	6	2.2	0.1	1.0	1.1	5
	Mean	56	15	12	8	3.9	1.3	2.6	1.9	
Type IV	Max.	44	57	7	18	3.5	0.9	4.1	1.9	
	Min.	21	34	3	6	2.6	0	1.0	0.6	16
	Mean	30	46	5	13	2.9	0.3	2.7	1.0	
Type V	Max.	54	49	5	15	3.9	0.6	2.3	1.2	
	Min.	35	24	1	6	2.4	0.1	0.7	0.8	22
	Mean	43	36	4	12	2.7	0.4	1.6	1.0	

associated with chlorides. Baumel [49] has found that cements with low Al_2O_3 contents ($\sim$ 4%) exhibit more active electrochemical behavior at lower $CaCl_2$ concentrations than cements containing a higher proportion of aluminates ($\sim$ 7%).

The remaining influences on the corrosion process which can be tied to cement compositional variables are mostly indirect in nature.

For example, a very fine cement may exhibit larger drying shrinkage than one which is not fine. This shrinkage increases the probability of cracking in the hardened concrete and allows aggressive agents, such as deicer salts, to penetrate more rapidly to the steel. The same effect may be seen in cements low in gypsum [50]. An increase in cement fineness may also increase the water demand of a concrete mix, thus increasing the net water-to-cement ratio (w/c) and consequently the permeability of the concrete. Blaine [51] et al. have found a similar relationship between Al_2O_3, C_3A, and the water demand.

It is believed that the C_3A of Portland cement may react with a chloride solution and take much of the chloride out of the solution by forming an insoluble compound, $C_3A \cdot CaCl_2 \cdot 10\ H_2O$ [52,53]. Roberts [54] found very little corrosion for type I Portland cement (9 percent C_3A) when 1.4 percent $CaCl_2$ by weight of cement was present, while considerable corrosion took place for the type V Portland cement (1 percent C_3A) containing the same amount of $CaCl_2$.

However, under some conditions even high C_3A Portland cements may not be effective chloride-removing agents, depending on the type of crystallographic form. A review of both published experimental data and theoretical considerations shows that the type of tricalcium aluminate present and the source of the chloride, as well as the amount, are necessary factors in predicting the corrosion behavior of steel in reinforced concrete.

Regourd [55] has done work on this chrystallographic form. He reported that the formation and the stability of the chloroaluminate hydrate in Portland cement pastes exposed to sea water may be related

to the crystallographic form of C_3A present in cement. C_3A can exist in commercial Portland cements in three crystallographic forms: cubic; orthorhombic; or tetragonal. In hydrated cement pastes exposed to sea water, Regourd found that ettringite rather than the chloroaluminate hydrate was the preferred phase in cement containing cubic C_3A, but significant proportions of the chloroaluminate hydrated co-existed with ettringite in cements containing orthorhombic or tetragonal C_3A.

2.5.4 Effect of pH. The pH of a corroding solution has a noticeable effect on the corrosion rate of metals. Large cracks in reinforced concrete allow the salt-containing solutions easy access to the interior. Furthermore, the solutions may be flowing into and out of the crack. This condition makes it difficult to maintain the normal PH of about 12.5 from saturation by $Ca(OH)_2$, which would exist in a crack if there were no flow. Several investigations have considered the influence of this chloride ion migration into concrete on pore water pH [56,57], and a decrease in pH from a value near that of water-saturated concrete (pH=12.35) has been observed.

Shalon and Raphael [36] have investigated the effect of pH in general and have found that the minimum pH for inhibition of steel varies from 11.5 to 12.75 depending on the nature of corrodent and the degree of aeration.

With the use of the Pourbaix diagram, Metzger [58] has indicated that corrosion would occur in an $Fe\text{-}H_2O$ system at 25°C for pH values between 0 and 10 and for pH values greater than 12. These values depend on the electrical potential of metal.

Mayne and Menler [59] have pointed out that steel becomes passive in calcium and sodium hydroxide solutions because of the formation of an impervious layer of ferric products on the steel surface. Weak areas in the initial rust layer are first repaired by the formation of ferrous hydroxide, which then reacts with oxygen to form Fe_3O_4 (magnetite) and Fe_2O_3 (ferric oxide). Direct electrochemical production of ferric oxide causes later repair. However, the protective film would be disrupted and corrosion would proceed if, for some reason, the hydroxide ion concentration were decreased.

2.5.5 The Effect of Moisture. Moisture induces corrosion reactions. All corrosive variables become ineffective in its absence [45]. In addition, moisture penetration is the way any external substances such as chloride, dissolved oxygen and carbon dioxide find access to the reinforcement. A corrosion cell will be set up along the reinforcement because of differential moisture content and the areas having the greatest moisture content will be anodic [12,60]. Thus, local corrosion occurs by the flow of current from anodic to cathodic areas. The conduction of electricity through moist concrete is believed to be the movement of ions in the absorbed water of the paste matrix and in some cases in the pores of the aggregate particles, any variables affecting the amount or properties of water-absorption, or the kind or number of ions will influence the resistance of concrete and therefore the current flow. Thus, the moisture content type of corrosion mechanism can be an important element in the corrosion of steel in concrete.

2.5.6 The Effect of CO_2. Calcium hydroxide is converted to calcium carbonate when carbon dioxide (CO_2) is absorbed into the concrete. This reaction will reduce the pH and consequently the protective value of the concrete [42,60,61,62]. A pH lower than 10 may result in the corrosion of steel in the concrete.

There is sufficient evidence to prove that the possibility of carbonation is not very great in high quality concrete, and when it does occur, is in the range of a few millimeters. Therefore, in these concretes, the pH is not affected [36]; however, it is in low quality concrete.

Carbonation increases the shrinkage of concrete which results in cracks [61] and an increase in porosity. These allow moisture and corrosive chemicals to penetrate into the concrete and promote corrosion.

2.5.7 Sulfate Attack. Salts in the solid form do not attack concrete, but when present in solution, they may react with the hardened cement paste. Sodium, calcium and magnesium sulfates and ground water are present in some clays, in the form of a sulfate solution. An attack by these sulfates in solution may then take place because of reactions with $Ca(OH)_2$ and calcium aluminate hydrate.

The products of the reactions, gypsum and calcium sulphoaluminate, have a greater volume than the compounds they replace. Therefore, these reactions with the sulfates lead to expansion and disruption of the concrete.

The reaction of sodium sulphate with $Ca(OH)_2$ may be expressed as follows:

$$Ca(OH)_2 + NaSO_4 \cdot 10\,H_2O \rightarrow CaSO_4 \cdot 2H_2O + 2NaOH + 8H_2O \qquad (3)$$

Calcium hydroxide is completely leached out in produced water, but if NaOH accumulates, equilibrium will be established and only a part of SO_3 will be deposited as gypsum. Therefore, disruption of the concrete will be less.

The reaction with calcium aluminate hydrate may be written as follows [53]:

$$\begin{aligned} &2(3CaO \cdot Al_2O_3 \cdot 12\,H_2O) + 3(NaSO_4 \cdot 10\,H_2O) \rightarrow \\ &3CaO \cdot Al_2O_3 \cdot 3CaSO_4 \cdot 31\,H_2O + 2Al(OH)_3 + 6NaOH + 17\,H_2O. \end{aligned} \qquad (4)$$

Calcium sulfate only reacts with calcium aluminate hydrate, forming sulphoaluminate ($3CaO \cdot Al_2O_3 \cdot 3CaSO_4 \cdot 31\,H_2O$). On the other hand, magnesium sulphate attacks calcium aluminate hydrate, calcium silicate hydrates and $Ca(OH)_2$. The pattern of the reaction is given as

$$3CaO \cdot 2SiO_2 \cdot aq + MgSO_4 \cdot 7H_2O \rightarrow CaSO_4 \cdot 2H_2O + Mg(OH)_2 + SiO_2 \cdot aq \qquad (5)$$

An increase in the strength of the solution increases the rate of the sulfate reaction, although beyond a concentration of 0.5 percent of $MgSO_4$ or 1 percent Na_2SO_4 the intensity of the attack does decrease [53]. Serious deterioration of concrete occurs in a saturated $MgSO_4$ solution with low water/cement ratio. This situation only occurs after 2 to 3 years [63].

However, it should be noted that $CaSO_4$ is not an important factor in attacking concrete because of its low water solubility.

These sulfate attacks start at the edges and corners of the concrete, followed by progressive cracking and spalling which reduce the

the concrete to a friable or even soft state. Low C_3A cement reduces the sulfate attack, and impermeability plays an important role in concrete's resistance as well.

2.5.8 Concrete Cover. Obviously, the thickness of the cover over the steel is very important because this cover protects the steel from factors promoting corrosion.

A thicker concrete cover over the reinforcement means a greater resistance to the penetration of environmental salts, oxygen, and carbon dioxide to the steel surface. Therefore, this thickness postpones the initiation of corrosion. Evans [64] even suggests that thicker covers, because of their greater strength, are dislodged less easily from intimate contact with the steel which may produce "rust stifling" and afford permanent protection.

Kinneman [65] states that a 1/2 inch cover of sound, high-grade concrete will preserve steel from salt-water corrosion although he also suggests a 2 to 2-1/2 inch cover for unprestressed concrete. Friedland [66] reports that a concrete with a maximum aggregate size of 3/8 inch shows an improvement in corrosion resistance when the cover is increased from 1/4 to 7/16 inch. It should be noted, however, that the required thickness is related to the quality of the concrete.

2.5.9 Quality of Concrete. The permeability of the concrete will determine the degree of penetration for a given thickness of cover in a given environment. The permeability of concrete depends on several variables. The most important ones being the water-cement ratio, aggregate grading, the cement-aggregate ratio and consistency [45]. An understanding of these factors allows modern concrete technology to

design a high quality, impermeable concrete which gives high protection for the life of a structure in a corrosive environment. Shalon and Raphael [36] have discussed these factors when they describe a high quality concrete as, "The kind of concrete which can be achieved only by close attention to every detail in connection with the selection of materials, proportioning of the mix to produce a truly plastic concrete having a relatively low water-cement ratio, and thorough consolidation of the concrete as placed."

Tyler [67] has found that, in general, a low water-cement ratio (0.4-0.5) concrete will afford better protection than a concrete with a similar consistency but having a high water-cement ratio (0.6 and higher). Usually a low water-cement ratio concrete also needs higher cement factors than normally required for strength requirements. Specification of the best water-cement ratio cannot be made, however, unless the mix consistency is also considered. This consistency has a tremendous effect on the corrosion rate, not accounted for by the water-cement ratio or the cement content [66].

Aggregate gradation is another factor which must be considered for high quality concrete since well-graded aggregate is important for low permeability [66,68]. Data taken by Fiedland [66] indicates that coarser grading increases the protective quality of concrete; however, the spread of the data is too great to guarantee the conclusions.

A consideration of these variables indicates that the protective quality of concrete may be increased by proper proportioning of the materials. It should be pointed out, however, that no matter how carefully the mix specifications are prepared, proper supervision and

site control are required to insure the careful mixing and placing techniques [45].

2.6 Variables Associated with Steel

Any heterogeneities in the steel's surface produces differences of effective potential and thus corrosion cells. This nonhomogeneity is caused by differences in chemical composition over the steel's surface, differences in texture, and discontinuous surface layers [30]. These differences in chemical composition may be due to grain boundaries, impurities, or a change in the corrosion resistance of the microstructure, and they produce the different potentials which increase the risk of corrosion, and, in addition, may tend to localize the action [29]. From the standpoint of total corrosion, however, these variables are not as important as the external conditions of the concrete [30].

Another factor causing differences in potential is stress, either static or cyclic, in the reinforcement. Borgmann suggests that this stress is simply a modification of the bimetalic couple problem: the crystalline structure in the strained areas has a somewhat different configuration from that in the unstrained areas [31]. The rearrangement is such that the strained regions become negative or anodic compared to the unstrained regions. Consequently, electrochemical couples [16] are set up. Tension stresses also cause trouble in corrosion. These stresses produce a force on the grain boundaries, at the steel surface, and in the cases where corrosion appears along these boundaries, the stresses will split up the grooves produced between grains. This effect causes further corrosive attack along the boundaries and simultaneously creates stress

concentrations which destroy the protective surface films and predispose the steel to continued attack [28,29].

The corrosion will be intergranular, in the case of static stresses. In the cases of cyclic stresses, the corrosion is transgranular and tends to follow those planes where resolved shear stresses are maximum. If the range of alternating stresses goes beyond a certain level, defined as the "fatigue limit", any crack starting at the steel surface will continue through the cross section until a fracture occurs. Failure never happens below the fatigue limit no matter how many cycles are applied when corrosive effects are absent. However, the steel structure becomes unstable when corrosive conditions are present. Consequently, deterioration will occur at the crack boundaries and the crack will extend no matter how low the stress range [28].

The stresses for reinforcing rebar in concrete are normally less than required to cause major corrosion.

Another characteristic of metal which reduces its tendency to corrode is its passivity, the ability to become inactive in a given environment. In other words, a passivated metal is one with more noble potential under certain environmental conditions. It should be noted that although passivity is due to a protective film on the metal's surface, it is still related to the metal's properties. Passivity, however, is affected by environmental conditions and can be reduced in a highly corrosive environment.

The mill scale on the reinforcing steel's surface has a tremendous effect on the corrosion of steel. Reinforcing rods of the deformed type are hot-rolled in air and therefore, have various types and

amounts of mill scale on their surfaces. The mill scale can act as the cathode of a couple whose anode is the steel base. Since the mill scale will not form a continuous coating, bare parts are found where the scale has flaked off. Scaled and bare surfaces combined with aeration or deaeration cause cells which in turn cause corrosion.

Passivity and Its Characteristics

Passivity is the loss of chemical reactivity of certain metals and alloys under particular environmental conditions. Two theories are more acceptable than the others in explaining passivity: (1) the oxide film theory; (2) the adsorption film theory. According to the former, a diffusion layer of reaction products forms a barrier in which metal oxide or other compounds keep the metal separate from its environment. Consequently, the reaction rate slows down. According to the latter theory, the metal is covered by a chemisorbed film--that is, oxygen. This chemisorbed layer displaces the adsorbed H_2O molecules and slows down the rate of the anodic reaction, or hydration of the metal ion. Passivity breaks down because of the presence of chloride ions. According to the oxide film theory, the chloride ion either penetrates the oxide film through the pores or may colloidally separate the oxide film and thus increase its permeability. According to the adsorption theory, Cl^- may adsorb on the metal surface in competition with dissolved O_2 or OH^- [75]. Cl^-, in contact with the metal, increases its dissolution.

A number of investigators, namely Hoar [69], Bianchi, et al. [70], Kortum and Bockris [71], Seijka, et al. [72], H.H. Uhlig [35], Vetter [73], Pourbaix [74], Okamoto [39], and others have done work on

the subject of passivity. Others have used analytical techniques to try and discover the nature of passive films. Some of the techniques used are:

1) auger electron spectroscopy
2) surface studies by electron diffraction
3) the x-ray diffraction method for analyzing the corrosion product
4) electron microscopy of surfaces
5) x-ray photo electron spectroscopy (ESCA)
6) ion-scattering spectrometry
7) nuclear microanalysis
8) ellipsometry techniques
9) low energy diffraction technique (LEED)
10) electron probe microanalysis

Greater detail on the experiments relating to passivity is beyond the scope of this study.

Characteristics of Passivation

Figure 1 is a behavior of an active-passive metal under corrosive environments. This figure indicates three possible cases which may exist for an active-passive metal in corrosive conditions. In Case 1, there is only one stable intersection which is in active region, and high corrosion rate occurs. This is a characteristic of stainless steel in sulfuric acid. Typical behavior of such a case is shown in Figure 2a. In Case 2, there are three possible intersection points like A, B, and C at which the total rate of anodic and cathodic reactions are equal. The system cannot exist at point C because it is not electrically stable, but points A and B are stable. This system may exist in active

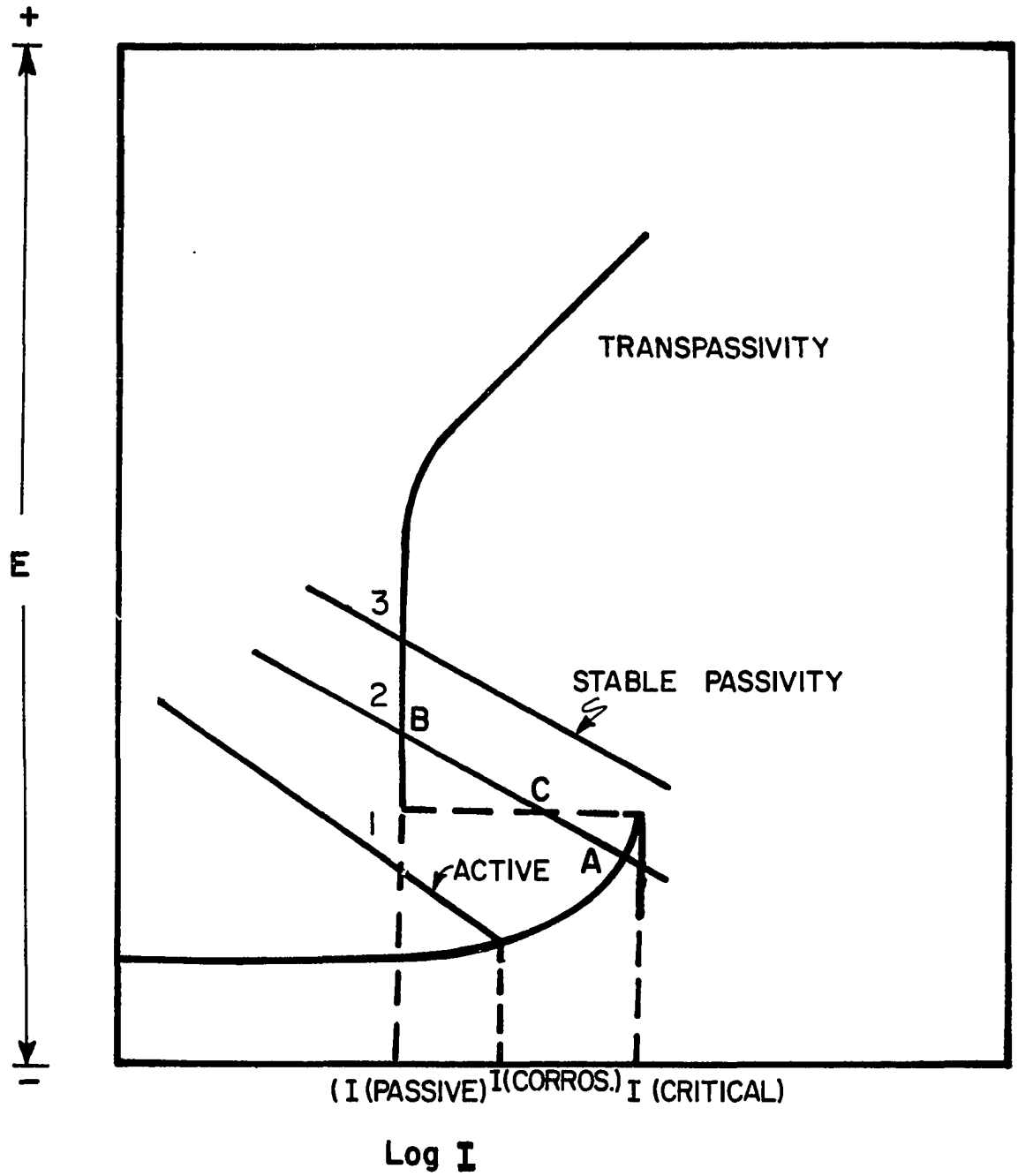

FIG. 1. ANODIC POTENTIOSTATIC POLARIZATION FOR EITHER ACTIVE OR PASSIVE METAL, DEPENDING ON OVERVOLTAGE OF CATHODIC AREAS.

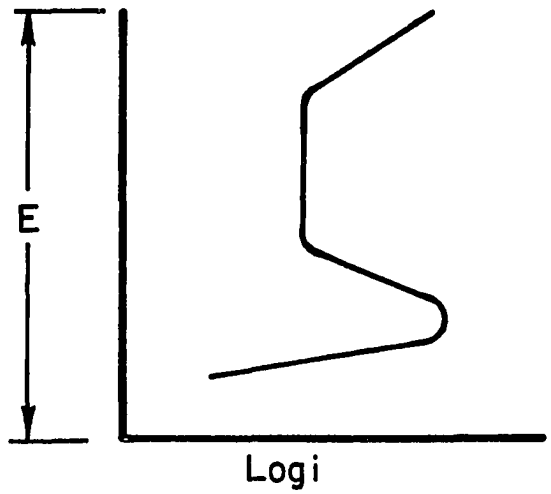

a) Case I

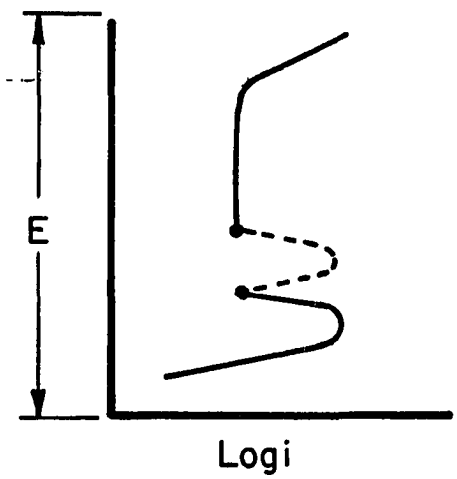

b) Case 2

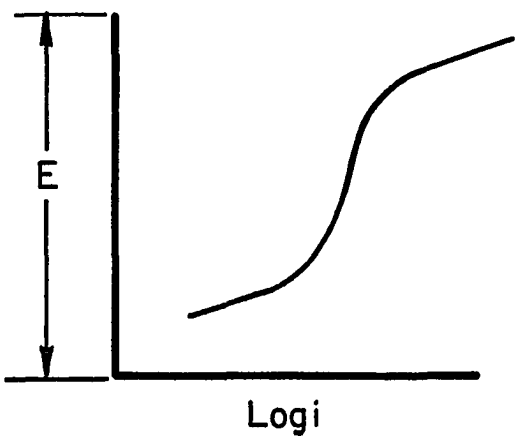

c) Case 3

FIG. 2. TYPICAL ANODIC POLARIZATION OF THREE CASES SHOWN IN FIGURE 1.

or passive state. This is a characteristic of steel in fertilizer solution, and typical behavior of this system is shown in Figure 2b.

In Case 3, there is only one stable point, and the metal spontaneously passivates and corrosion rate is small. This is a characteristic of steel in concrete, and typical behavior of the system is shown in Figure 2c.

Molybdenum/Molybdenum Oxide (Mo/MoO_3) Reference Electrode

Solid molybdenum/molybdenum oxide is a newly developed electrode [76,77]. It is small and compact, and can be used in any orientation. Mo/MoO_3 electrodes can be embedded permanently in concrete adjacent to the reinforced structures (such as bridge decks and pipelines), which makes regular measurement and control of the potential of structures possible. This electrode also reduces the potential measurement error significantly.

The Mo/MoO_3 electrode is stable when manufactured to produce MoO_3 on the surface. The electrode's behavior with a variation of OH^- concentration is given as follows:

$$Mo^{+6} + 6\bar{e} \rightleftarrows Mo \tag{6}$$

$$MoO_3 \rightleftarrows Mo^{+6} + 3\bar{\bar{O}} \tag{7}$$

$$3\bar{\bar{O}} + 3H_2O \rightleftarrows 6OH^- \tag{8}$$

$$6OH^- + 6H^+ \rightarrow 6H_2O \tag{9}$$

Table 5 indicates the potential of the Mo/MoO_3 electrode compared to an external $Cu/CuSO_4$ electrode in various salt-contaminated concretes.

Table 5

Potential of the Mo/MoO_3 Electrode in Concrete, Compared to $Cu/CuSO_4$

Chloride Content, wt %	Average Potential, mv	Standard Deviation, mv
0	309	15.6
0.1	262	17.7
0.2	267	10.7
0.5	294	10.6

Table 6 shows the potential of Mo/MoO_3, compared to a saturated calomel electrode in a saturated $Ca(OH)_2$ solution with varying salt concentration.

Table 6

Potential of the Mo/MoO_3 Electrode in a Saturated $Ca(OH)_2$ Solution, Compared to a Saturated Calomel

Chloride Content, wt %	Potential, mv
0	-420
0.25	-420
0.5	-420
1	-420
2	-420

Potential Measurement in Electrochemical Cells

2.7 Cathode - Solution Gradient

The work of Stammen and Townsend [78] has shown that differences in potential are found at various points around a cathode when a current is introduced from the cathode to a chemical solution.

It was concluded that the potential would increase for a constant level of current as the distance from the cathode was increased. The change in the level of current gives essentially the same pattern, with potential values proportional to the current.

Hoar and Kasper [79,80] also found a gradient in potential in the solution adjacent to the electrode and a tangential as well as normal components of current at the electrode surface.

2.8 Cell Design and Potential Distribution

The potential and current distribution in the cell are of primary importance. Electrode placement and cell geometry have a great impact on the potential and current distribution, which consequently influence analytical and kinetic measurements.

The most basic elements to be taken into account are the dimensions and relative positioning of the cell component, which may create a local variation of electrode potential at the working electrode [81,82, 83,84]. For instance, the positioning of the reference electrode in the electrochemical cell may create a potential error for the working electrode, because of the IR drop between the working and the reference electrode.

To an extent, uniform current density indicates a uniform

potential distribution. This may be required for all controlled potential methods. However, because the relation between current and potential distribution over the electrode surface is dependent upon the current potential characteristics of individual portions of the surface, considerable change in current density may occur without any variation in electrode potential and vice versa. For example, an electrode which operates with virtually a uniform potential distribution may indicate quite non-uniform current distribution either because of differences in mass transfer at various parts of an electrode or because all regions of an electrode are operating at points on the steeply rising portion of current-potential characteristics. In a controlled-potential method, neither of these two conditions of non-uniform current distribution can necessarily be determined.

CHAPTER III

EXPERIMENTAL PROCEDURES

Sample Preparation

3.1 Mix Design

The mix design for the concrete was obtained from the Oklahoma Department of Transportation. The specifications for one cubic yard of concrete are given below:

658 lbs cement

1250 lbs dry sand

2000 lbs dry aggregate

276 lbs water

w/c = 0.42

These amounts were lowered proportionally to the smallest amount of concrete necessary to make the sample blocks. For example, for making 10 - 1x2x3 inch blocks, the amounts used were as follows:

0.854 lbs cement

1.620 lbs fine sand (dry)

2.590 lbs aggregate (dry)

0.350 lbs water

Because the sand and aggregate were stored outside the mixing room, weather conditions resulted in a variation in water content.

Therefore, the amount of water specified in the mix design was lowered by the water content of the sand and aggregate.

The concrete was stirred with a trowel until very well-mixed. This concrete mix was placed in the mold and rodded with a reinforcing bar to remove any large air pockets. These blocks were then placed in a water cabinet for 28 days to be cured.

3.2 Test Specimen

3.2.1. Samples for Electrochemical Studies of Steel in Salt-Contaminated Concrete. For this test program, sixty concrete blocks of 1x2x3 inch were cast. Each concrete block had a steel plate of 1.5x2 inches placed in the center with a 1/2 inch cover, and one solid molybdenum/molybdenum oxide (Mo/MoO_3) reference electrode [76,77] placed adjacent to the steel to reduce the IR drop in potential measurement. The steel plates were acid-pickled and cleaned with acetone and distilled water prior to usage. The chemical analysis of the steel plate used in these experiments was performed by Midstates Analytical Laboratory, Inc. The results of this analysis is given in Table 7.

Half these concrete blocks were made of Type I and the other half of Type V Portland cement. The composition of these two types is given in Table 8.

Salt (NaCl) was mixed with some of each of these types. The salt concentration was in the range of 0.1 to 2% by weight of concrete. The salt was first added to the concrete mixing water in order to distribute the salt uniformally throughout the concrete.

After the 28 days of curing, a number of samples from both Type I and V with a salt content from 0 to 2% were placed in water and in dry

Table 7

Chemical Analysis of the Steel Used in This Study

Element	Concentration %
Carbon	0.06
Sulfur	0.017
Phosphorous	0.009
Silicon	0.03
Maganese	0.28
Chromium	0.02
Molybdenum	0.01
Copper	0.02
Aluminum	0.01

Table 8

Cement Composition of Type I and V Portland Cement Used in This Study

Type of Cement	Compounds				
	C_3S	C_2S	C_3A	C_4AF	Total Alkalies (Na_2O)
V	60.83	19.10	4.51	8.60	0.37
I	51	25	9	8	

conditions, in the laboratory. Some of the slabs with no salt content, from both Type I and V, were placed in a salt solution (NaCl) with concentrations ranging from 0.1 up to 2% salt. The time of exposure of these samples to the above environments will be discussed in the Exposure Section.

In addition, three more 1 x 2 x 3 inch concrete blocks of Type I Portland cement with 0.5, 1, and 2% salt content by weight of concrete were cast. Each of the three had a 1/2 x 2 inch platinum plate (thickness, 0.002 inch) placed in the center with a 1/2 inch cover. One Mo/MoO_3 solid electrode was placed adjacent to the platinum plate in each block.

3.2.2 Samples for the Effect of Wire Mesh on Current and Potential. For this study, a series of test specimens were made.

Initially, five 3 x 3 x 3 inch concrete slabs of Type I Portland cement were cast. Each block had one 1.5 x 2 inch steel plate and one solid Mo/MoO_3 reference electrode adjacent to the plate. Four of these concrete slabs had a reinforcing wire mesh and one had none. Two of the slabs had a screen wire mesh. On one, this was lying on the plate and on the other was 2 inches away from the plate, with no connection. The screen wire mesh was degalvanized in acid prior to usage. The other two slabs had an expanded wire mesh with the same locations as the screen wire mesh. In addition, another Mo/MoO_3 electrode was mounted adjacent to each wire mesh. The arrangement of the plate and wire mesh in these concrete slabs is shown in Figures 3A and 4.

One 3 x 6 x 3 inch concrete block having one steel plate and four screen wire meshes were cast in order to study the effect of potential gradient in the concrete. The screen wire meshes were mounted in the

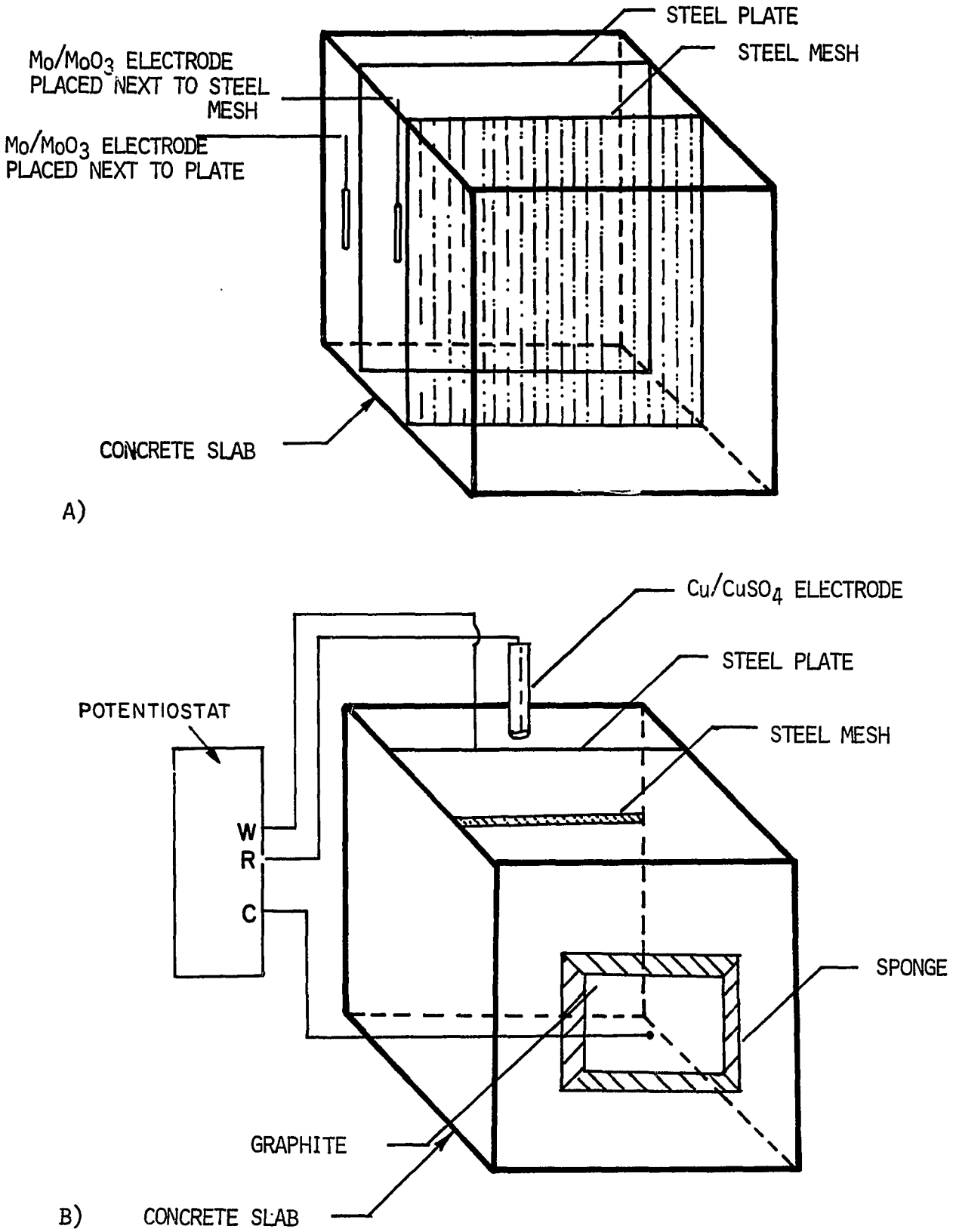

FIG. 3 . SCHEMATIC DIAGRAM OF CONCRETE SLABS FOR MESH SHIELDING STUDIES

A) ELECTRODES, MESH AND PLATE LOCATIONS
B) EXPERIMENTAL APPARATUS FOR ELECTROCHEMICAL STUDIES

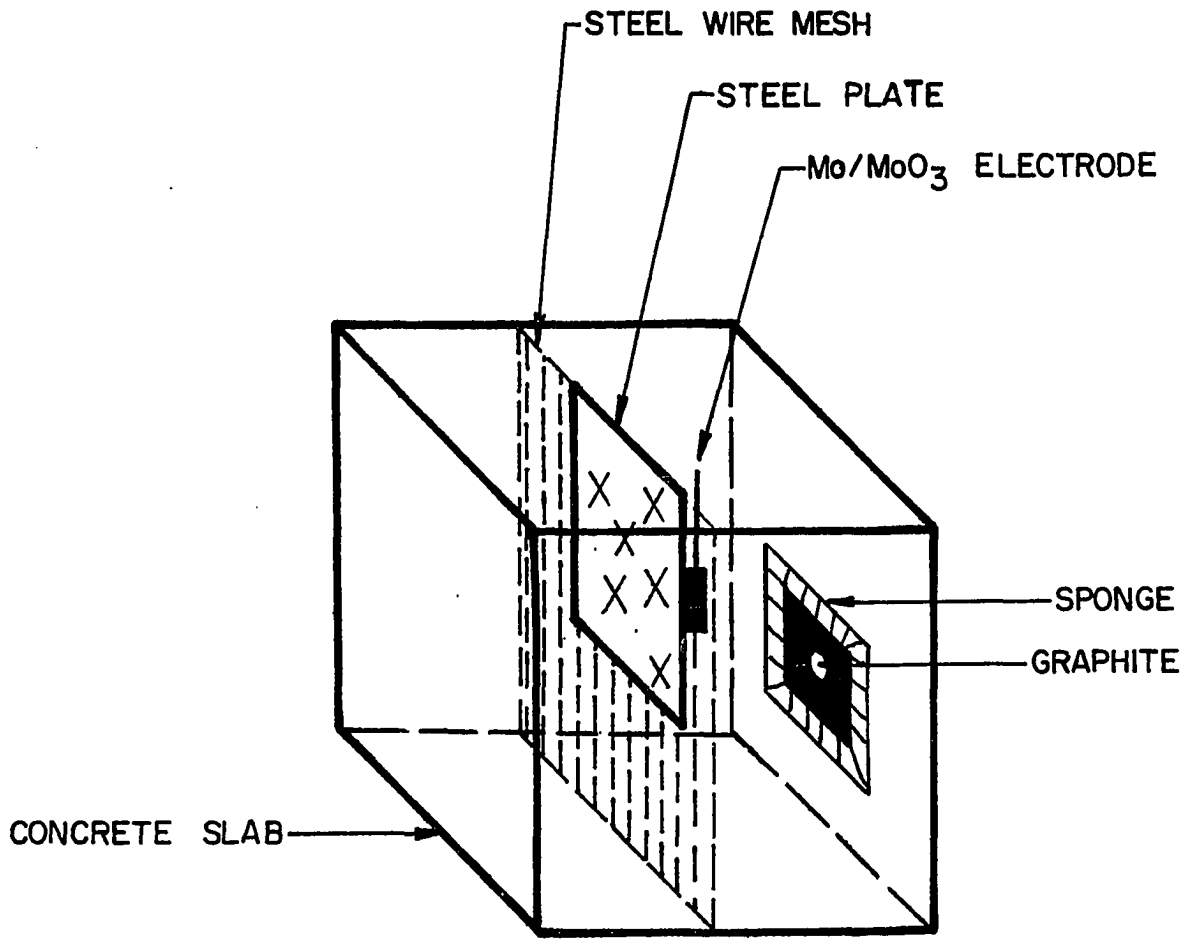

FIG. 4. CELL ASSEMBLY FOR CONCRETE SLAB WITH WIRE MESH LAYING AGAINST STEEL PLATE.

concrete at distances of 3, 6, 9, and 12 centimeters from the plate. In this concrete sample, one Mo/MoO_3 reference electrode was placed adjacent to the steel plate and each mesh. The arrangement of the screen wire meshes, the steel plate, and the reference electrodes in this concrete sample is shown in Figure 5.

Finally, another 3 x 6 x 2 inch concrete slab with five 1/2 x 1 inch platinum plates (thickness, 0.002 inch) was cast. The platinum plates were 2 inches apart. In this concrete sample, each plate had one Mo/MoO_3 electrode adjacent to it, as shown in Figure 6.

3.3 Exposure Time

After 28 days of curing, some of the 1 x 2 x 3 inch concrete blocks were placed in distilled water, some in salt solutions, and some in a dry condition in the laboratory. These concrete blocks were kept under these conditions for six to seven months and periodically, the polarization test was conducted on them.

After 28 days of curing, the concrete blocks used for the wire mesh study were placed in a dry condition in the laboratory.

Electrochemical Measurements

In this study, the Potentiostat/Galvonostat Model 173, combined with a logarithmic current converter Model 376 and Universal Programer Model 175 purchased from Princeton Applied Research were used for obtaining the polarization data. The data were recorded by a Varian Recorder Model F100. Potentiostat Model PEC-1B from Floyd Bell Associates, Inc. and a volt-ohm microammeter Model 269 from Simpson Electric Company were also used. The potential measurements were made by a digital voltmeter

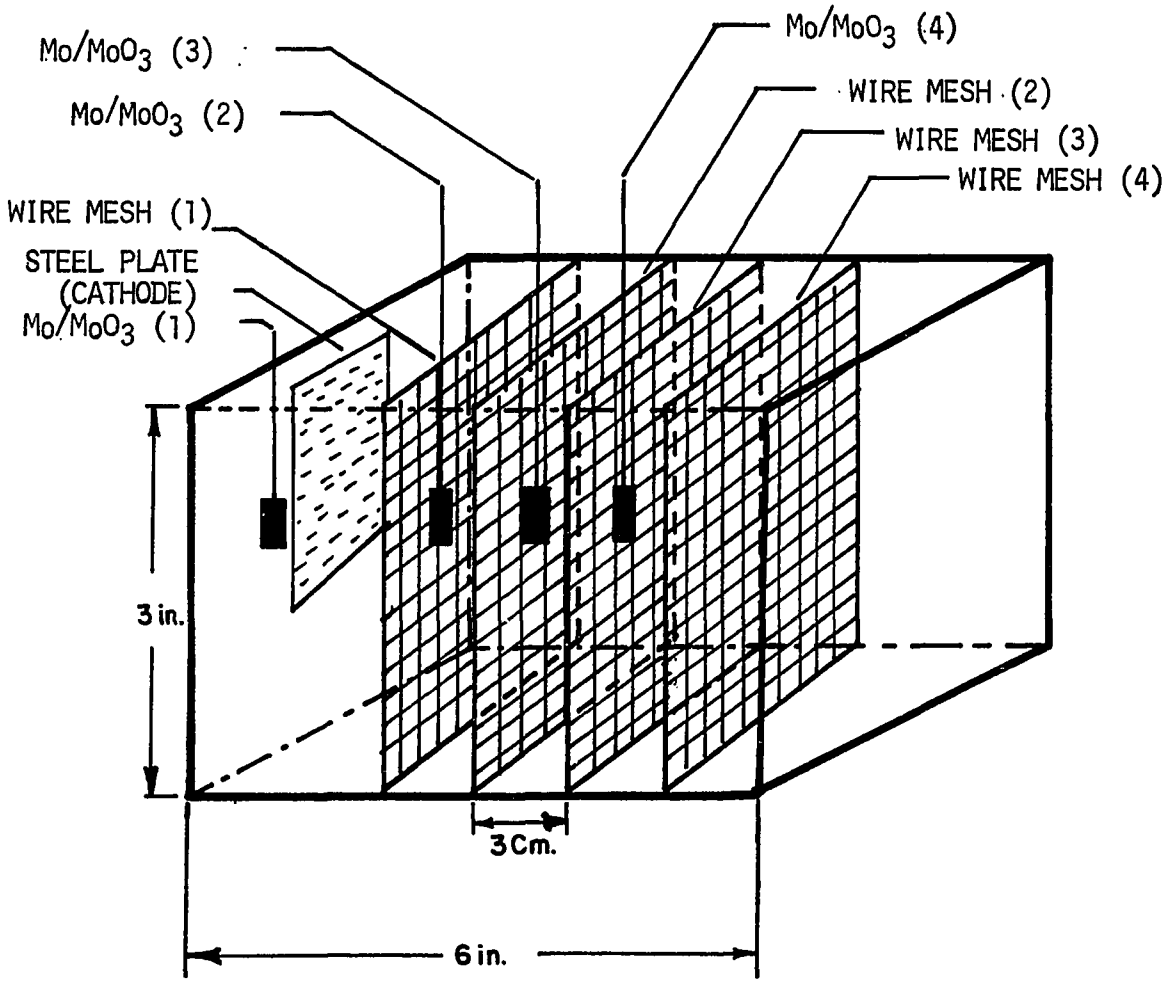

FIG. 5. CONCRETE SAMPLE WITH ONE STEEL PLATE AND FOUR STEEL WIRE MESHES AT THE DISTANCES 4 CM APART EMBEDDED IN CONCRETE BETWEEN ANODE AND CATHODE.

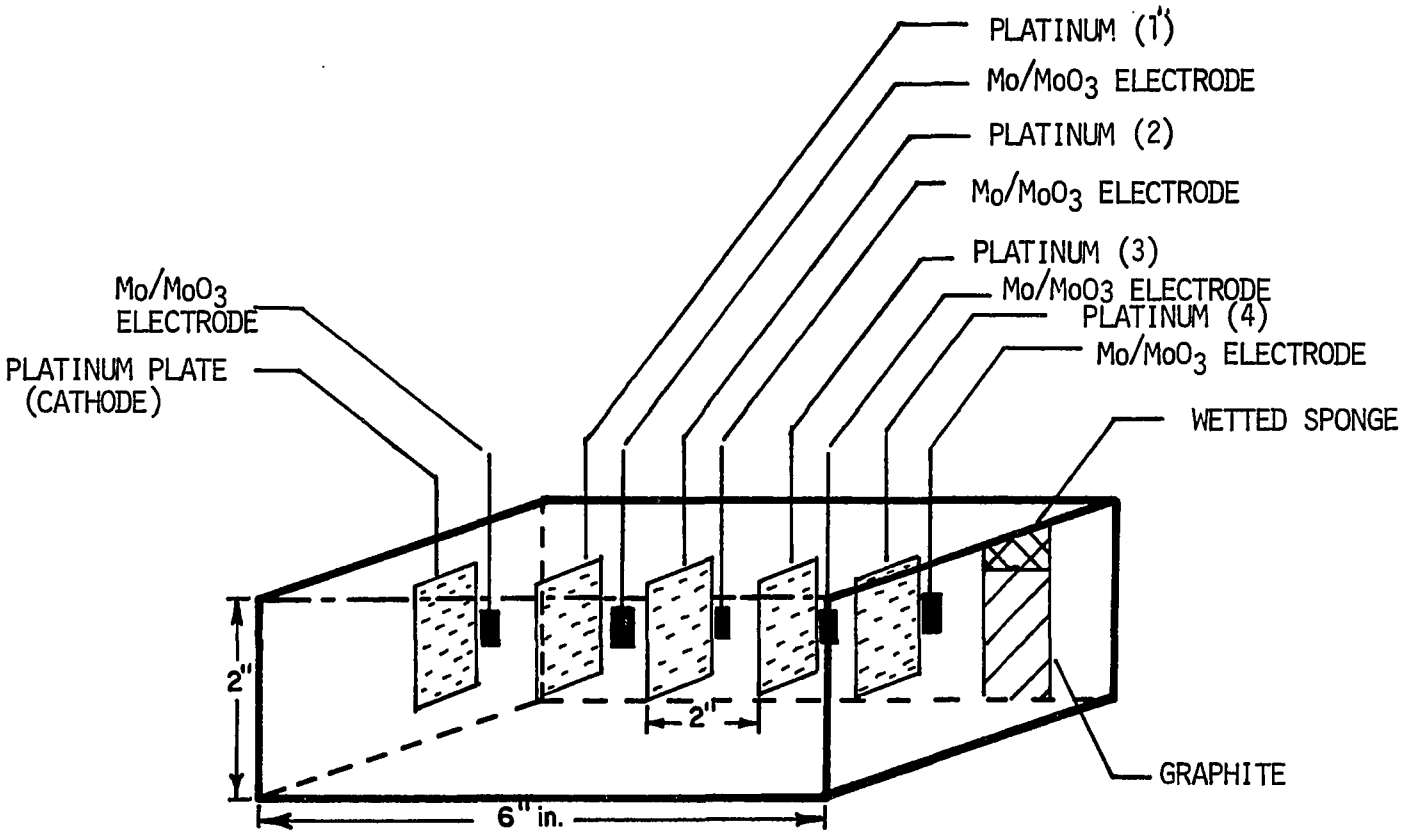

FIG. 6. CONCRETE SAMPLE WITH FIVE PLATINUM PLATES AND FIVE Mo/MoO_3 ELECTRODES ADJACENT TO PLATES. PLATINUM PLATES ARE AT THE DISTANCE OF 2 INCHES APART FROM ONE ANOTHER.

Model 3460A and 3440A from Hewlett, Packard.

3.4 Electrochemical Study of Steel in Salt-Contaminated Concrete

The anodic and cathodic potentiostatic polarization curves were obtained periodically for all 1 x 2 x 3 inch concrete slabs. In these polarizations, the potential of the steel plates was compared by an embeddable solid Mo/MoO_3 reference electrode adjacent to the plate and the potential shifted by 50 mv every three minutes. A graphite anode was used in this study. A sponge wetted with saturated KCl was used to conduct the current through the concrete. A diagram of this assembly is shown in Figure 3B.

A potentiodynamic anodic polarization test was also carried out on these samples. In this test, the potential of the steel plate was kept at -1300 mv, in comparison to the Mo/MoO_3 electrode, for ten minutes. Then the potential was scanned towards the more positive, up to +2000 mv. A slow sweep rate was used (0.28 mv/sec).

3.5 Effect of Wire Mesh and Potential Measurement Error on Current and Potential

The experiments for this study were divided into two parts: solution and those concerning concrete environments.

3.5.1 Solution. A series of tests was conducted in a saturated calcium hydroxide [$Ca(OH)_2$] solution, used to simulate the concrete environment. In these tests, a saturated calomel electrode was used as a reference electrode and a platinum electrode as an anode.

Different cell arrangements with various wire mesh sizes were

used in order to investigate fully the effect of wire mesh on current and potential measurements.

3.5.1.1 Polarization of the Steel Plate

3.5.1.1.1 Wire Mesh was Between the Anode and the Cathode with no Connection. Initially, an experimental set up as shown in Figure 7 was used. The wire mesh was placed between the anode (platinum plate) and cathode (steel plate). Anodic and cathodic polarization of the steel plate was obtained. The wire mesh potential was determined simultaneously with a separate Luggin probe.

3.5.1.1.2 The Wire Mesh was Lying on the Steel Plate. Another test was conducted while the wire mesh was lying on the steel plate. A cell assembly for this experiment is shown in Figure 8. The anodic and cathodic polarization curves were obtained for the steel plate.

3.5.1.1.3 The Wire Mesh was Connected to the Top and Bottom of the Steel Plate and Raised in an Arc about 1 Inch. In a third experiment, the wire mesh was connected at the top and bottom of the steel plate and raised in an arc about one inch in the center. A cell set-up for this test is shown in Figure 9. The anodic and cathodic polarization curves for the steel plate were obtained. Note: the wire mesh was degalvanized in nitric acid prior to use in all the above experiments.

3.5.1.2 Potential Shift of the Platinum Electrode as a Function of Distance, Because of the Passage of Current. (Platinum Plates were Between the Anode and the Cathode with no Connection).

The experimental set-up shown in Figure 10 was used, to determine the potential gradient between anode and cathode. In this experiment, five platinum electrodes were placed in 3% salt solution one inch apart.

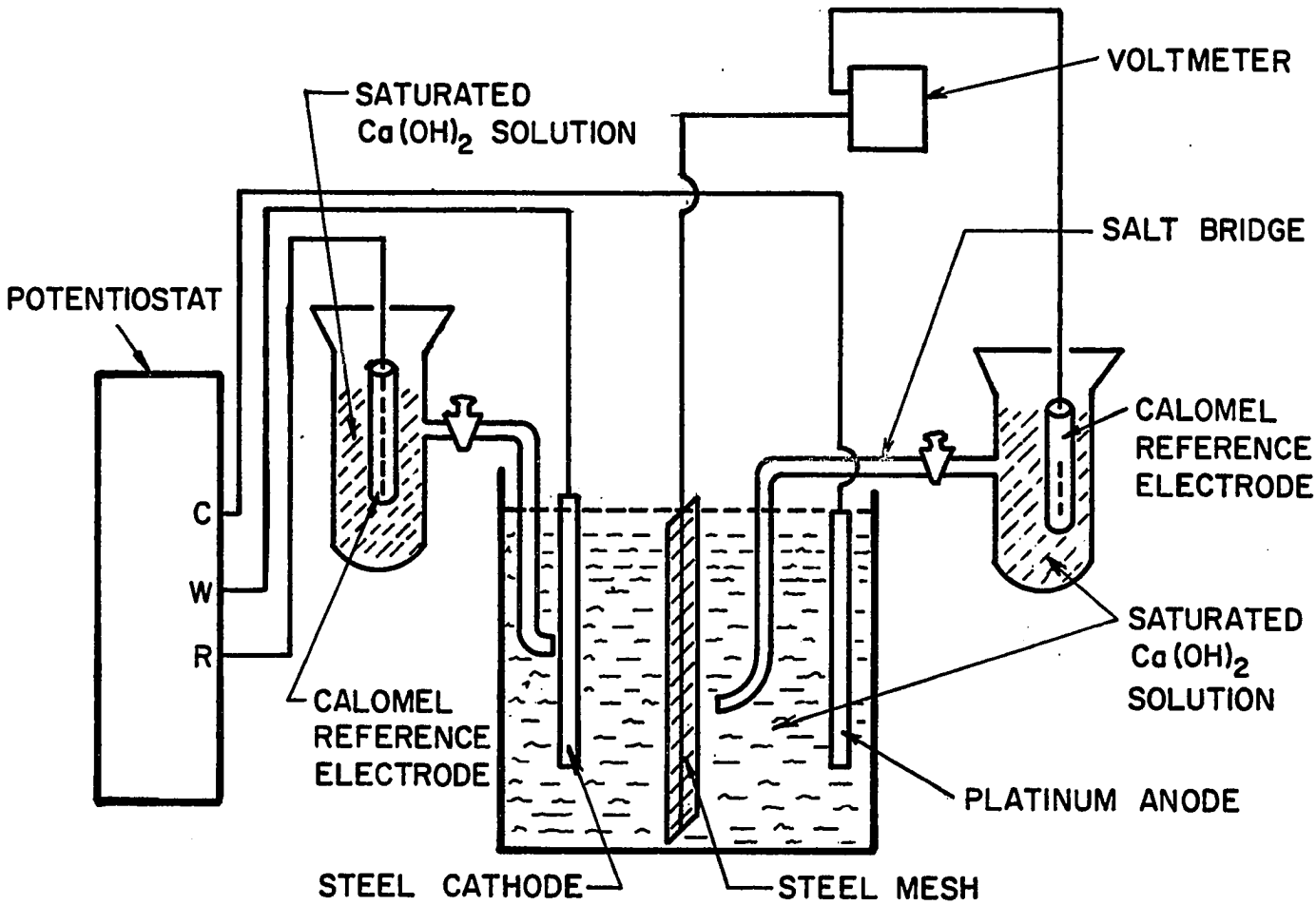

FIG. 7. EXPERIMENTAL SCHEMATIC FOR STEEL MESH STUDY.

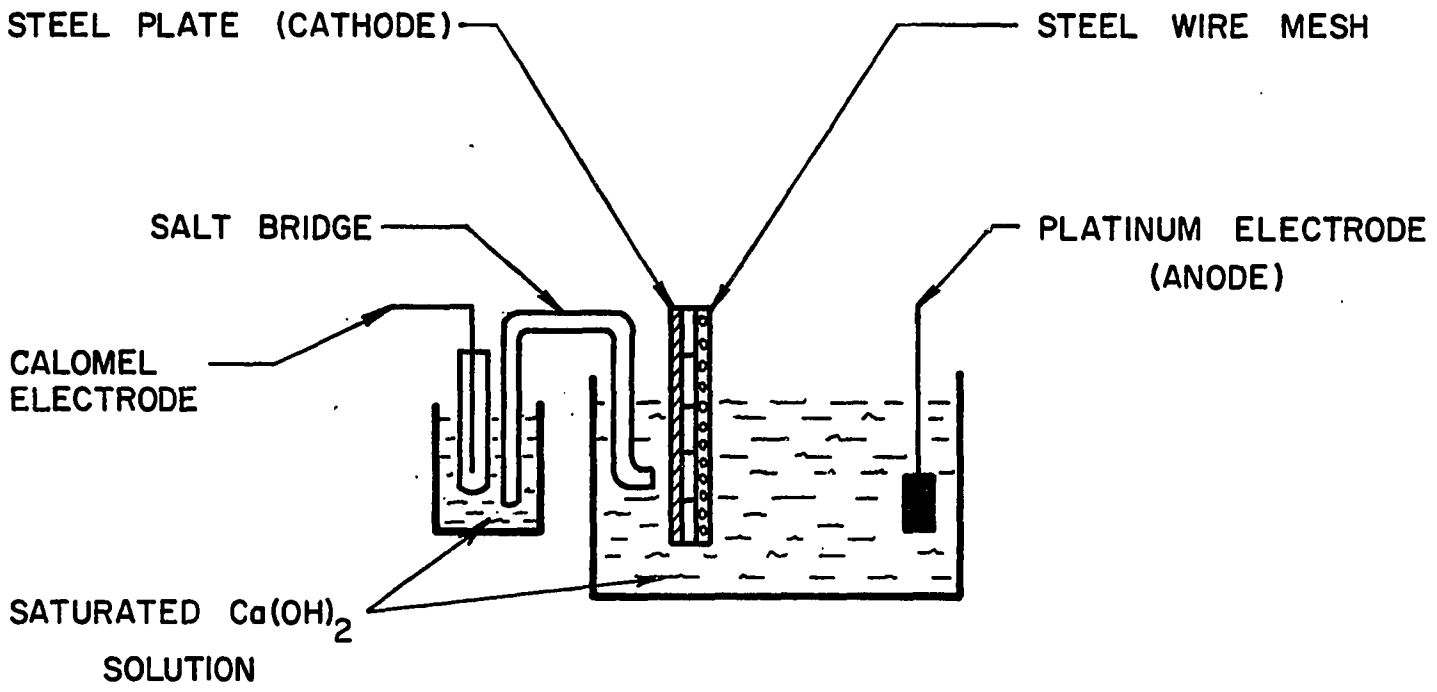

FIG. 8. CELL ASSEMBLY FOR ANODIC AND CATHODIC POLARIZATION OF STEEL PLATE WHEN WIRE MESH IS LYING ON STEEL PLATE IN SATURATED $CA(OH)_2$ SOLUTION.

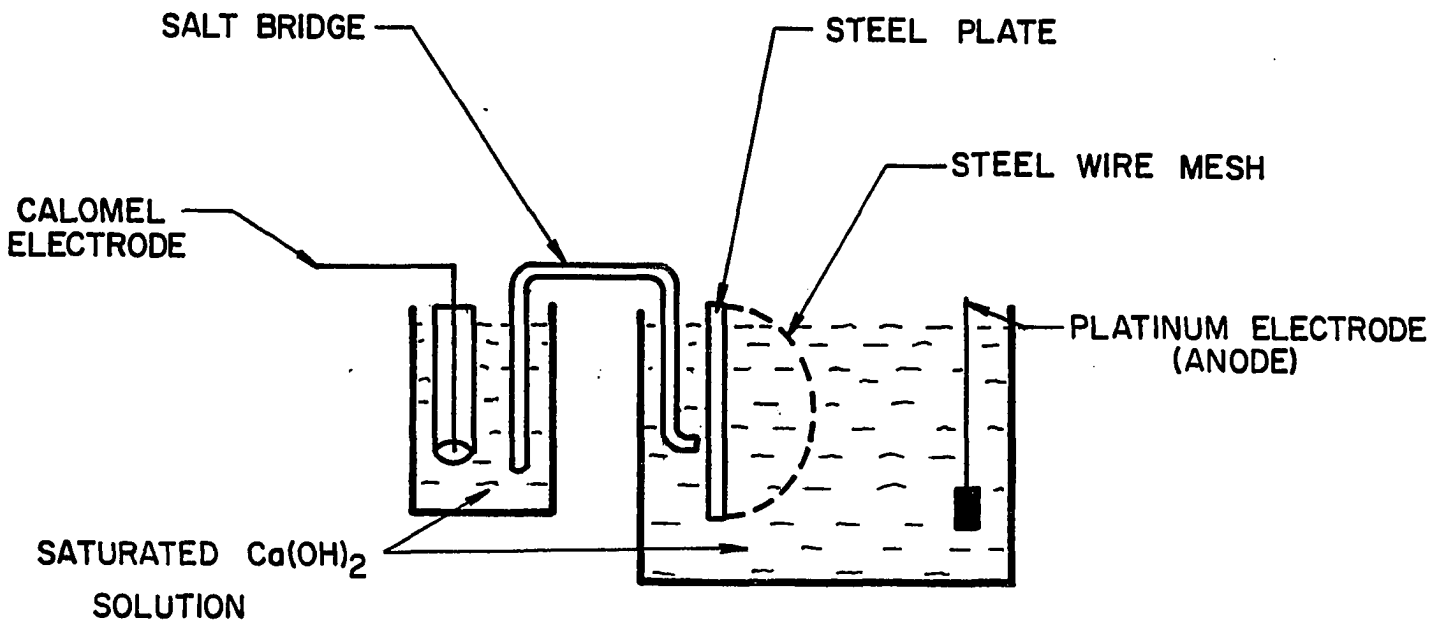

FIG. 9. CELL ASSEMBLY FOR ANODIC AND CATHODIC POLARIZATION OF STEEL PLATE WHEN STEEL WIRE MESH IS ATTACHED TO TOP AND BOTTOM OF STEEL PLATE IN SATURATED $CA(OH)_2$ SOLUTION.

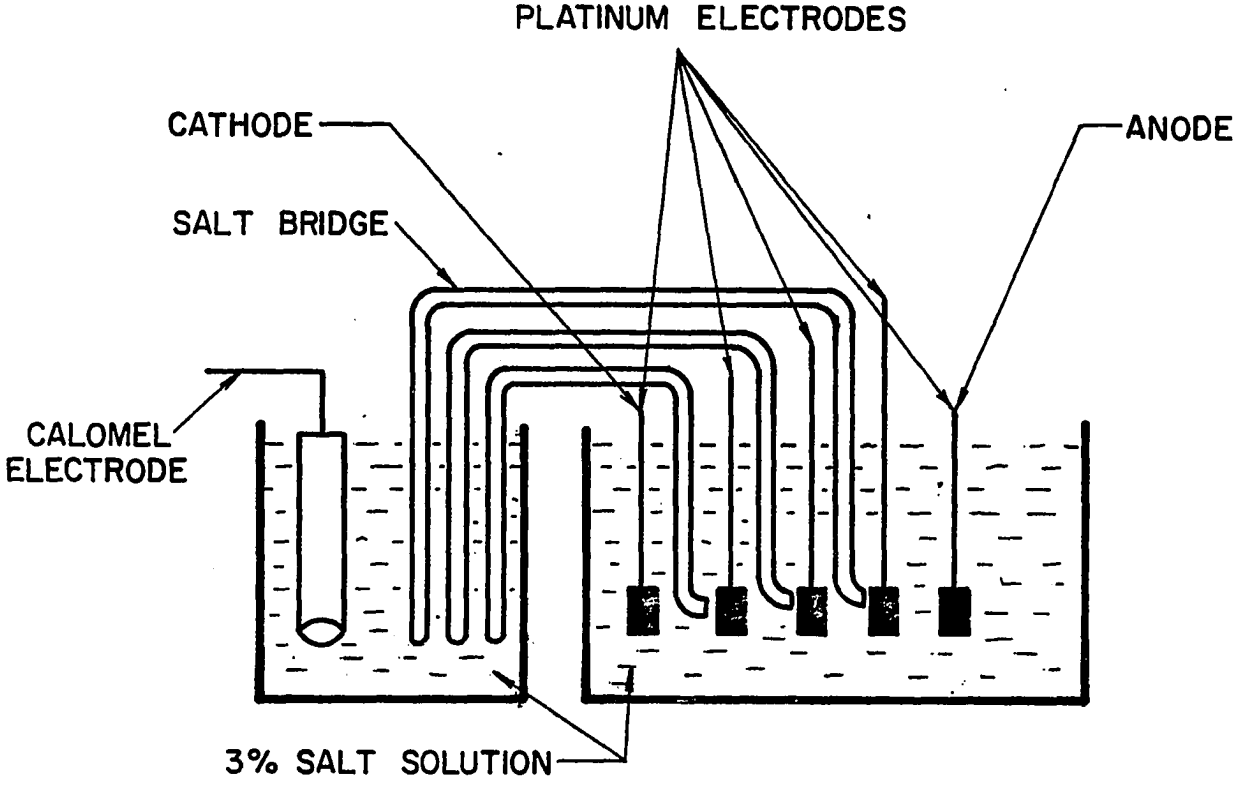

FIG. 10. CELL ASSEMBLY FOR ANODIC AND CATHODIC POLARIZATION OF PLATINUM ELECTRODE AND ITS EFFECT ON THREE OTHER PLATINUM ELECTRODES PLACED BETWEEN ANODE AND CATHODE IN 3% SALT SOLUTION.

One of these platinum electrodes was used as an anode and another as a cathode. The potential of the three platinum electrodes between the anode and the cathode was measured simultaneously by three separate Luggin probes.

3.5.2 Concrete Environments.

3.5.2.1 Polarization of the Steel Plate at the Presence of the Wire Mesh.

Anodic and cathodic polarization curves were obtained for the steel plate in the concrete samples with the screen and expanded wire mesh connected and disconnected to the steel plate. The potential of the steel plate and wire mesh was measured by the two separate solid Mo/MoO_3 electrodes placed adjacent to the plate and wire mesh. A typical concrete sample with wire mesh disconnected from the plate is shown in Figure 3B.

The anodic and cathodic polarization curves of the sample having the platinum plate and wire mesh were obtained. The potential of the wire mesh was measured with respect to the Mo/MoO_3 electrode placed adjacent to it. This test was performed to check the potential variation of the wire mesh in the presence of platinum plate instead of the steel plate.

3.5.2.2 Potential Shift of the Wire Mesh as a Function of Distance from the Cathode Because of the Passage of Current. (Wire Meshes were Between the Anode and the Cathode with no Connection).

Two different test series were conducted in order to determine the potential gradient in concrete. (1) The polarization test was carried out on the sample with four wire meshes placed at the distances

of 3, 6, 9, and 12 centimeters from the steel plate. The potential of each mesh was measured simultaneously by the solid Mo/MoO_3 electrodes mounted adjacent to them. The schematic diagram of this sample is shown in Figure 5. (2) The polarization test was conducted on the sample with five platinum plates placed at distances of 2 inches from one another. One of these platinum plates was chosen as cathode and the potential of the other four platinum plates between the anode and cathode was measured with the Mo/MoO_3 electrodes placed close to them (see Figure 6). For all of these tests, a sponge wetted with saturated KCl solution was used between the anode (graphite) and the concrete.

CHAPTER IV

RESULTS

The Electrochemical Behavior of Steel in a Salt-Contaminated Concrete

The results presented here consist of anodic and cathodic polarization curves for steel in concrete.

These results represent a qualitative assessment of these curves rather than a quantitative determination of corrosion current densities. The shape and position of the curves provide a reasonably good indication of the corrosiveness of the environment with regard to steel. The relationship between this corrosivity of an environment and polarization curves will be explained below.

Note: In this study, the word "salt" refers to sodium chloride.

4.1 Samples in Dry Condition

Figure 11 presents the anodic and cathodic potentiostatic polarization curves for Type I Portland cement concrete. (The samples were in a dry condition in the laboratory for 200 days.) The results indicate that the current density requirements for the sample with no salt are much higher than for the samples containing up to 2% salt. This result was repeated in the potentiodynamic anodic polarization (see Figure 12). The cathodic polarization in Figure 11 also indicates that current density increases as the salt content of the concrete increases

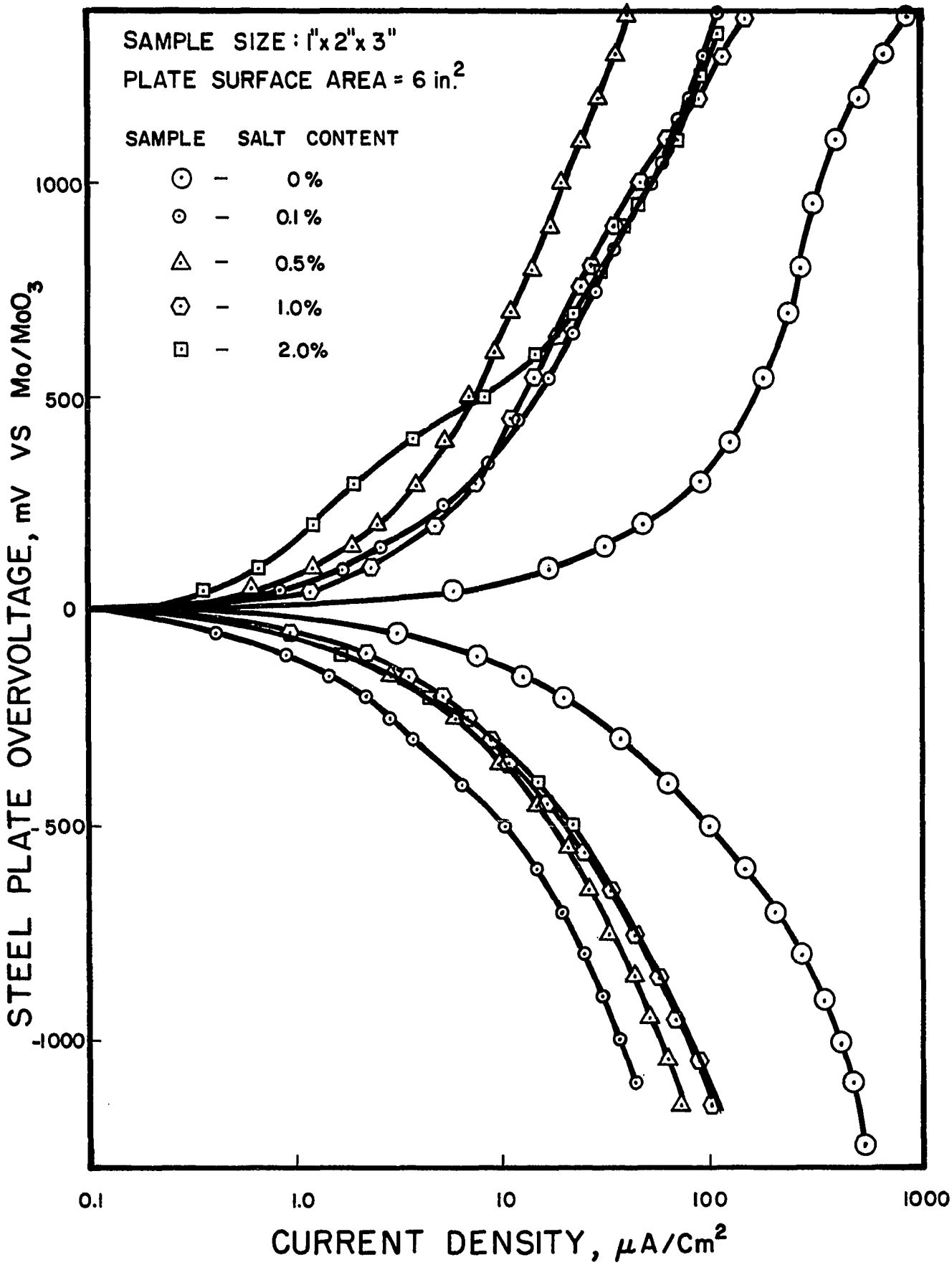

FIG. 11. ANODIC AND CATHODIC POLARIZATION OF STEEL IN TYPE I PORTLAND CEMENT CONCRETE WITH VARIOUS SALT CONTENTS. THE CONCRETE SAMPLES WERE IN DRY CONDITION OF LABORATORY FOR 200 DAYS.

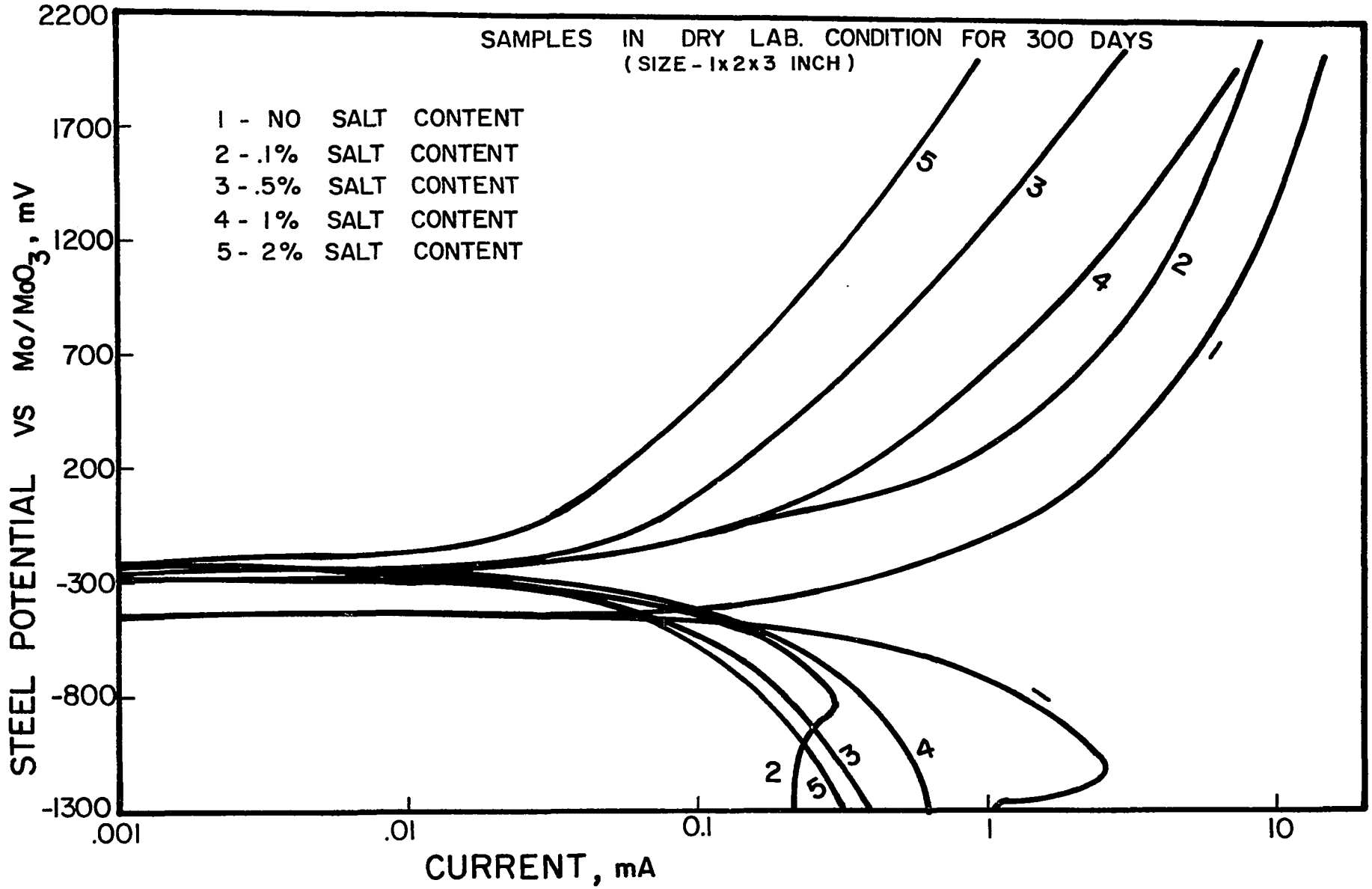

FIG. 12. POTENTIODYNAMIC ANODIC POLARIZATION OF STEEL PLATE IN TYPE I PORTLAND CEMENT CONCRETE CONTAING VARIOUS PERCENTAGES OF SALT (NACL)
(SWEEP RATE 0.28 mV/S)

from 0.1 to 2%.

The potentiodynamic anodic polarization curves in Figure 12 show that the anodic current requirements decrease as the salt content of the concrete increases. The cathodic parts of these polarization curves show that at -1300 mv with respect to the Mo/MoO_3 electrode the current requirements for the samples are different.

Figure 13 gives the anodic and cathodic potentiostatic polarization curves for the Type V Portland cement concrete samples with various salt contents which had been exposed to dry conditions for 200 days. The data indicates that the cathodic current density requirements for the concrete sample with no salt is higher than for the samples with salt content, but the anodic current density for the sample with no salt is about the same as for the sample with 0.5% salt, but higher than for the rest of samples with various salt contents. The potentiodynamic anodic polarization indicates that the current density requirements for the sample with no salt is almost the same as for the samples with various salt contents (see Figure 14).

The cathodic polarization curves in Figure 13 indicate that the current density requirements decrease as the salt content increases. The anodic polarization curves also show approximately the same trend.

A comparison of Figures 11 and 13 indicates that the anodic and cathodic polarization of steel in Type I and V Portland cement are not alike. The shape and the position of the anodic and cathodic curves are different for these two types of cement. Figure 11 shows that the current density requirements for steel in Type I Portland cement increase as the salt content increases except for the sample with no salt. The

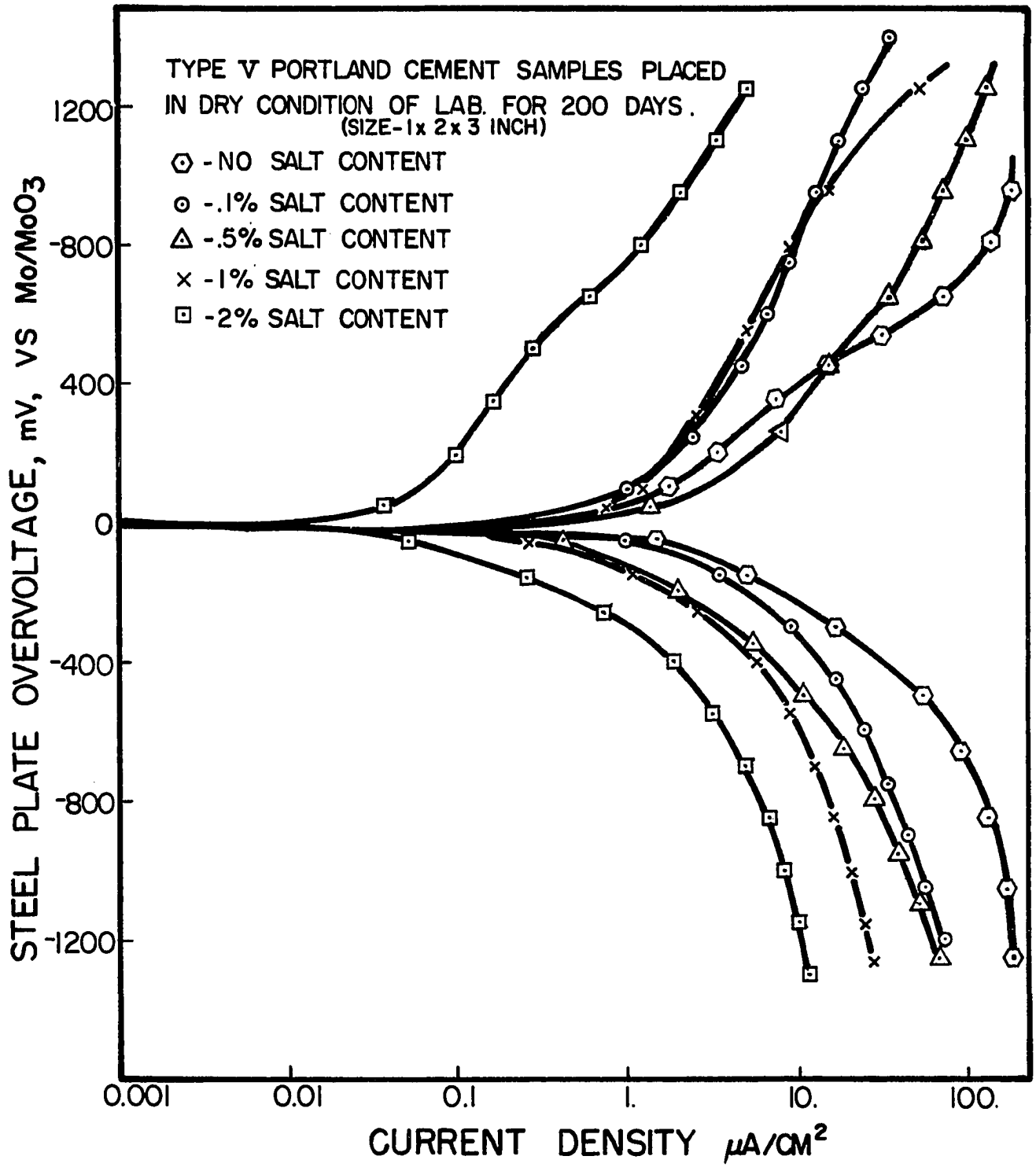

FIG. 13. ANODIC AND CATHODIC POLARIZATION OF STEEL PLATE IN TYPE V PORTLAND CEMENT CONCRETE. THE CONCRETE SAMPLES WERE IN DRY CONDITION OF LABORATORY FOR 200 DAYS.

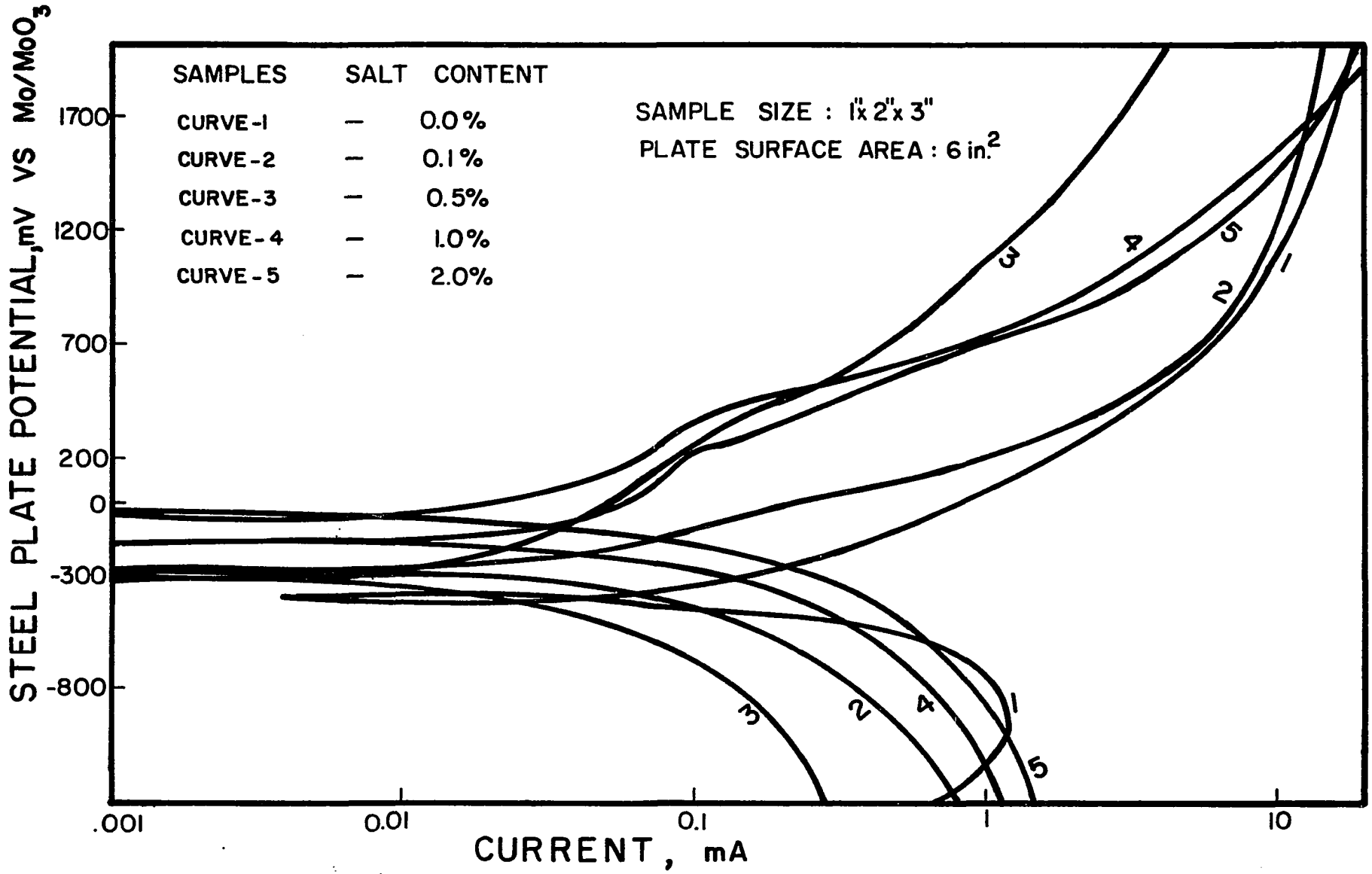

FIG. 14. POTENTIODYNAMIC ANODIC POLARIZATION OF STEEL PLATE IN TYPE V PORTLAND CEMENT CONCRETE CONTAINING VARIOUS PERCENTAGES OF SALT (NACL). SAMPLES WERE IN DRY CONDITION OF LABORATORY FOR 300 DAYS. [SWEEP RATE = 0.28 MV/SEC.]

opposite trend was seen for Type V Portland cement containing various percentages of salt. The anodic current density requirements for Type I Portland cement were about the same, but some differences were found for Type V Portland cement.

In general, the current density requirements for the anodic and cathodic polarization of steel in Type I Portland cement are higher than in Type V Portland cement with and without salt content.

Figure 15 is a plot of the steel plate potential compared to $Cu/CuSO_4$ in Type I and V Portland cement samples versus the salt concentration obtained after the samples were exposed to the dry conditions of the laboratory for 200 days. The potentials of steel in Type I Portland cement were approximately constant for salt concentrations up to 1% (potentials in the range of -530 mv), but the potential shifted toward a more positive value (-470 mv) for a 2% salt concentration. In Type V Portland cement, the steel potential for the samples with zero and 0.1% salt content were the same (-500 mv), and the potential shifted toward a more negative value (-590 mv) for 0.5% salt content. The potential then shifted toward a more positive value for 1 and 2% salt content.

4.2 Samples in Distilled Water

Figure 16 presents the anodic and cathodic potentiostatic polarization curves for steel in Type I Portland cement concrete containing various salt contents. (The samples had been in distilled water for 90 days.) The results indicate that the current density requirements increase as the salt content increases. Passivity was observed for the steel in the zero and 0.1% salt content samples. The anodic polarization

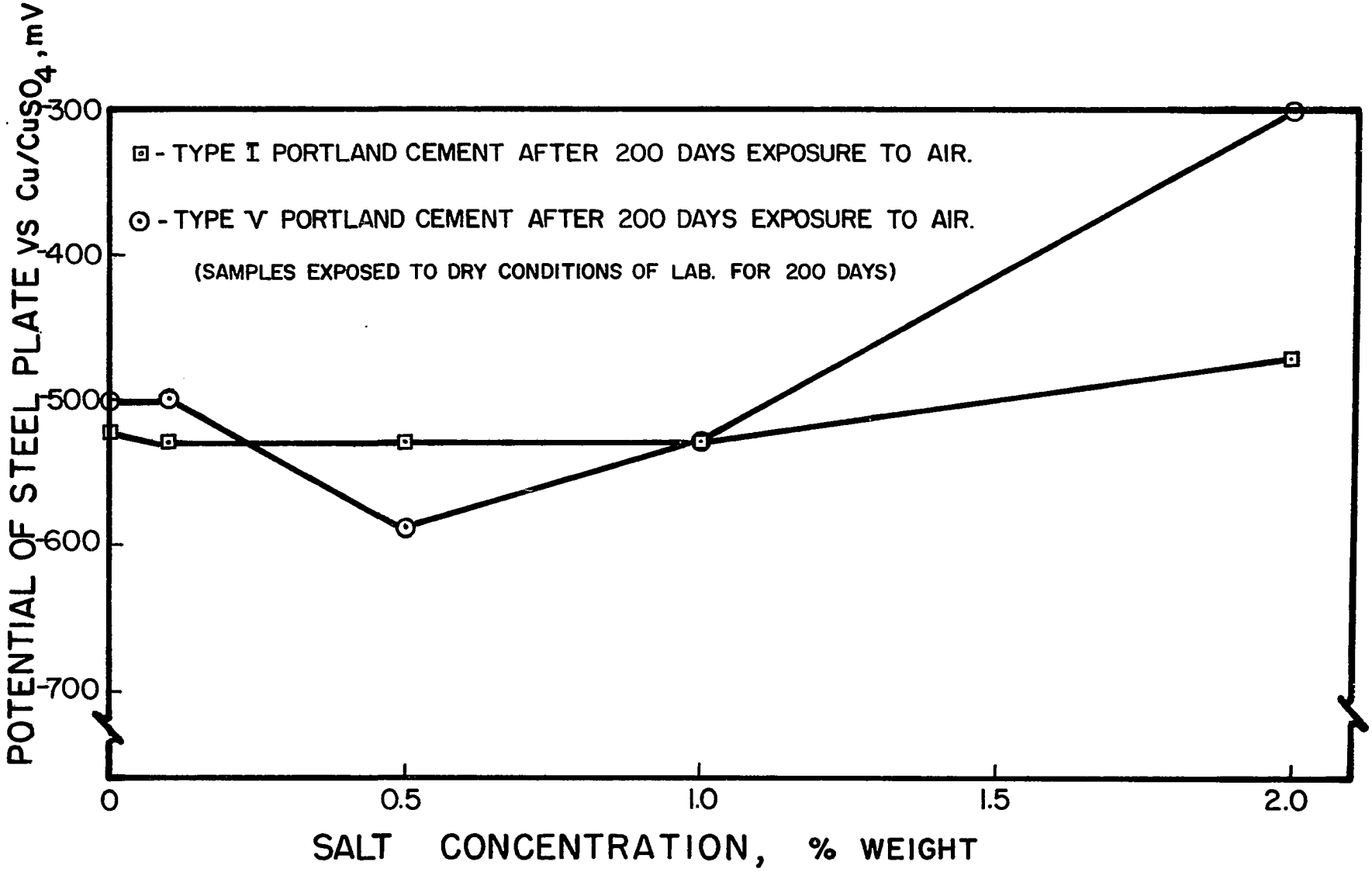

FIG. 15. CORROSION POTENTIAL OF STEEL AS A FUNCTION OF SALT CONTENT IN TYPE I AND V PORTLAND CEMENT CONCRETE.

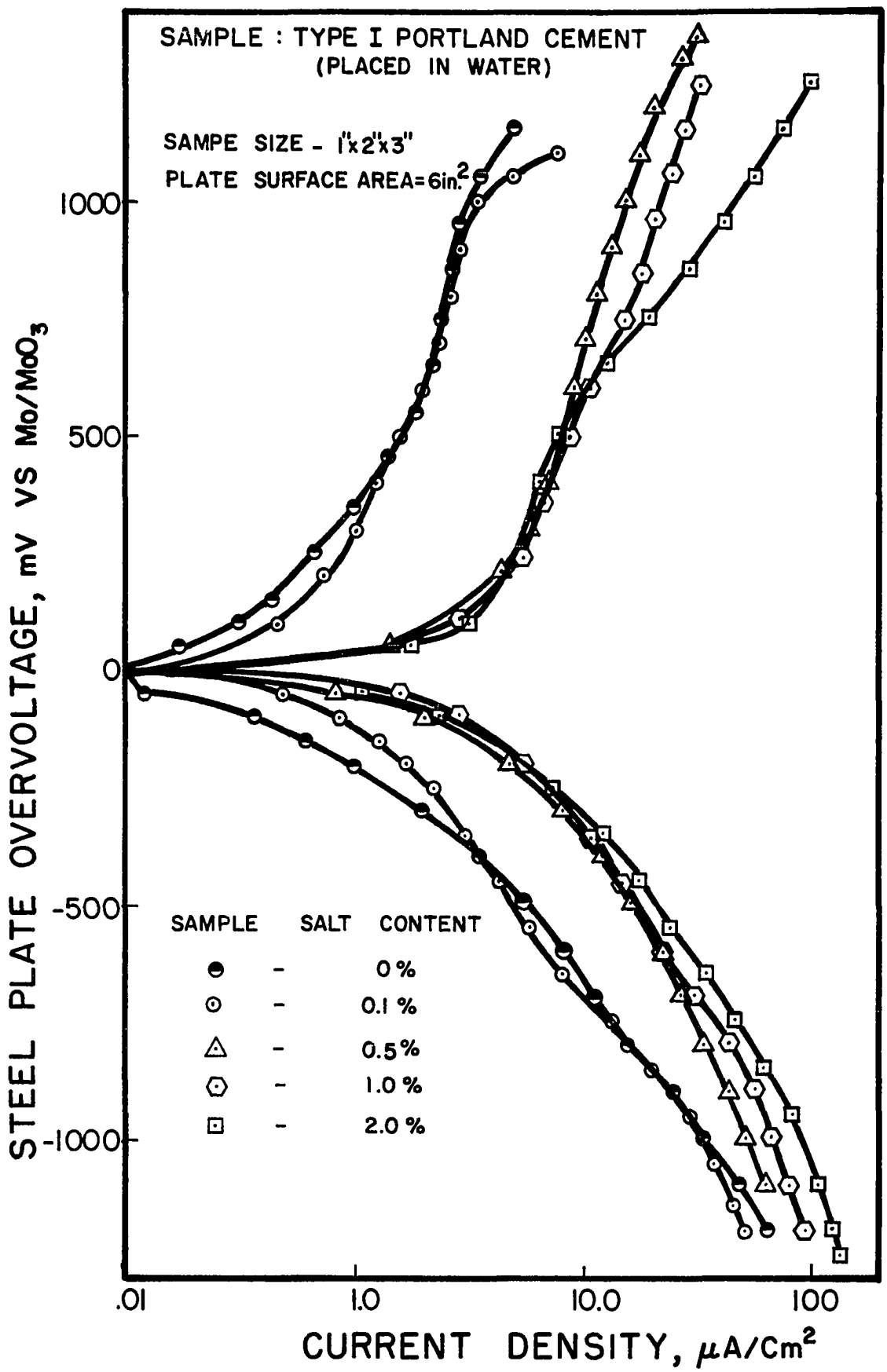

FIG. 16. ANODIC AND CATHODIC POLARIZATION OF STEEL IN TYPE I PORTLAND CEMENT CONCRETE WITH VARIOUS SALT CONTENTS. THE SAMPLES WERE IN WATER FOR 90 DAYS.

curves presented in Figure 16 indicate that the current density requirements for the 0.5 to 2% salt content samples were much higher than for the sample with zero and 0.1% salt.

Figure 17 shows the anodic and cathodic polarization of steel in the Type V Portland cement samples containing various percentages of salt (NaCl). (The samples had been in distilled water for 90 days.) The data indicates the same trend as found for Type I Portland cement. That is, the current density increases as the salt content increases. The anodic polarization indicates the existence of passivity for the samples with zero, 0.1, and 0.5% salt content. The anodic current density for the samples with zero, 0.1, and 0.5% salt content was approximately the same, but this density was much higher for the samples with 1 and 2% salt content.

A break at the potentials about -500 to -600 mv compared to the Mo/MoO_3 electrode for the cathodic polarization curves and about 500 to 600 mv for the anodic polarization curves for the samples of Type I and V Portland cement containing various salt contents was observed.

A comparison of Figures 16 and 17 indicates that the anodic and cathodic current requirements for steel in the samples with zero, 0.1, and 0.5% salt content are higher for Type I than for Type V Portland cement, but the opposite trend was found for the samples of 1 and 2% salt content.

Figure 18 presents the anodic and cathodic potentiostatic polarization of steel in Type I Portland cement containing various salt contents. (The samples had been in distilled water for 170 days.) The results in this figure indicate that the current density for the sample

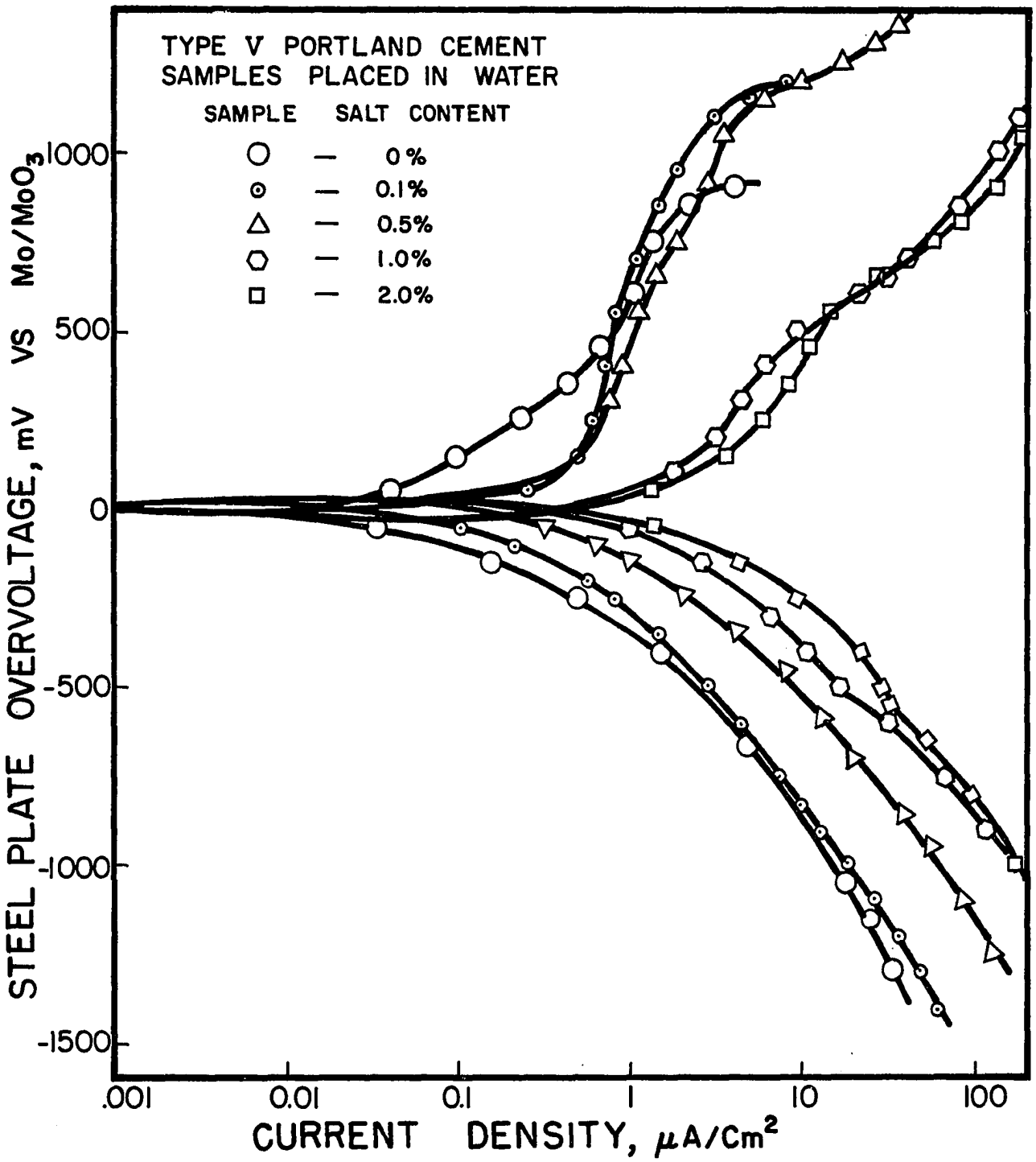

FIG. 17. ANODIC AND CATHODIC POLARIZATION OF STEEL IN TYPE V PORTLAND CEMENT CONCRETE WITH VARIOUS SALT CONTENTS. THE CONCRETE SAMPLES WERE IN WATER FOR 90 DAYS.

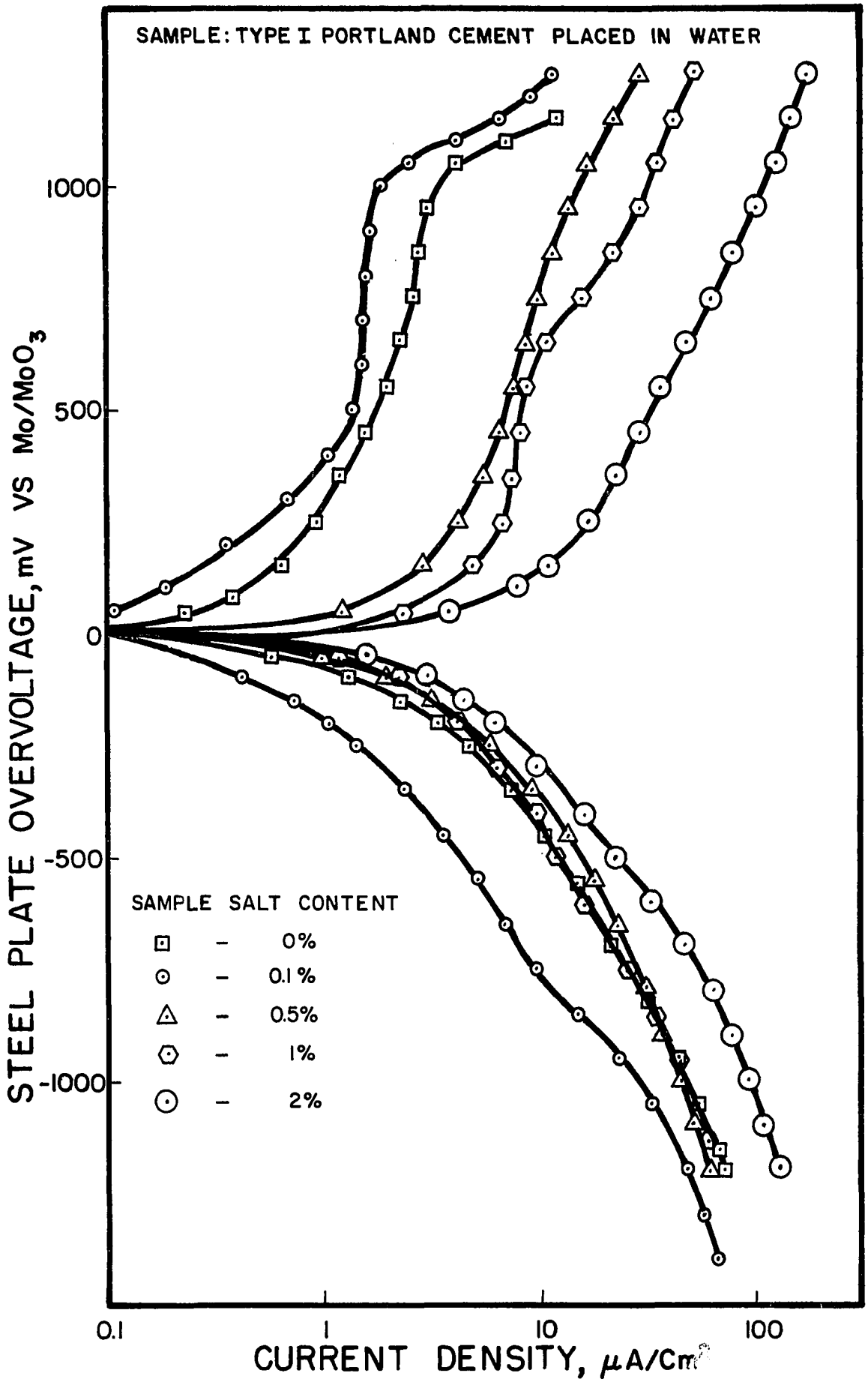

FIG. 18. ANODIC AND CATHODIC POLARIZATION OF STEEL IN TYPE I PORTLAND CEMENT CONCRETE WITH VARIOUS SALT CONTENTS. THE CONCRETE SAMPLES WERE IN WATER FOR 170 DAYS.

with 0.1% salt is lower than for the sample with no salt. The anodic current density of the steel increases as the salt content increases. The cathodic current density of the steel in the samples with zero, 0.5, and 1% salt content is approximately the same, but this density is higher than the 0.1% and lower than the 2% salt content samples. The anodic curves also indicate the existence of a passive region for the samples with zero and 0.1% salt content. The potentiodynamic anodic polarization also indicates the same results. The passive region was smaller for the sample with 0.1% salt content than for the sample with no salt. (See Figure 19.)

Figure 20 presents the anodic and cathodic potentiostatic polarization curves for steel in the Type V Portland cement samples having various amount of salt. (The samples had been in distilled water for 170 days.) The data shows that the current density requirements increase as the salt content increases. The anodic polarization indicates the presence of a passive film on the steel surface for the samples with zero, 0.1, and 0.5% salt content. The same result was found in the potentiodynamic anodic polarization curves. (See Figure 21.)

A comparison of Figures 18 and 20 indicates that the anodic and cathodic current density requirements for the samples of Type I Portland cement with zero, 0.1, and 0.5% salt contents are higher than for the samples of Type V Portland cement with the same amounts of salt. However, these current density requirements are about the same for the samples with 1 and 2% salt content. The anodic and cathodic current density for the sample of Type I Portland cement with 0.1% salt content was lower than for the sample with no salt, but higher for the samples

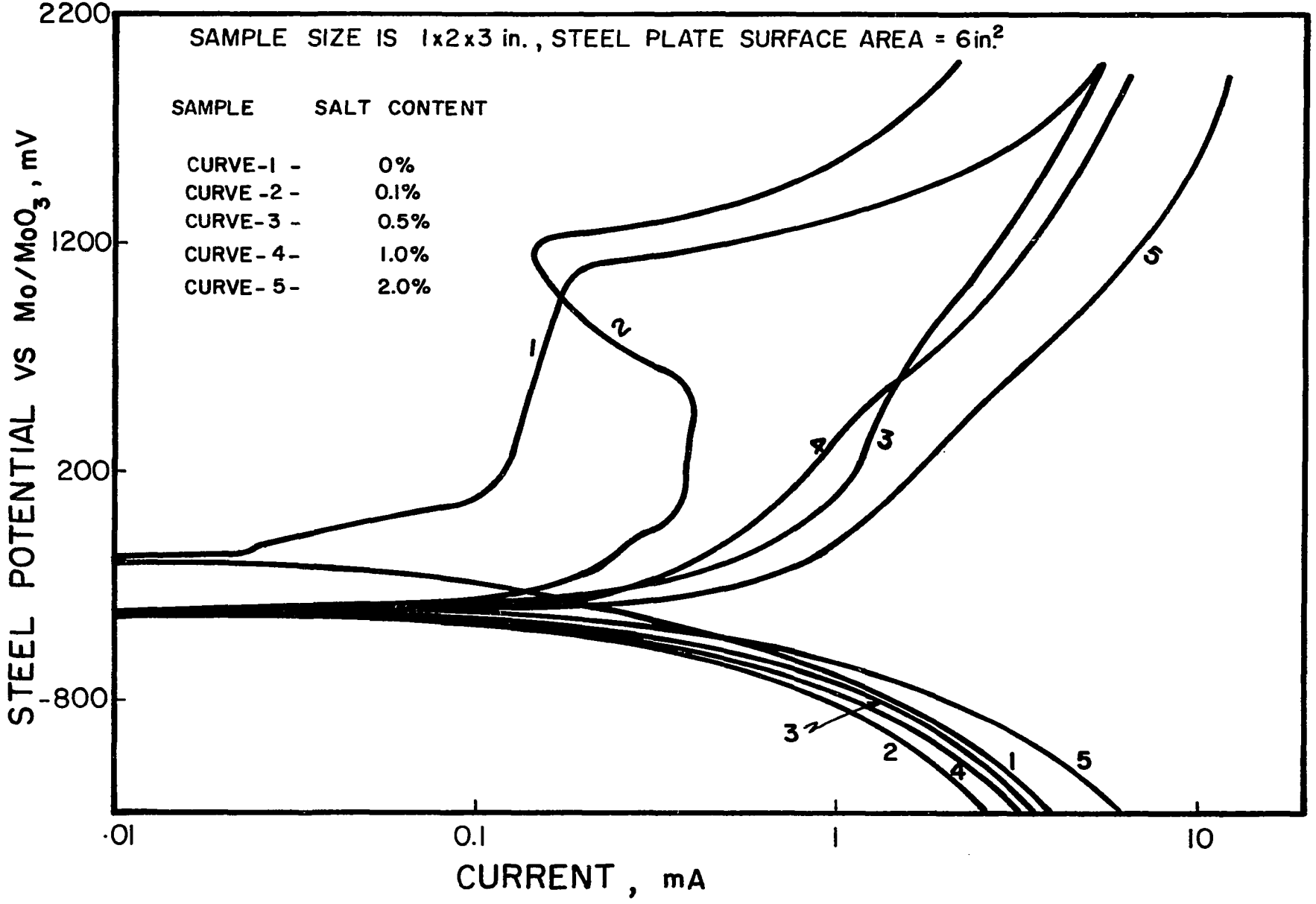

FIG. 19. POTENTIODYNAMIC ANODIC POLARIZATION OF STEEL PLATE IN TYPE I PORTLAND CEMENT CONCRETE CONTAINING VARIOUS PERCENTAGES OF SALT (NACL). SAMPLES WERE IN DISTILLED WATER FOR 300 DAYS. [SWEEP RATE = 0.28 MV/SEC.]

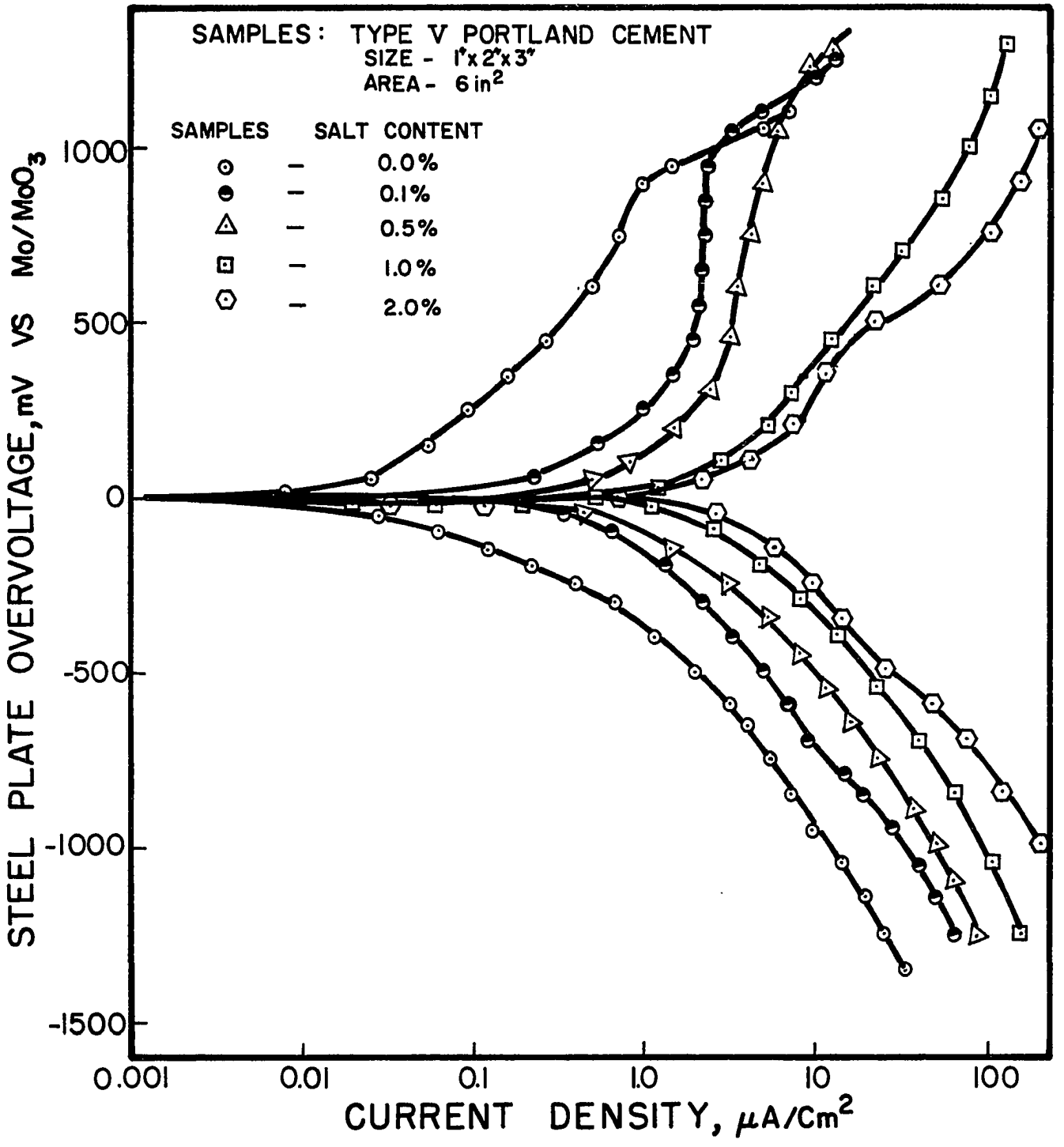

FIG. 20. ANODIC AND CATHODIC POLARIZATION OF STEEL IN TYPE V PORTLAND CEMENT WITH VARIOUS SALT CONTENTS. THE CONCRETE SAMPLES WERE IN WATER FOR 170 DAYS.

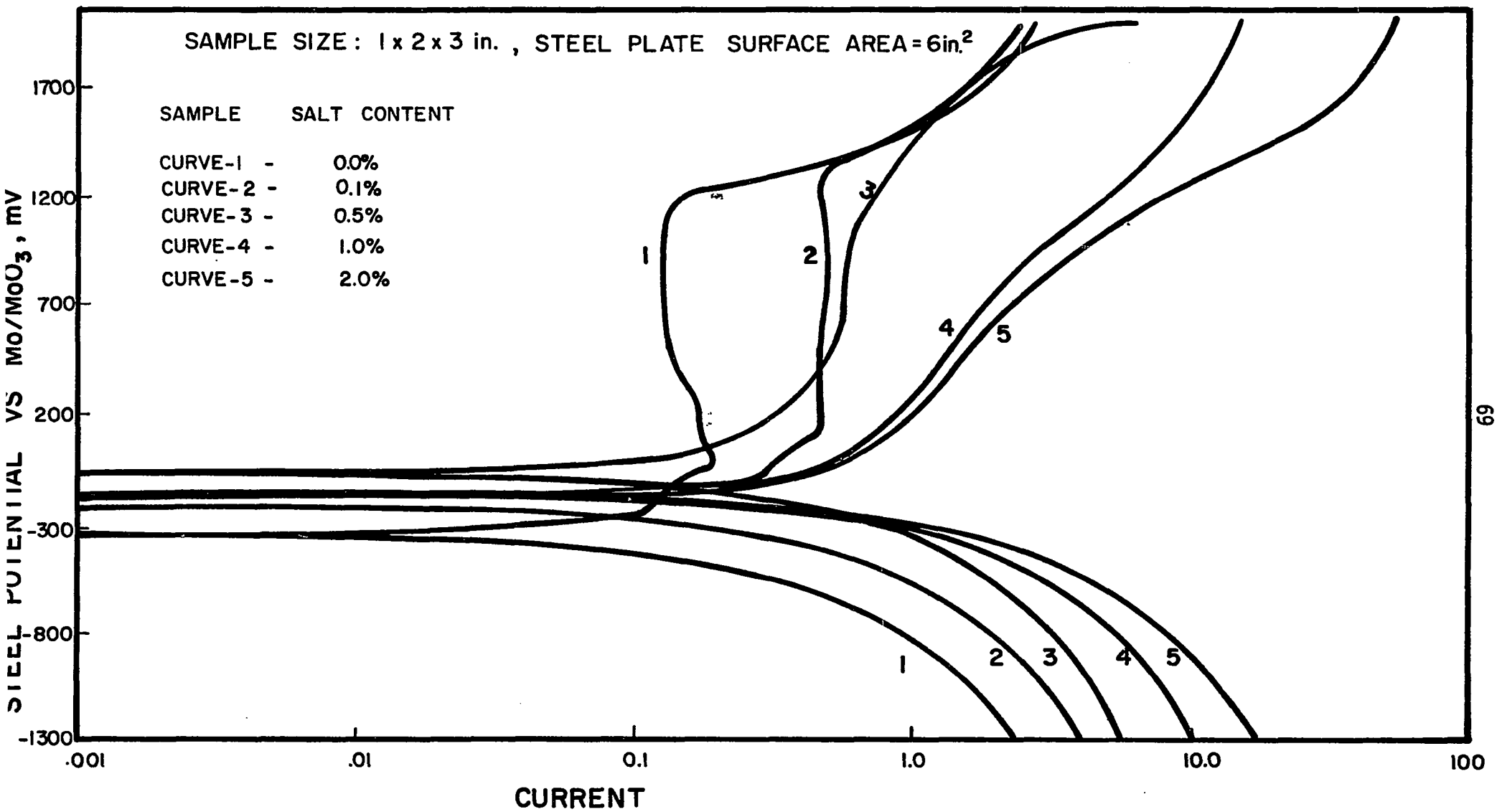

FIG. 21. POTENTIODYNAMIC ANODIC POLARIZATION OF STEEL PLATE IN TYPE V PORTLAND CEMENT CONCRETE CONTAINING VARIOUS PERCENTAGES OF SALT (NACL). SAMPLES WERE IN DISTILLED WATER FOR 300 DAYS. [SWEEP RATE = 0.28 MV/SEC.]

of Type V Portland cement with zero and 0.1% salt content. The anodic polarization curves also indicate that the steel will remain in a passive state for the samples of Type I Portland cement with a salt content up to 0.1% but up to 0.5% for the samples of Type V Portland cement. These results were repeated in the potentiodynamic anodic polarization curves. (See Figures 19 and 21).

Figure 22 represents the potentiodynamic anodic and cathodic polarization curves for a platinum plate in 0.5, 1, and 2% salt-contaminated concrete of Type I Portland cement. (The samples had been in distilled water for 45 days.) A break occurred at the potentials about 500 to 750 mv versus the Mo/MoO_3 electrode for the anodic and about -500 to -800 mv for the cathodic polarization curves. This was the same potential range indicated by the samples with the steel plate.

Figure 23 is a plot of steel potential versus salt content for the samples of Type I and V Portland cement exposed to distilled water for 90 to 170 days. The potentials of the steel plate in Type I Portland cement samples shifted toward a more positive value for 0.1% salt content, then toward more negative values for higher salt concentrations. The exposure time to distilled water (from 90 to 170 days) for the samples of Type I Portland cement caused a little shift in steel potential for the samples containing salt content up to 1%, but this shift was higher for samples with 2% salt content.

The potentials of steel in Type V Portland cement shifted toward more negative values as the salt concentration increased except for the sample with 1% salt which has been exposed to distilled water for 170 days. The exposure time to distilled water had a little effect

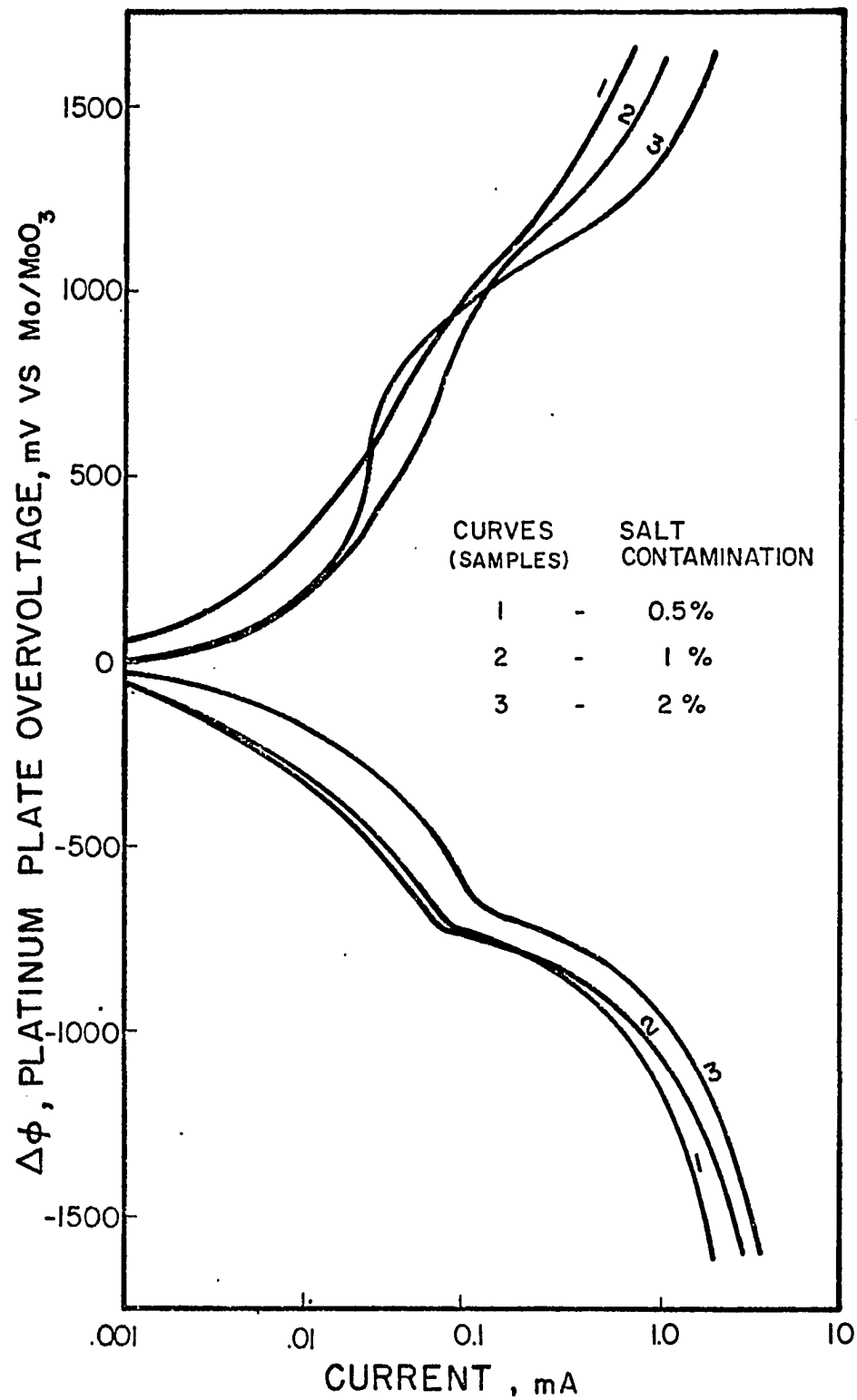

FIG. 22. POTENTIODYNAMIC ANODIC AND CATHODIC POLARIZATION OF PLATINUM PLATE IN TYPE I PORTLAND CEMENT CONTAINING VARIOUS PERCENTAGES OF SALT (NACL). THE SAMPLES HAVE BEEN SOAKED IN DISTILLED WATER FOR 35 DAYS.

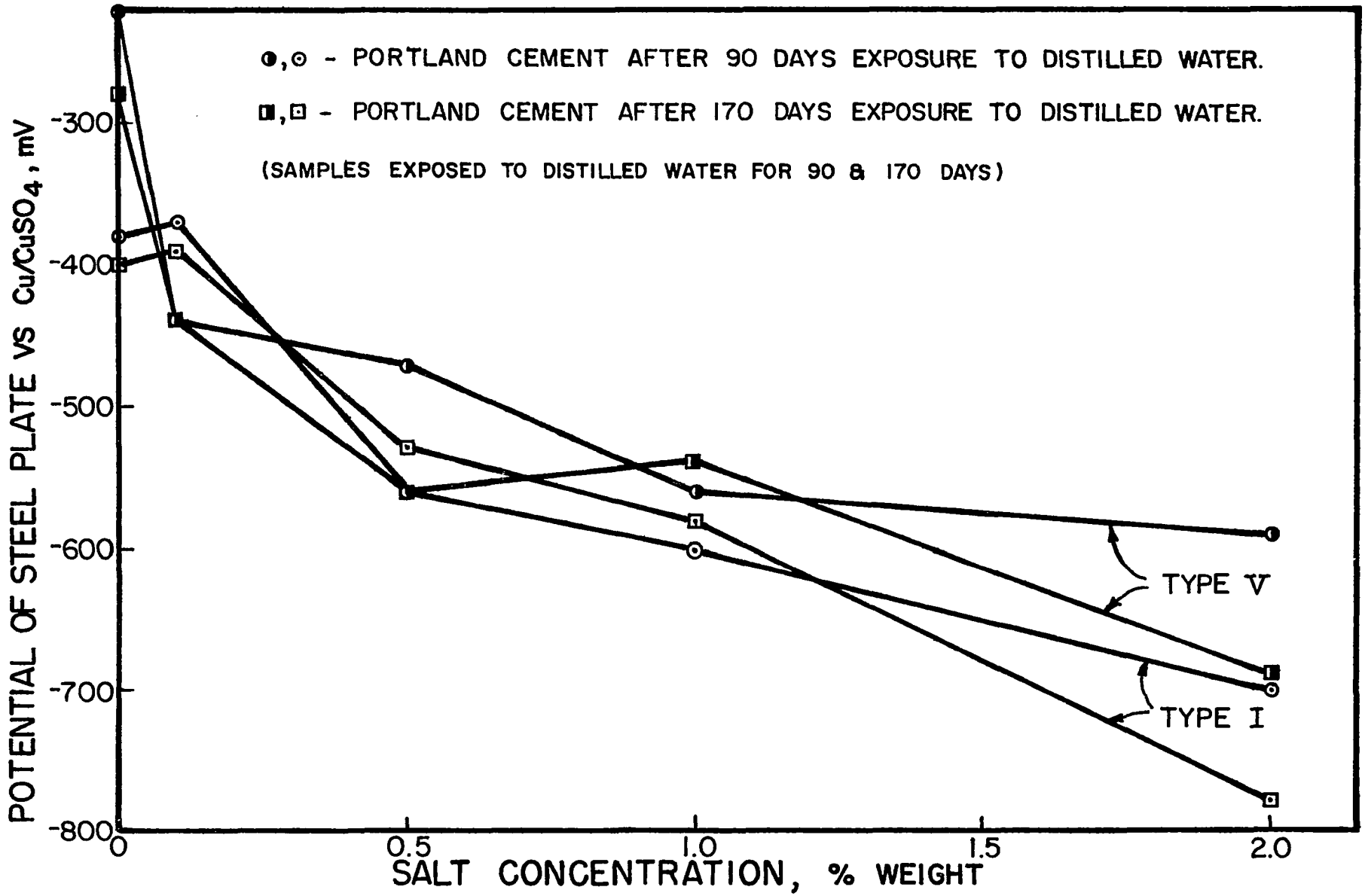

FIG. 23. CORROSION POTENTIAL OF STEEL AS A FUNCTION OF SALT CONTENT IN TYPE I AND V PORTLAND CEMENT CONCRETE.

on the potential for the samples of Type V Portland cement up to 1% salt content, but it had a significant effect for the sample with 2% salt content.

4.3 Samples in Salt Solutions

No salt was mixed with the samples described in this section. Figure 24 presents the anodic and cathodic potentiostatic polarization of steel in Type I Portland cement. (The samples had been exposed to the various salt solutions for 90 days.) The result indicates that the anodic and cathodic current density requirements increase as the salt concentration of the solution increases. A break in the cathodic polarization curves was also observed. There was no break in the anodic and cathodic polarization curves for the sample exposed to distilled water.

Figure 25 represents the anodic and cathodic potentiostatic polarization curves for the samples of Type V Portland cement. (The samples had been exposed to the various salt concentrated solutions for 90 days.) The data indicates that the anodic current density requirements increase as the salt concentration of the solution increases. The cathodic curves show that the samples exposed to the salt solutions require more current density than the sample exposed to distilled water but the current density requirements for the samples exposed to the various salt solutions are approximately the same. A break in the cathodic polarization curves for the samples placed in the salt solutions was observed at the same potentials mentioned for the samples with salt content exposed to distilled water.

A comparison of Figures 24 and 25 indicates that, in general, the anodic and cathodic current density requirements for the samples of

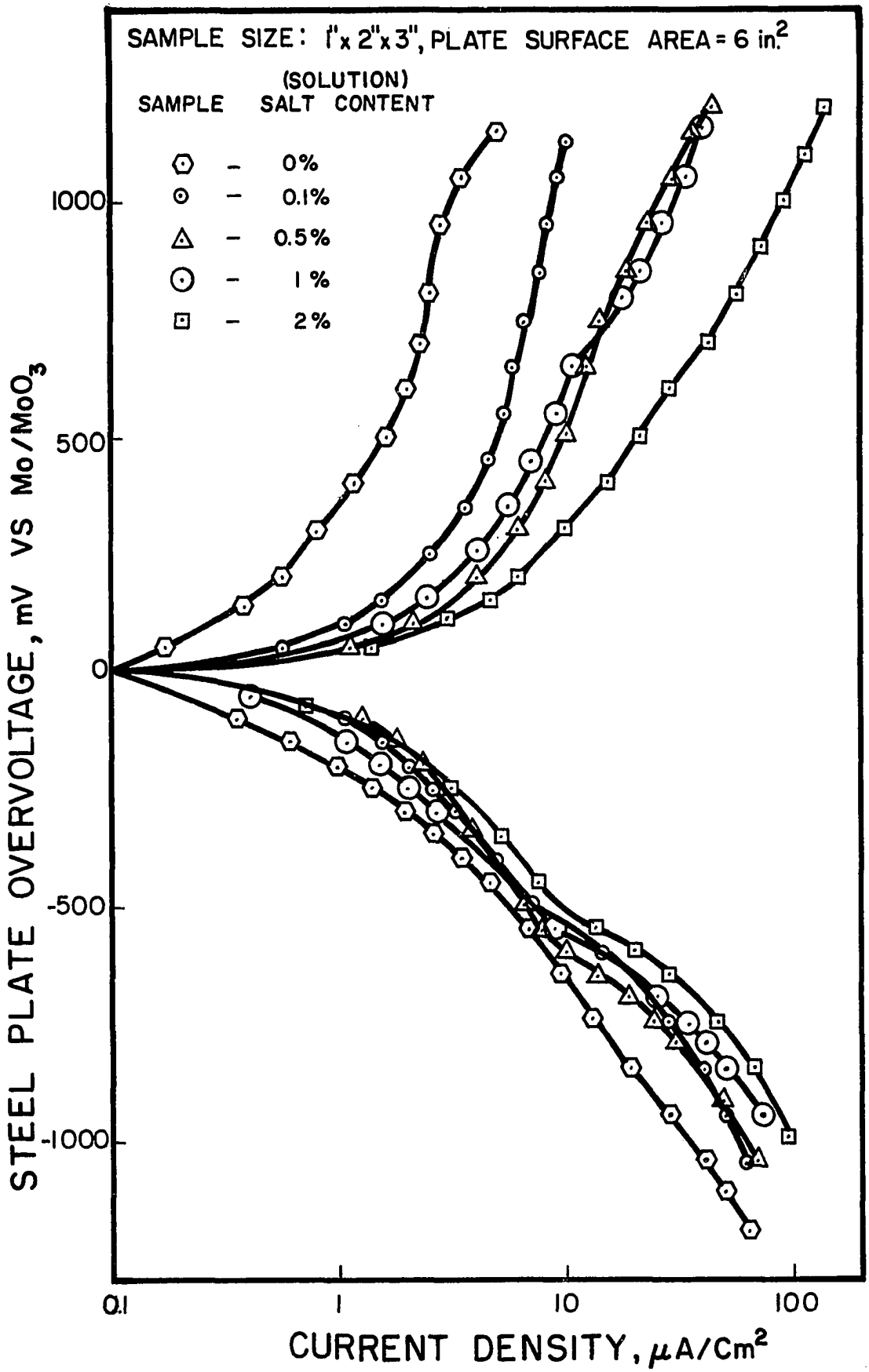

FIG. 24. ANODIC AND CATHODIC POLARIZATION OF STEEL PLATE IN CONCRETE SAMPLE OF TYPE I PORTLAND CEMENT. SAMPLES WERE IN VARIOUS SALT CONTAMINATED SOLUTIONS FOR 90 DAYS.

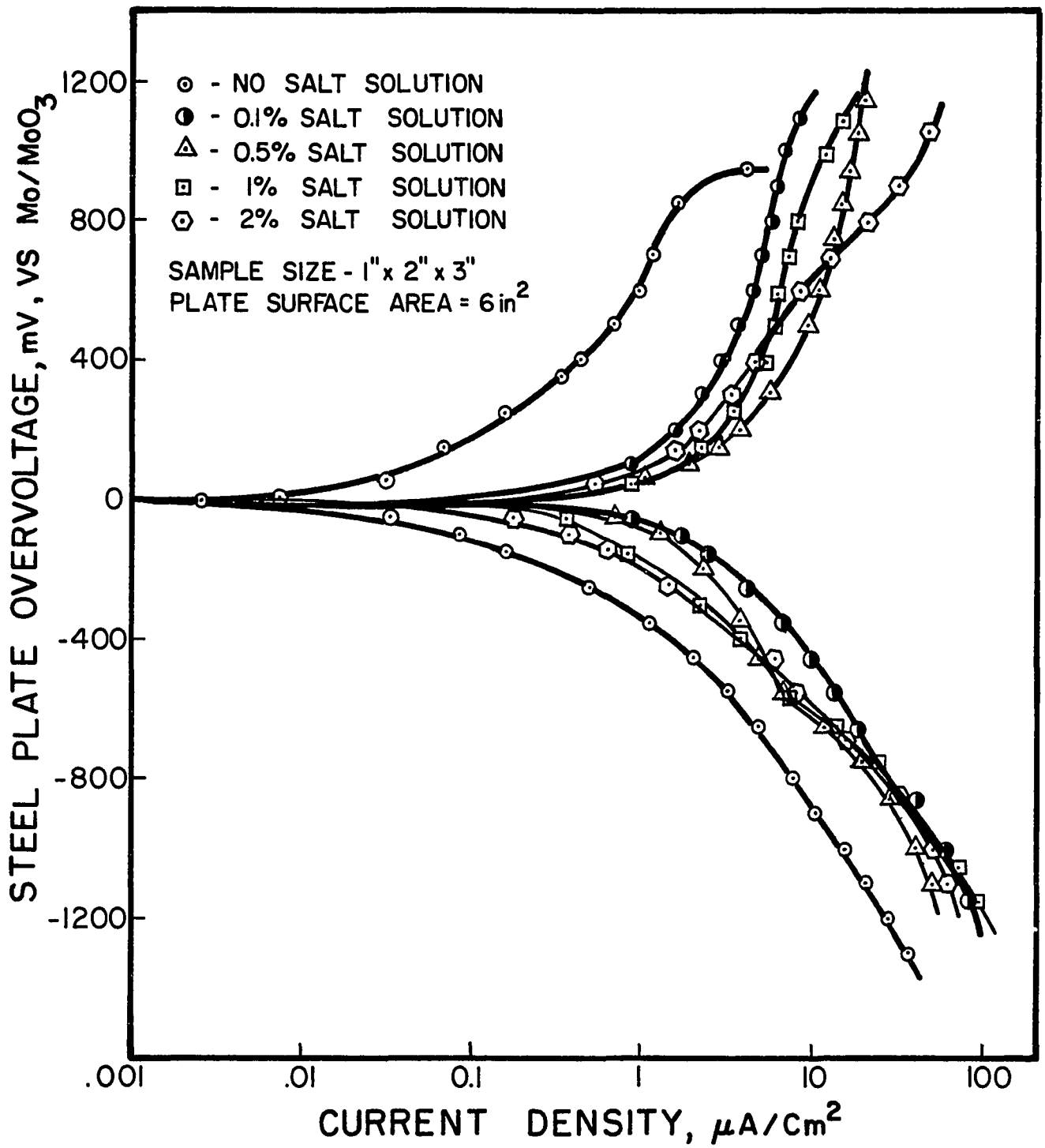

FIG. 25. ANODIC AND CATHODIC POLARIZATION OF STEEL IN TYPE V PORTLAND CEMENT CONCRETE IN VARIOUS SALT CONCENTRATED SOLUTIONS. THE CONCRETE SAMPLES WERE IN SALT SOLUTION FOR 90 DAYS.

Type I Portland cement soaked in the salt solutions are higher than for the samples of Type V Portland cement exposed to the same salt solutions.

Figure 26 presents the anodic and cathodic potentiostatic polarization curves for Type I Portland cement. (The samples had been soaked in various salt-concentrated solutions for 170 days.) These curves show that the current density requirements increase as the salt concentration of the solutions increases. Anodic polarization curves indicated a passivity for the steel only on the sample exposed to zero salt solution. This result was also found in Figure 27 for the potentiodynamic anodic polarization. (The samples had been soaked in salt-concentrated solutions for 300 days.) The results also indicate that the region of passivity was much greater for the sample soaked in distilled water than for the sample in 0.1% salt solution.

Figure 28 represents the anodic and cathodic potentiostatic polarization curves of steel in Type V Portland cement. (The samples had been soaked in various salt-concentrated solutions for 170 days.) The result indicates that the current density requirements increase as the salt content of the solution increases. A significant variation in current density was observed for the samples exposed to salt solutions, compared to the samples exposed to distilled water. The steel was passivated only in the samples exposed to no salt solutions. Figure 29, which represents the potentiodynamic polarization curves, indicated the same result. (The samples had been exposed to salt solution for 300 days.)

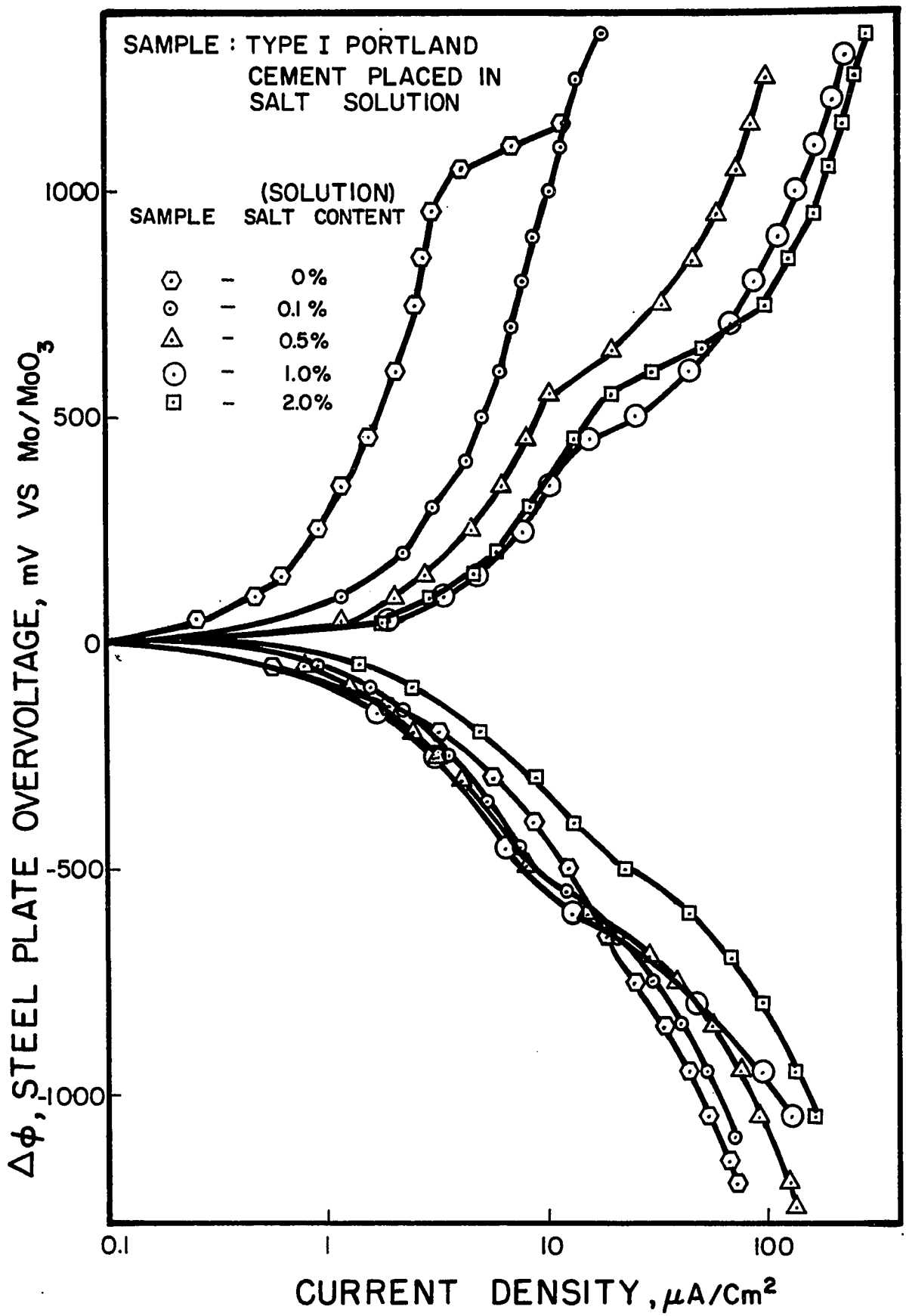

FIG. 26. ANODIC AND CATHODIC POLARIZATION OF STEEL IN TYPE I PORTLAND CEMENT CONCRETE. THE CONCRETE SAMPLES WERE IN VARIOUS SALT CONTAMINATED SOLUTIONS FOR 170 DAYS.

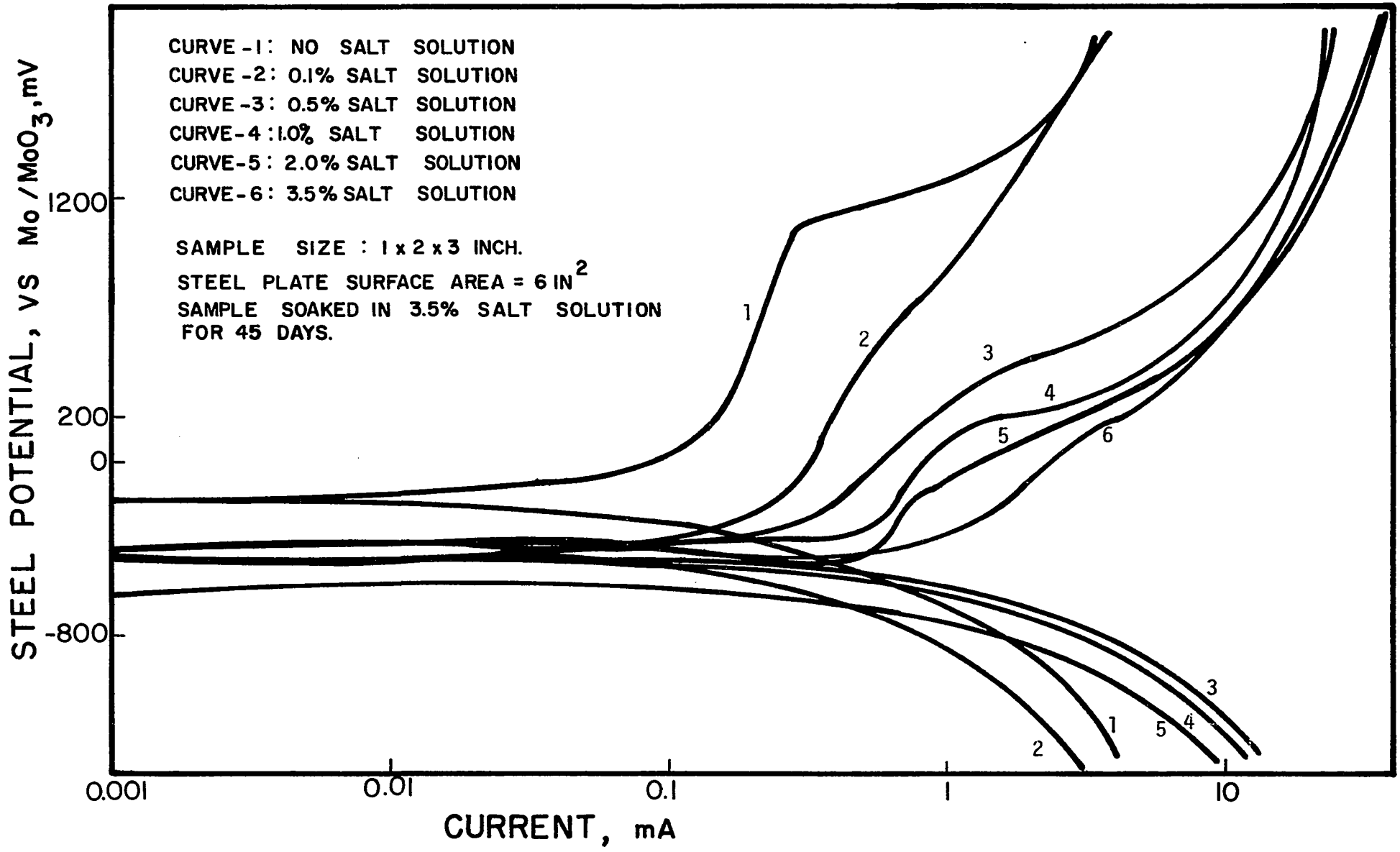

FIG. 27. POTENTIO — DYNAMIC ANODIC POLARIZATION OF STEEL PLATE IN TYPE I PORTLAND CEMENT CONCRETE PLACED IN VARIOUS SALT CONCENTRATED SOLUTIONS FOR 300 DAYS. (SWEEP RATE - 0.28 mV/S)

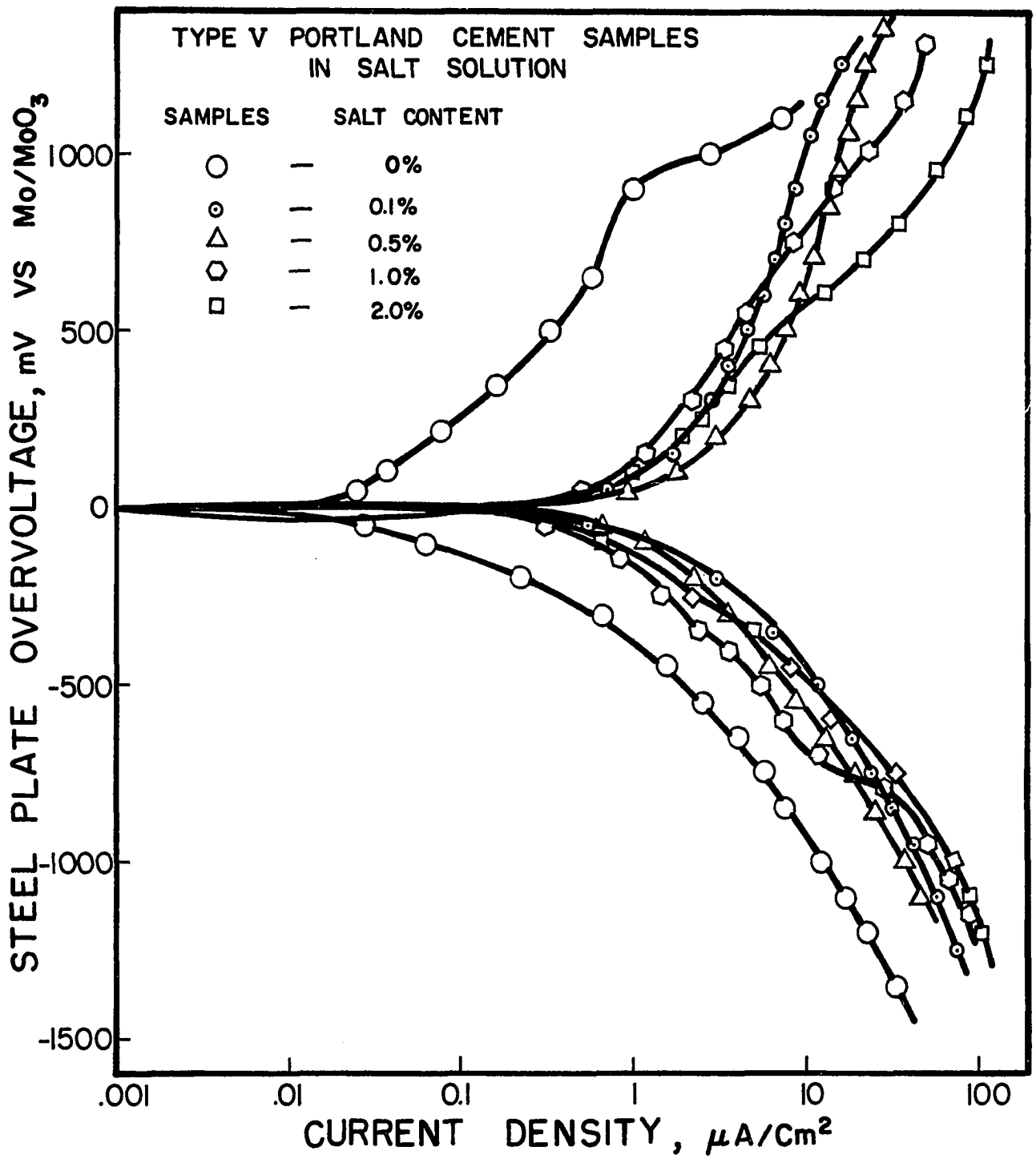

FIG. 28. ANODIC AND CATHODIC POLARIZATION OF STEEL IN TYPE V PORTLAND CEMENT CONCRETE. THE CONCRETE SAMPLES WERE IN VARIOUS SALT CONTAMINATED SOLUTIONS FOR 170 DAYS.

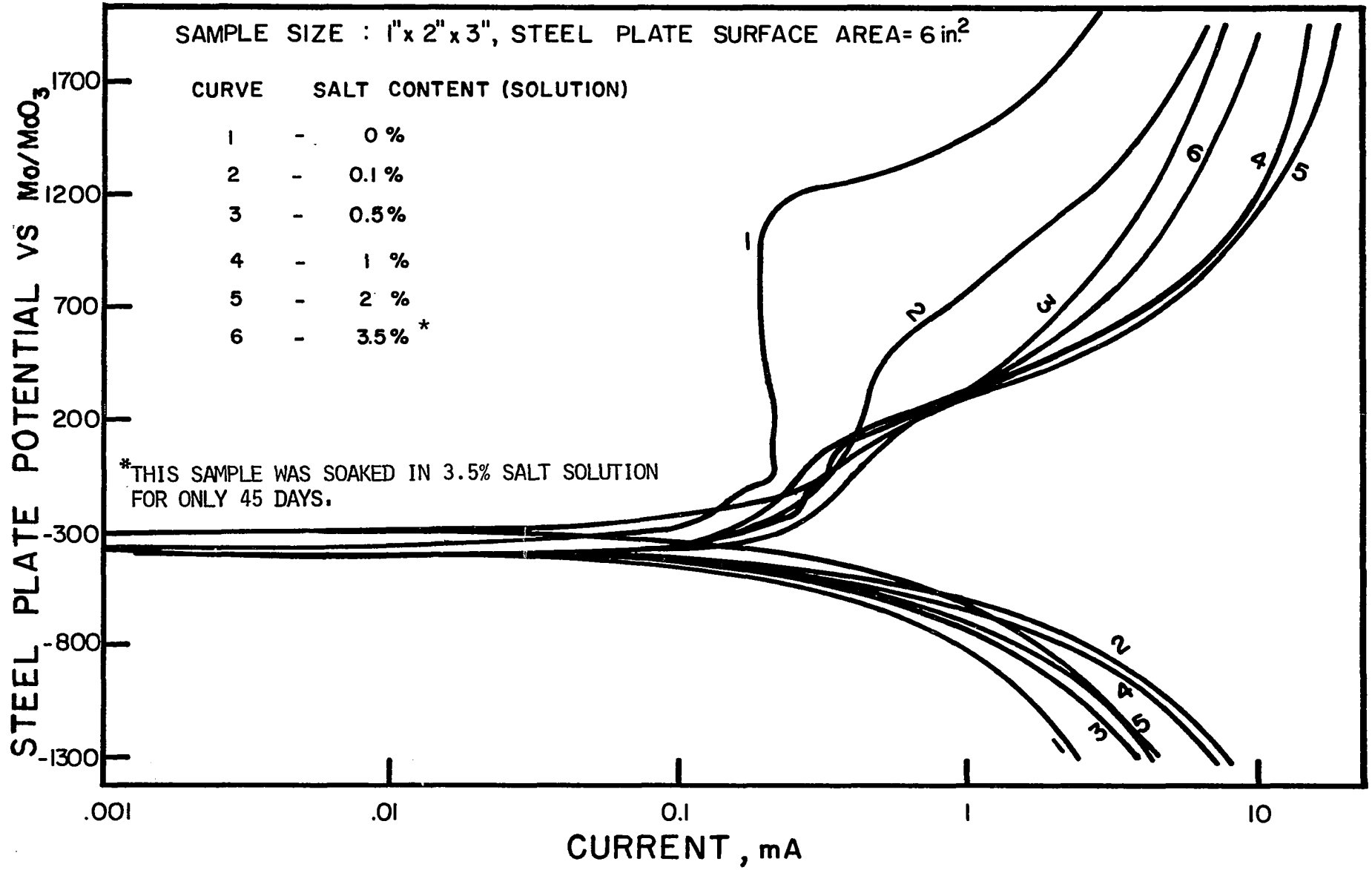

FIG. 29. POTENTIODYNAMIC ANODIC POLARIZATION OF STEEL PLATE IN TYPE V PORTLAND CEMENT CONCRETE PLACED IN VARIOUS SALT CONCENTRATED SOLUTIONS FOR 300 DAYS. [SWEEP RATE = 0.28 MV/SEC.]

A comparison of Figures 26 and 28 indicates that the anodic and cathodic current density requirements for the samples exposed to the salt solutions, compared to the samples soaked in distilled water, are higher for Type I than for Type V Portland cement.

Figure 27 indicates that the anodic current requirements for steel in the sample of Type I Portland cement exposed to 3.5% salt solution for 45 days are about the same as for the samples exposed to 0.5, 1, and 2% salt solutions but higher than for the samples exposed to zero and 0.1% salt solutions for 300 days. Figure 29 also indicates that the anodic current requirement for steel in Type V Portland cement exposed to 3.5% salt solution for the period of 45 days is higher than for the samples exposed to 0.1 and 0.5% salt solutions but lower than that for the samples exposed to 1 and 2% salt solutions for 300 days.

Figure 30 indicates that the anodic current density of steel in Type I and V Portland cement exposed to salt solutions increases as the salt content and exposure time to salt solution increases.

A comparison of Figures 27 and 29 indicates that the salt penetrates at a much faster rate for the samples of Type I Portland cement exposed to the salt solutions ranging from 0.1 up to 3.5% than for Type V exposed to the same solutions. (See also Figure 30.)

A comparison of Figures 24 and 26 indicates that the exposure time to salt solutions has a significant effect on the increase of anodic and cathodic current density for Type I Portland cement. (See also Figure 30.)

No break in the anodic polarization curves was seen for the samples soaked in 0.5, 1, and 2% salt solutions for 90 days, but a break

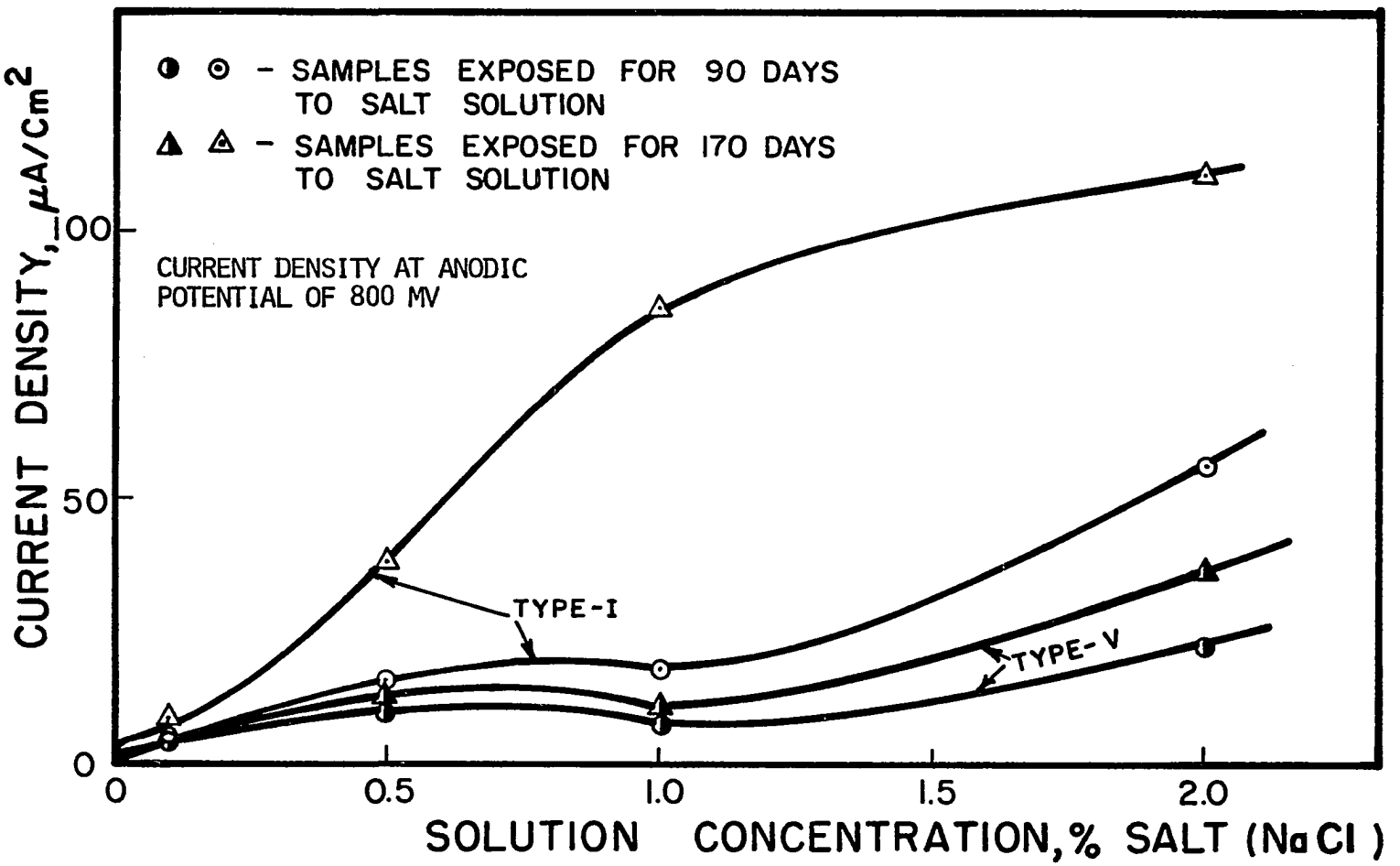

FIG. 30. PRESENTS THE ANODIC CURRENT DENSITY AS A FUNCTION OF SALT CONCENTRATED SOLUTIONS FOR TWO DIFFERENT TIME OF EXPOSURE.

was observed after 170 days of exposure at the same potentials as mentioned for the samples with salt content exposed to distilled water.

A comparison of Figures 25 and 28 indicates that the exposure time to the salt solutions (for a period of 90 to 170 days) has a fairly small effect on the anodic and cathodic current density requirements for the samples of Type V Portland cement.

Figure 31 presents the differential anodic current density at the potential of 800 mv (with respect to a Mo/MoO_3 electrode) as a function of the salt-concentrated solution. The differential anodic current density was determined by subtracting the anodic current density requirement at +800 mv for the samples of Types I and V Portland cement concrete exposed to distilled water from the current density requirement for the samples of Types I and V exposed to solutions with various salt concentrations at the same potential (+800 mv). Figure 31 also presents the current, calculated by the diffusion process equation (see Appendix B). The result in Figure 31 indicates that the differential anodic current increases as the salt content of the solution increases. The current calculated by the diffusion process increases linearly with the increase of the salt content in the solution.

Figure 32 is a plot of the steel potential in Types I and V Portland cement samples exposed to various salt-concentrated solutions for 90 to 170 days. The potentials of steel in Type I Portland cement shifted toward more negative values as the salt concentration of the solutions increased except for the samples exposed to a 0.5% salt solution. The shift in potential for the samples exposed to 0.1, 0.5, and 1% salt solutions after 90 days was constant. There was no significant

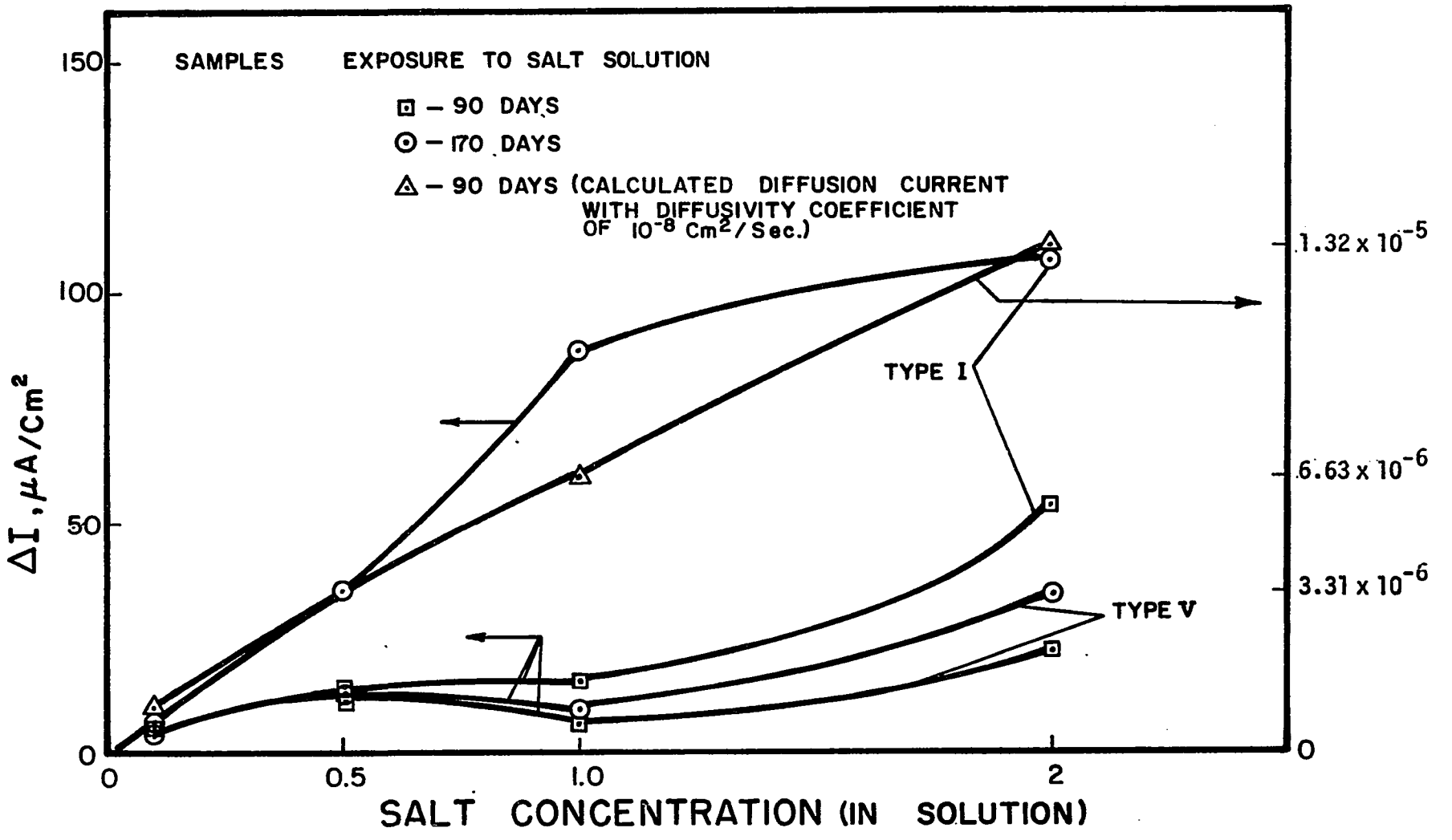

FIG. 31. DIFFERENTIAL ANODIC CURRENT DENSITY CAUSED BY CHLORIDE IONS AT POTENTIAL OF +800 MV VS Mo/MoO_3 ELECTRODE. THE CURRENT CALCULATED BY THE CHLORIDE DIFFUSION PROCESS IS ALSO SHOWN. THE CONCRETE SAMPLES OF TYPE I AND V PORTLAND CEMENT WERE EXPOSED TO VARIOUS SALT SOLUTIONS FOR A PERIOD OF 90 TO 170 DAYS.

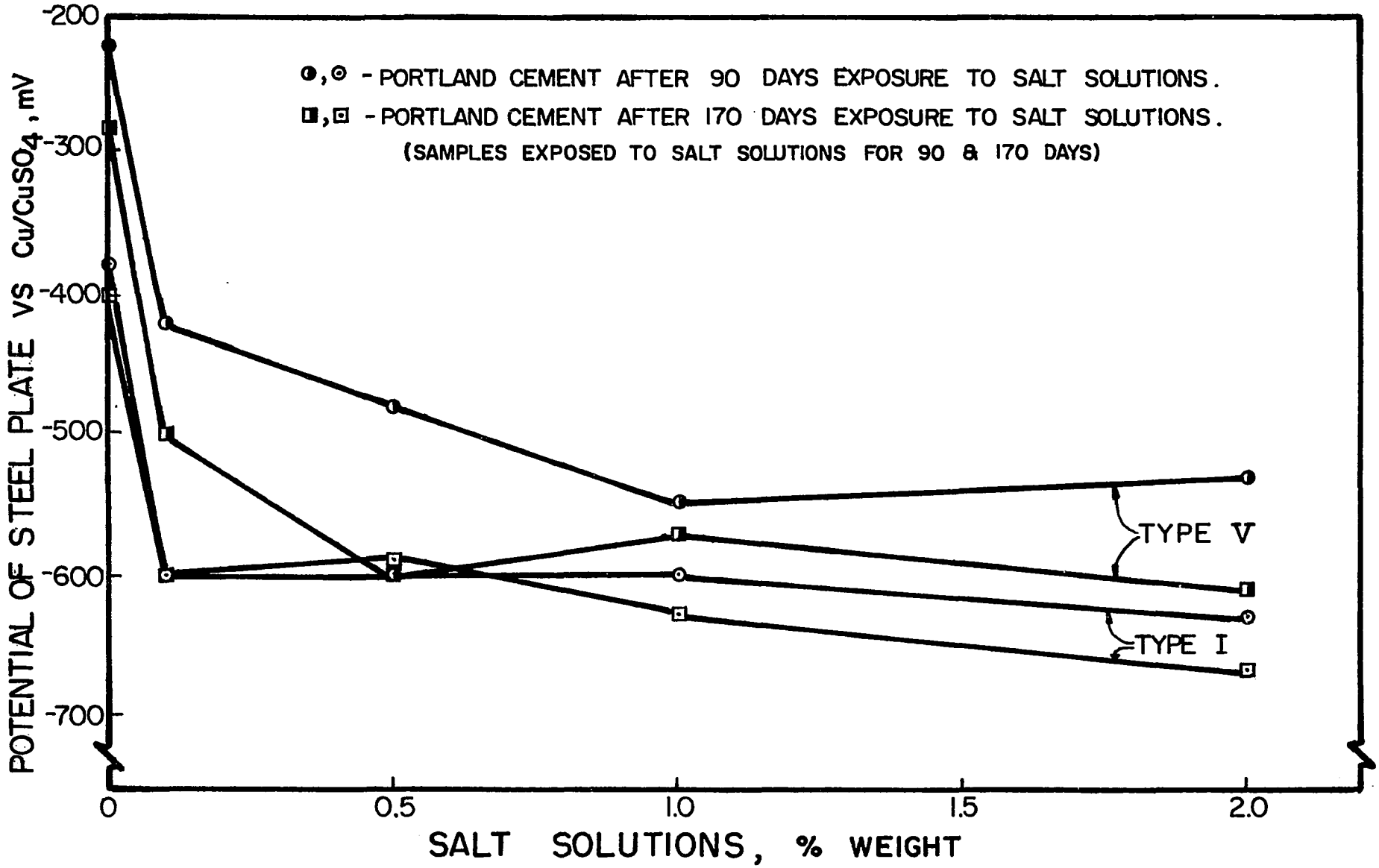

FIG. 32. CORROSION POTENTIAL OF STEEL IN TYPE I AND V PORTLAND CEMENT CONCRETE SAMPLES EXPOSED TO VARIOUS SALT CONCENTRATED SOLUTIONS. SAMPLES WERE EXPOSED TO SALT SOLUTIONS FOR 90 AND 170 DAYS.

shift in potentials for samples exposed to salt solutions with a salt concentration lower than 1%, but an appreciable potential shift was observed for the samples exposed to 1 and 2% salt solutions.

The potentials of steel in Type V Portland cement samples also shifted toward the negative direction as the salt concentration of the solutions was increased, except for the sample exposed to 1% salt solution for 170 days. The exposure time to salt solutions (from 90 to 170 days) for the samples of Type V Portland cement had a significant effect on the steel potential.

Figure 33 presents the potentiodynamic cathodic polarization of steel with and without IR drop compensation in 2% salt-contaminated concrete of Type V Portland cement. In this test, the potential of the steel was controlled by the Mo/MoO_3 electrode embedded adjacent to the steel plate. The result indicates no change in the Tafel slope of the polarization curves and a very small shift in the current requirements (see curves 1 and 2 in Figure 33). Figure 34 also represents the potentiodynamic polarization of steel with and without IR drop compensation in 2% salt-contaminated concrete of Type V Portland cement. In this experiment, the potential of the steel plate was controlled by an external $Cu/CuSO_4$ reference electrode. The data indicates no significant change in the Tafel slope, but a small shift in the current requirements (see curves 1 and 2 in Figure 34).

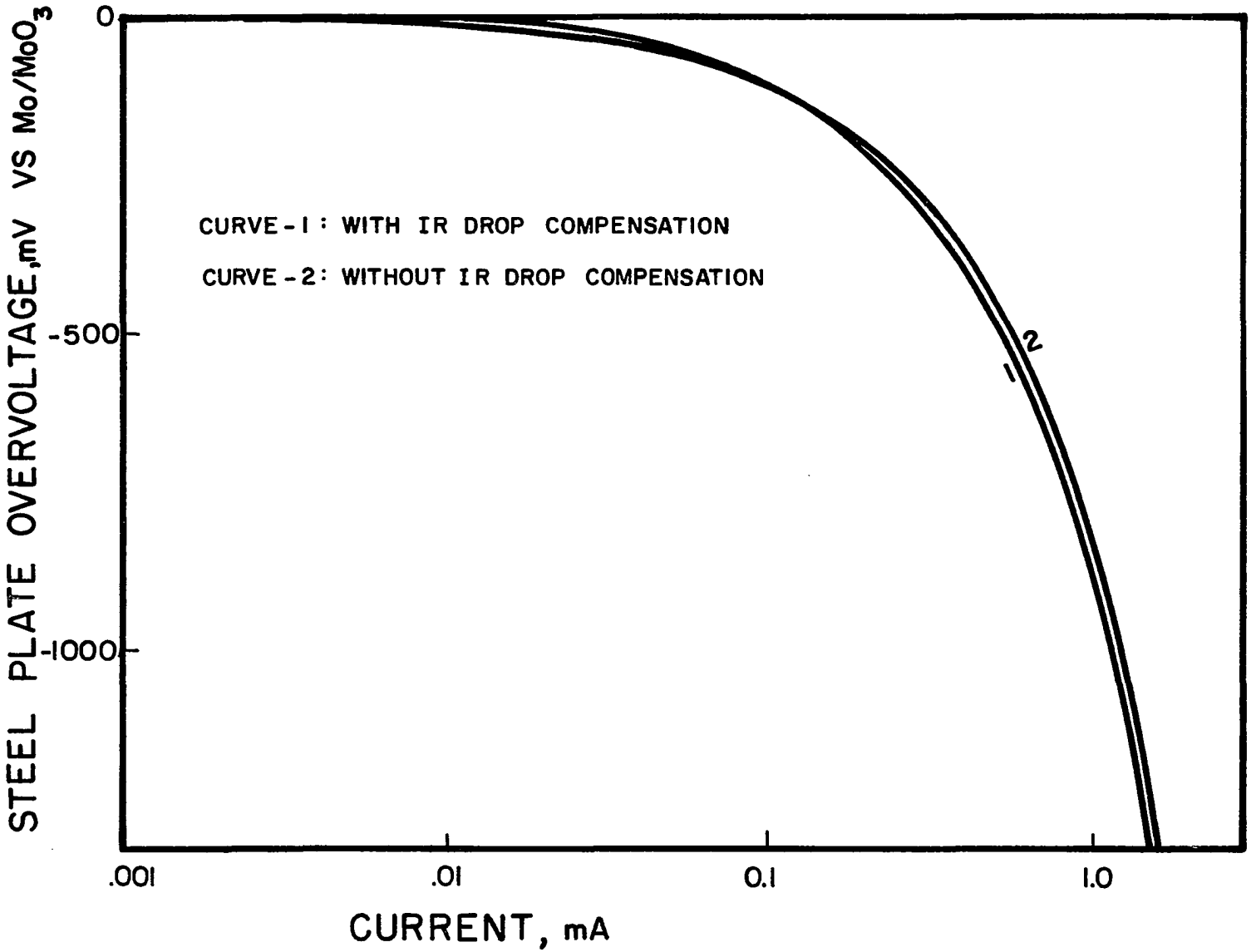

FIG. 33. POTENTIODYNAMIC CATHODIC POLARIZATION OF STEEL PLATE WITH AND WITHOUT IR DROP COMPENSATION COMPARED TO Mo/MoO_3 ELECTRODE IN 2% SALT CONTAMINATED CONCRETE OF TYPE V PORTLAND CEMENT. CONCRETE SAMPLE WAS IN DRY CONDITION OF LABORATORY FOR 300 DAYS.

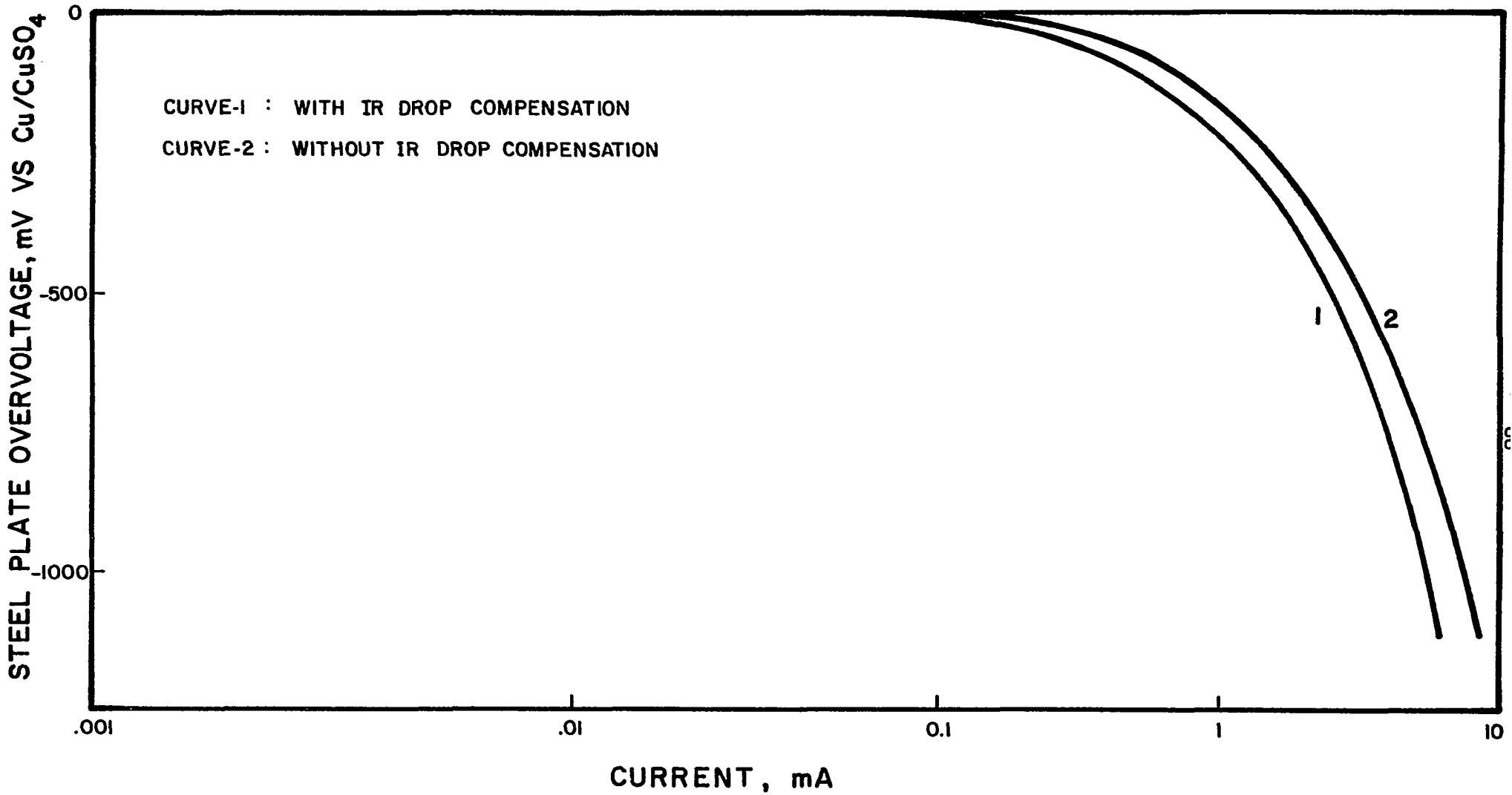

FIG. 34. CATHODIC POLARIZATION OF STEEL PLATE COMPARED TO $Cu/CuSO_4$ ELECTRODE WITH AND WITHOUT IR DROP COMPENSATION IN 2% SALT CONTAMINATED CONCRETE OF TYPE V PORTLAND CEMENT.

Effect of Steel Wire Mesh and Potential Measurement Error on Current and Potential

The results in this section will be divided into two parts, solution and concrete environments.

4.4 Solution

The potential measurements in the solution were made by saturated calomel reference electrodes. Luggin probes were used to reduce the IR drop in potential measurements.

4.4.1 Polarization of the Steel Plate.

4.4.1.1 The Wire Mesh was Between the Anode and Cathode with no Connection.

Figure 35 presents the anodic and cathodic polarization curves for the steel plate in a saturated calcium hydroxide [$Ca(OH)_2$] solution with the presence and the absence of a steel wire mesh. Different sizes of wire mesh were used to discover the effect of hole size in shielding the current. The cell assembly for this test is shown in Figure 7. The results indicate no significant differences in current density requirements with the wire mesh compared to those with no wire mesh.

4.4.1.2 The Wire Mesh was Connected to the Top and Bottom of the Steel Plate and Raised in an Arc About One Inch.

Figure 36 presents the anodic and cathodic polarization of the steel plate in a saturated $Ca(OH)_2$ solution when the wire mesh was connected to the top and bottom of the steel plate. The cell assembly for this experiment is shown in Figure 9. The results indicate that the cathodic current density does not change significantly with the wire mesh connected to the steel plate or without any wire mesh. The anodic

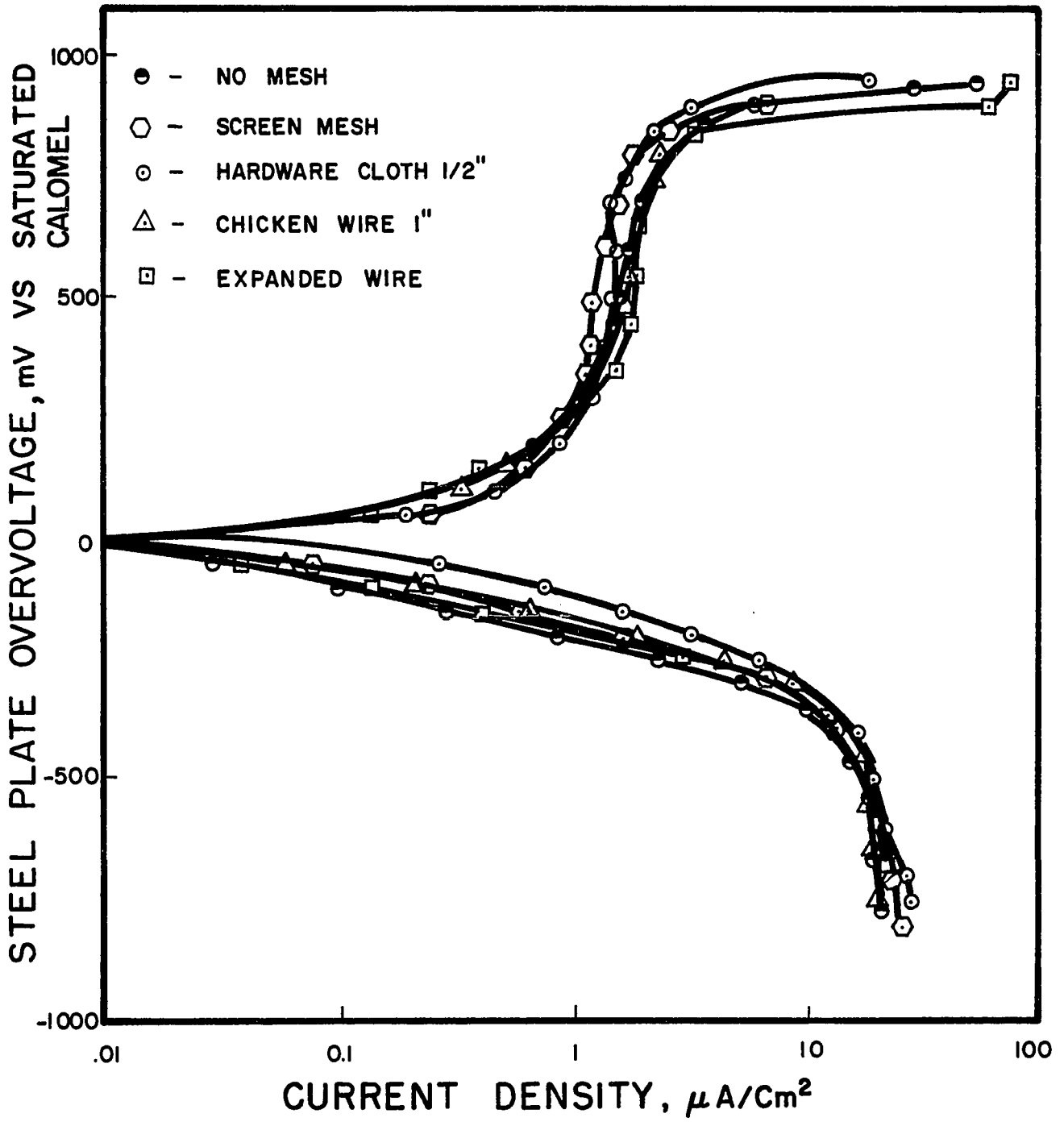

FIG. 35. ANODIC AND CATHODIC POLARIZATION OF STEEL IN SATURATED $CA(OH)_2$ SOLUTION WITH AND WITHOUT PRESENCE OF WIRE MESH (VARIOUS SIZES). WIRE MESH WAS PLACED BETWEEN ANODE AND CATHODE WITH NO CONTACT.

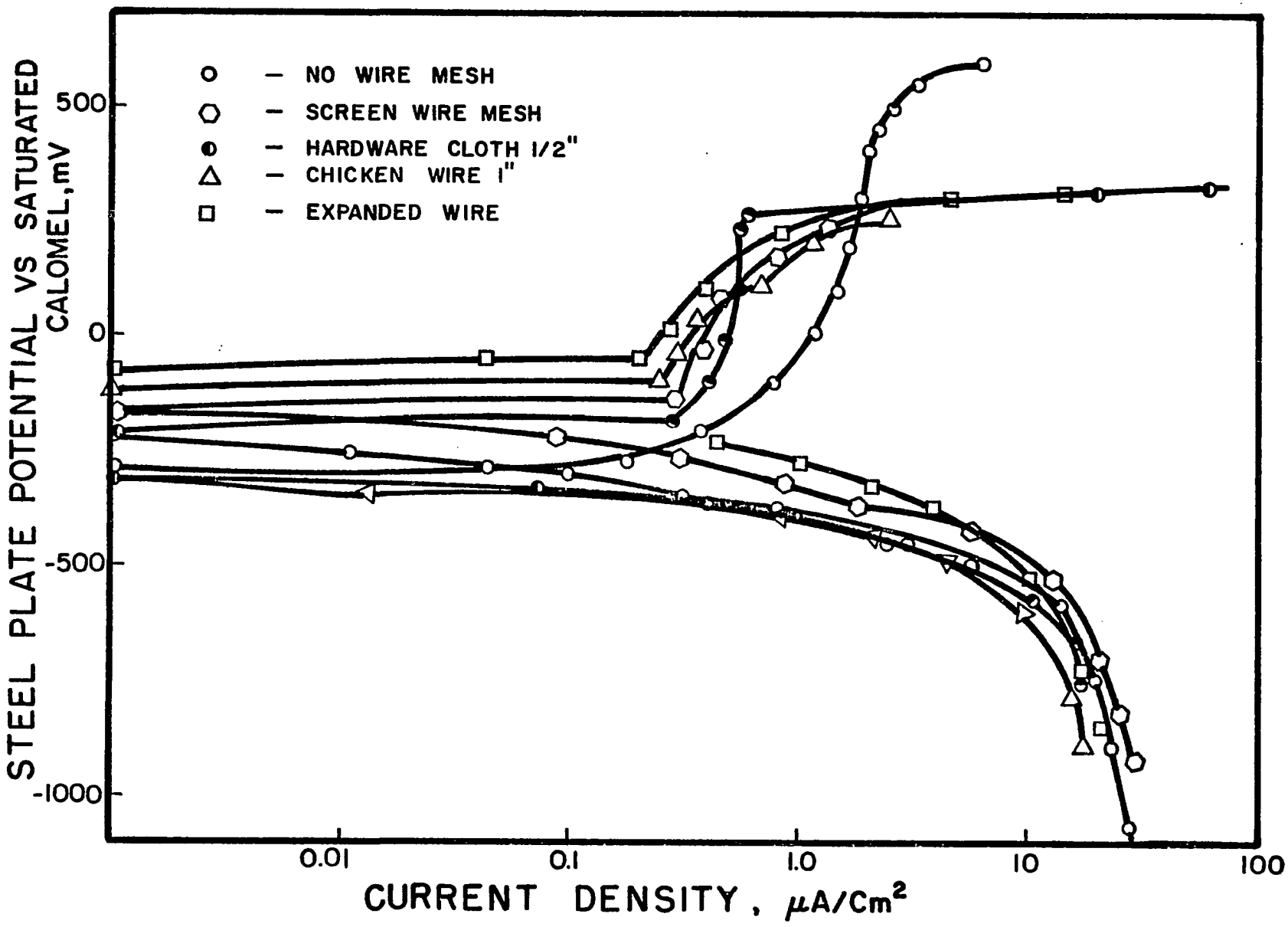

FIG. 36. ANODIC AND CATHODIC POLARIZATION OF STEEL IN SATURATED $CA(OH)_2$ SOLUTION WITH AND WITHOUT WIRE MESH (VARIOUS MESH SIZE) ATTACHED TO TOP AND BOTTOM OF STEEL PLATE, REST ABOUT 1" FROM PLATE.

curves show that the passive region is greater for the steel plate without any wire mesh than it is when the wire mesh is connected to the steel plate. The results also indicate that the anodic current density requirements for the steel without wire mesh are higher than when the wire mesh is connected to the plate. In calculating the current density for the case where the wire mesh was connected to the plates, the cell current was divided by the sum of the plate and wire mesh surface areas.

4.4.1.3 The Wire Mesh was Lying on the Steel Plate.

Figure 37 presents the anodic and cathodic polarization curves for the steel plate in a saturated $Ca(OH)_2$ solution when the wire mesh was lying on the plate. The cell assembly for this test is shown in Figure 8. The results show no significant differences in the cathodic current density for the steel plate with and without the wire mesh. The anodic polarization curves indicate that the passive region for the steel plate without the wire mesh is greater than when the wire mesh is present. In this test, the current density was calculated as the cell current divided by the sum of the plate and wire mesh surface areas (for the case where wire mesh was connected to the plate).

4.4.2 Shift in Wire Mesh Potential Because of the Passage of Current (The Wire Mesh was Between the Anode and Cathode.) Figure 38 shows that the potential of the wire mesh shifted with the polarization of the steel plate. The shift in wire mesh potential was toward the positive for the cathodic polarization and toward the negative for the anodic polarization of the steel plate.

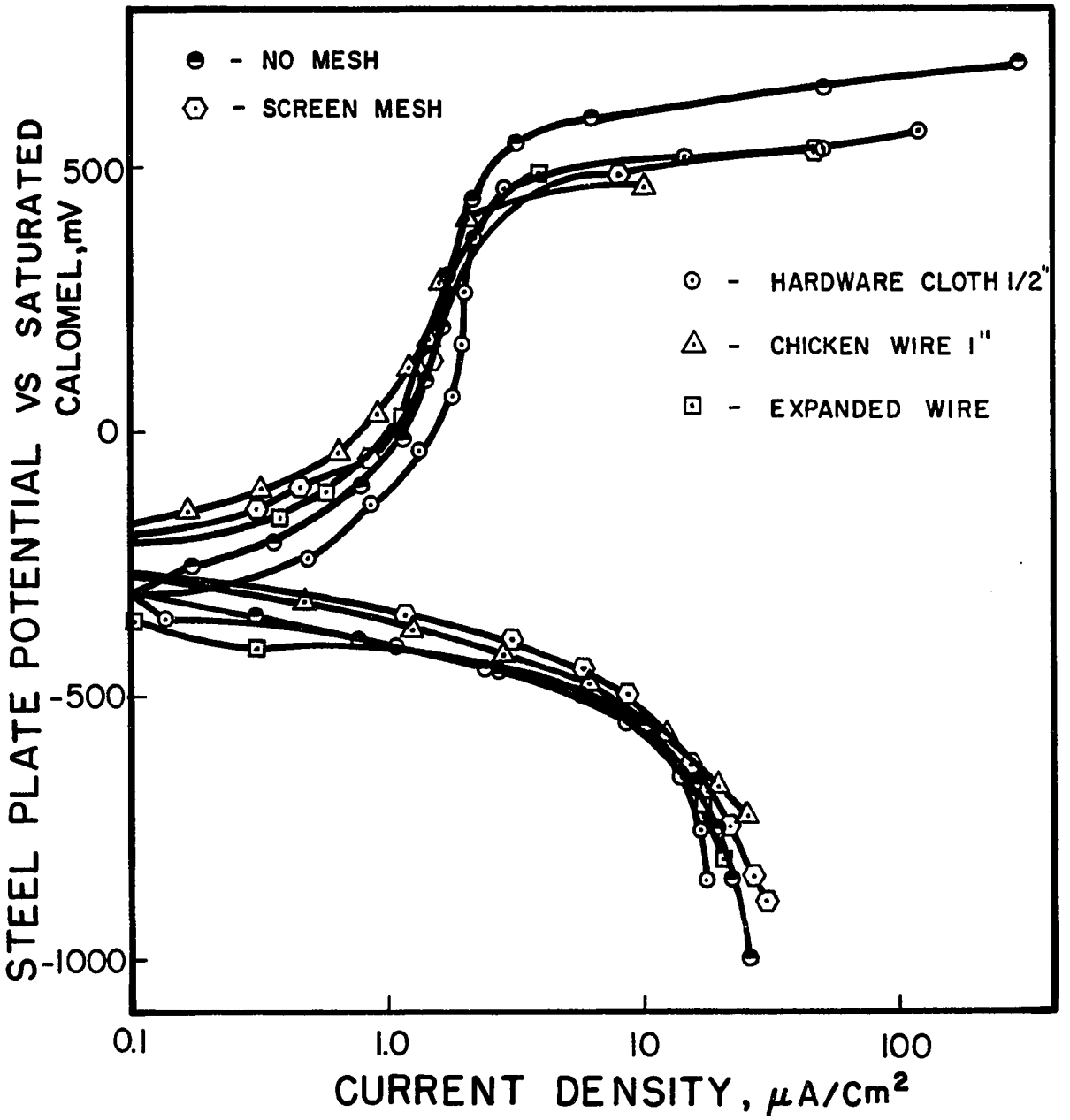

FIG. 37. ANODIC AND CATHODIC POLARIZATION OF STEEL IN SATURATED $CA(OH)_2$ SOLUTION WITH AND WITHOUT WIRE MESH (VARIOUS SIZES) LYING ON STEEL PLATE.

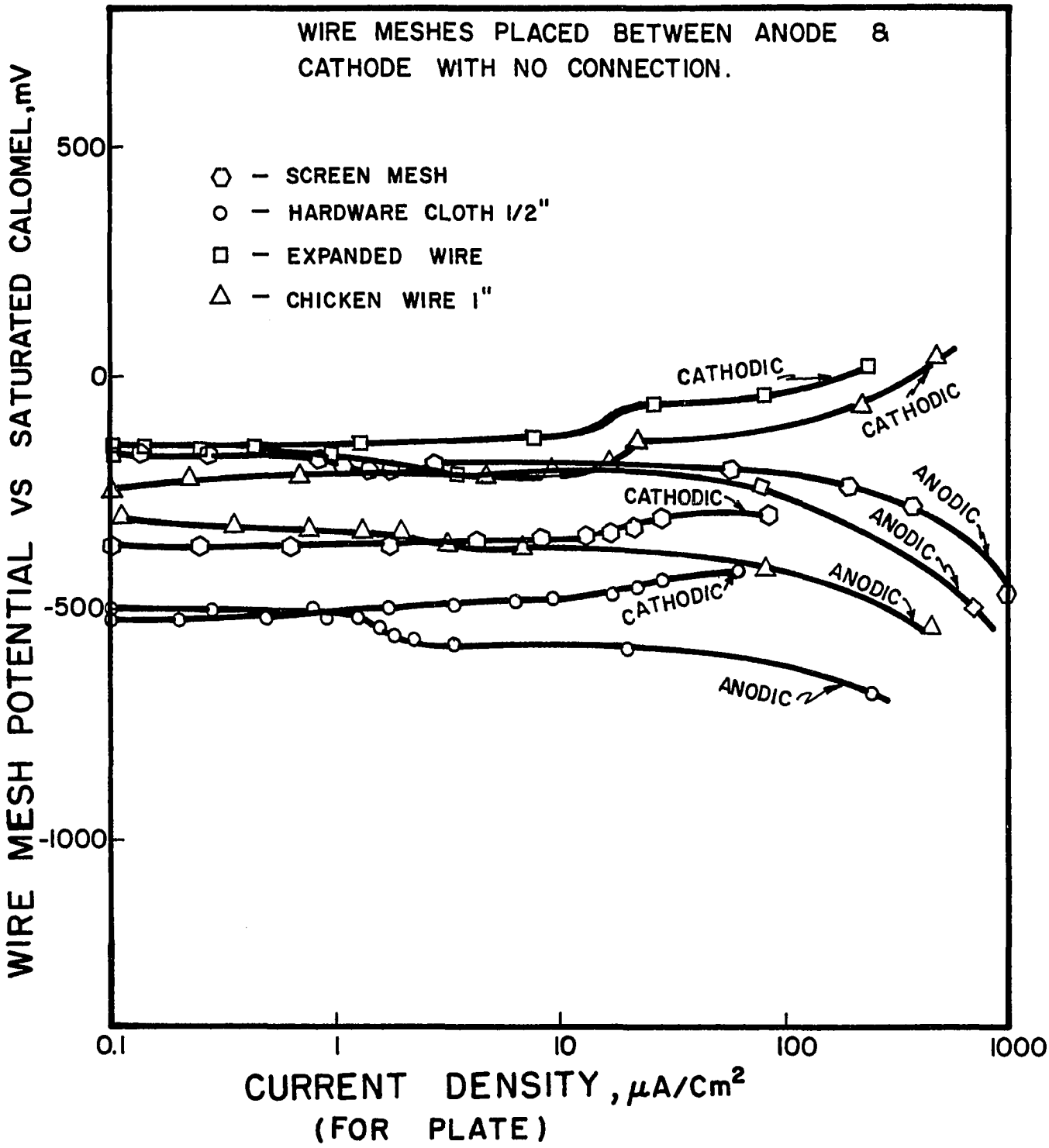

FIG. 38. POTENTIAL VARIATION OF WIRE MESH IN SATURATED $CA(OH)_2$ DURING ANODIC AND CATHODIC POLARIZATION OF STEEL PLATE.

4.4.3 Potential Shift of the Platinum Electrode as a Function of Distance Because of the Passage of Current (Platinum Plates were Between the Anode and the Cathode with no Connection.) The experimental set-up shown in Figure 10 was conducted to determine the potential gradient between anode and cathode. This experiment was conducted in 3% salt solution with five platinum electrodes. Two of these acted as anode and cathode and three were between the anode and the cathode. The potential of the three platinum electrodes between the anode and cathode was measured simultaneously during cathodic polarization. The results presented in Figure 39 indicate that the potential of these three platinum electrodes shifted toward more negative values as the cathodic current increased. Also, the potential shifted toward less negative values as the distance of platinum electrode from the cathode was increased (see also Figure 40). Figure 40 presents the shift in the potential of the platinum electrode as a function of distance from the cathode at three constant levels of current. The results indicate that the potential shift is not linear as a function of distance from the cathode.

4.5 Concrete

4.5.1 Polarization of the Steel Plate in the Presence of a Wire Mesh. Figure 41 presents the anodic and cathodic polarization of the steel plate with a wire mesh connected and disconnected to the plate (a cell assembly for this concrete sample is shown in Figures 3B and 4). The results indicate that the cathodic current density requirements for the sample with the wire mesh connected to the plate are higher than for the sample with no wire mesh. The opposite effect was found for samples

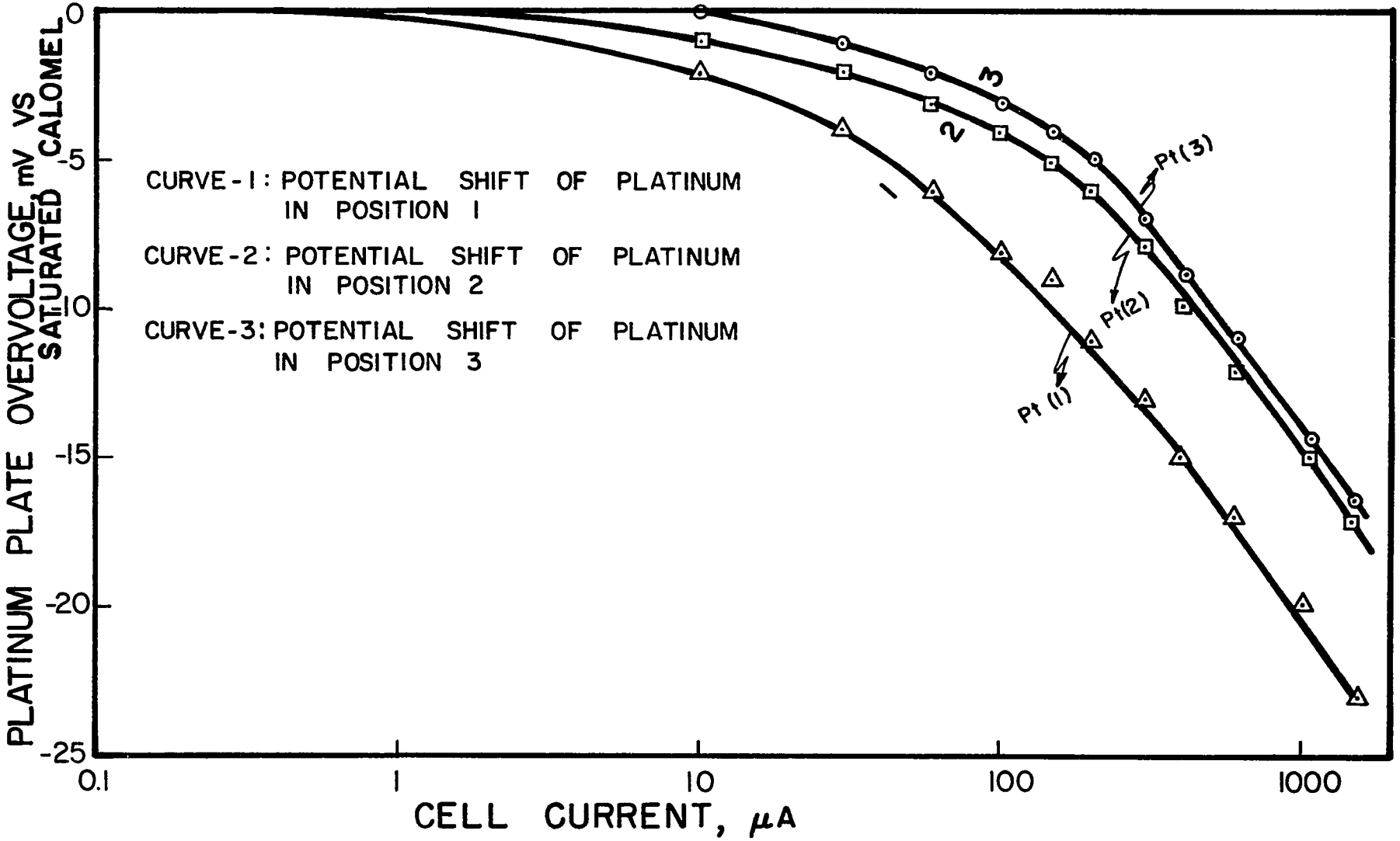

FIG. 39. POTENTIAL SHIFT OF PLATINUM ELECTRODES AS A RESULT OF CATHODIC POLARIZATION OF CATHODE IN 3% SALT SOLUTION.

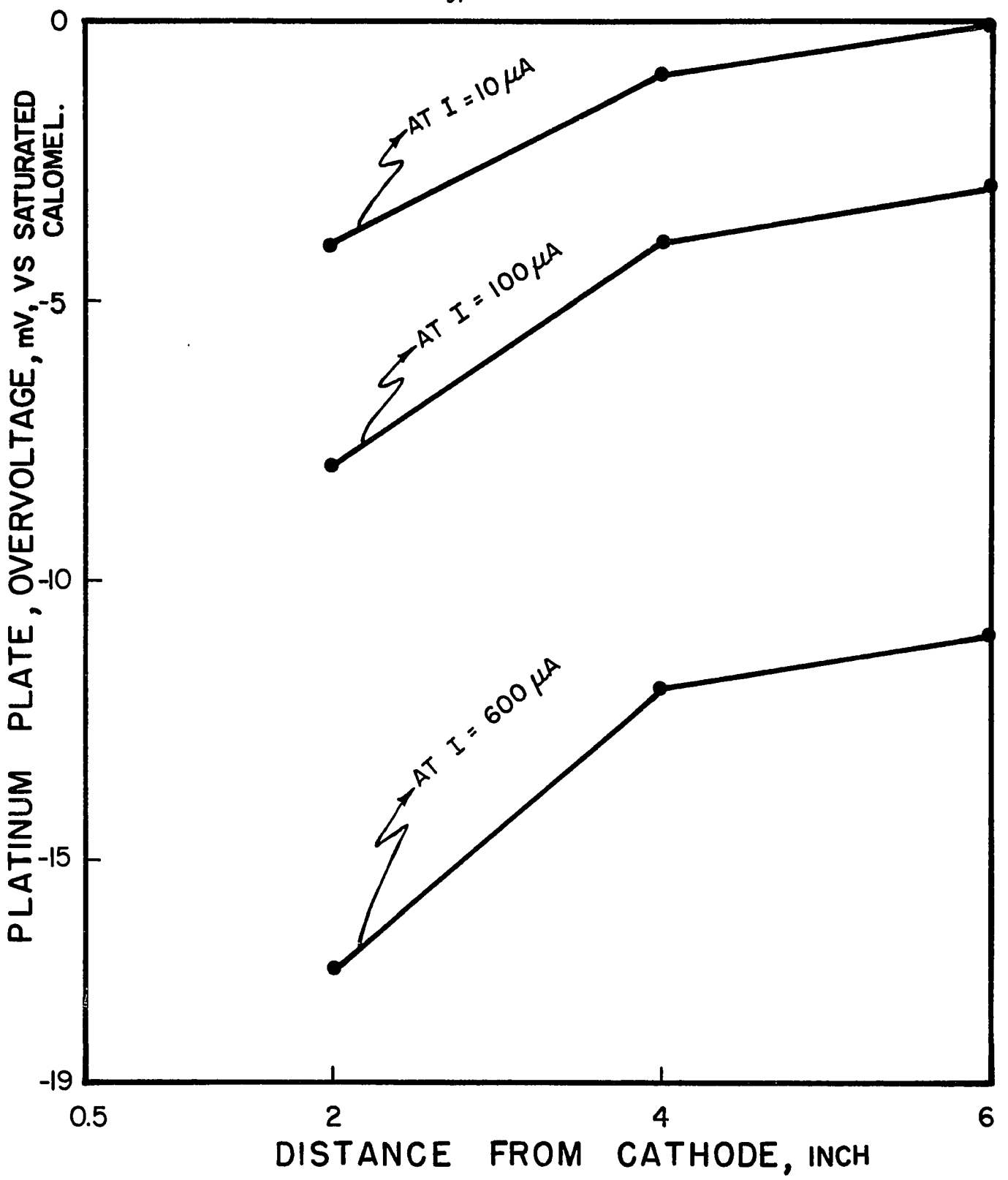

FIG. 40. POTENTIAL SHIFT OF PLATINUM PLATE BETWEEN ANODE AND CATHODE AS A FUNCTION OF DISTANCE AT THREE LEVELS OF CATHODIC CURRENT IN 3% SALT SOLUTION.

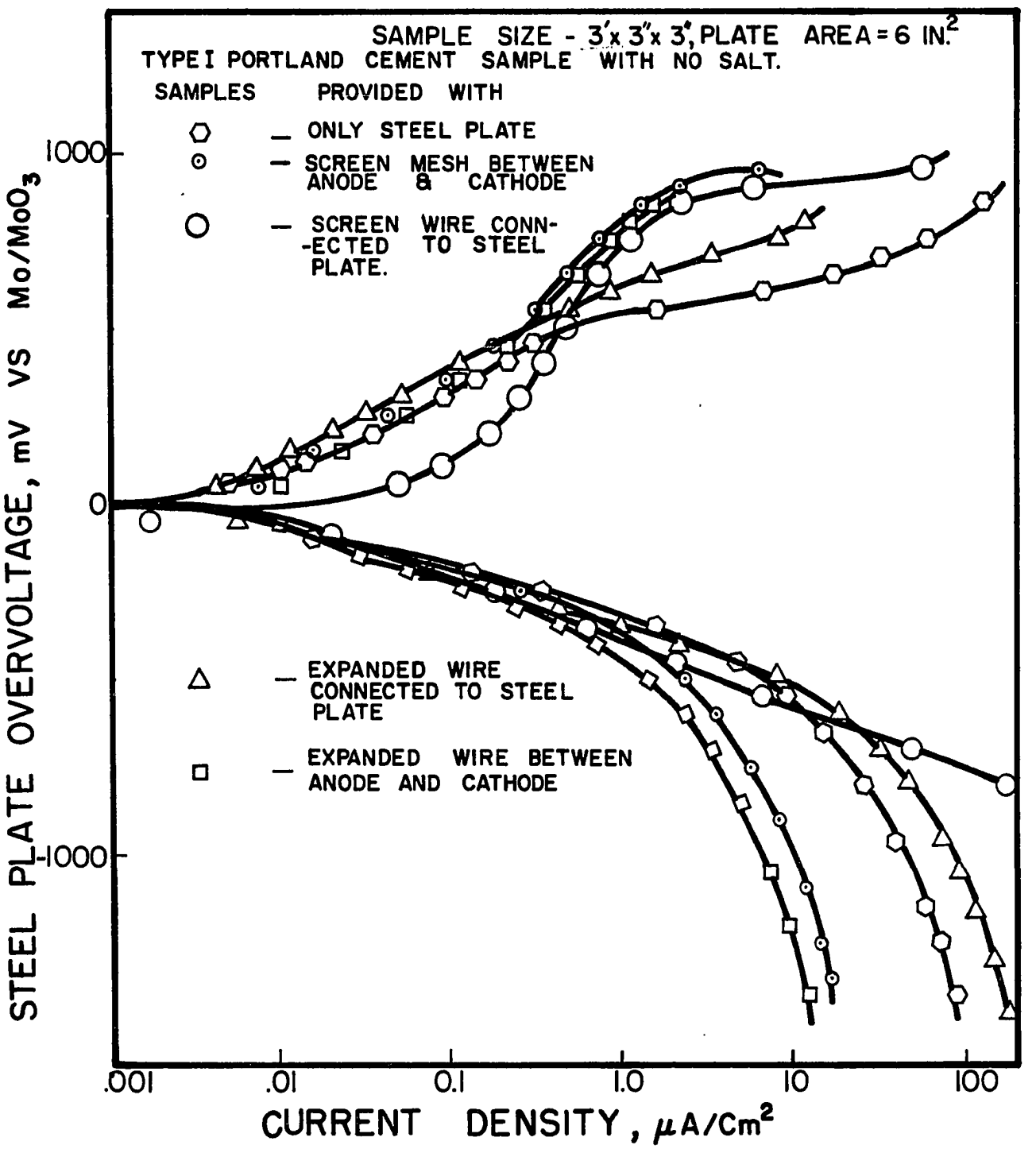

FIG. 41. ANODIC AND CATHODIC POLARIZATION OF STEEL PLATE IN PRESENCE OF WIRE MESH IN TYPE I PORTLAND CEMENT CONCRETE. SAMPLES WERE IN DRY CONDITION OF LABORATORY FOR 20 TO 30 DAYS AFTER CURING.

with the wire mesh disconnected from the plate. The anodic polarization curves indicate that the anodic current density requirements for the samples with wire mesh connected and disconnected to the plate are lower than the sample with no wire mesh.

Figure 42 also presents the anodic and cathodic polarization of the steel with a wire mesh connected and disconnected to the plate. In this experiment, the samples were exposed to distilled water for four months. The results indicate that the cathodic current density requirements for the sample with no wire and those with wire mesh placed between the anode and cathode with no connection, are about the same. The cathodic current density for the samples with wire mesh connected to the plate is higher than the sample with no wire mesh. The anodic current density requirements for the samples with wire mesh connected and disconnected to the plate were a little scattered for the wire meshes with different hole sizes. In these experiments, the current density for samples with the wire mesh connected to the plate was calculated as the cell current divided by the sum of the surface areas of the plate and wire mesh.

Figure 43 presents a potentiodynamic cathodic polarization of the steel for the samples of Type I Portland cement concrete with the wire mesh (between the anode and cathode with no connection) and without the mesh. The potential of the steel was first controlled by an embedded Mo/MoO_3 electrode place adjacent to the steel plate, then by an external $Cu/CuSO_4$ electrode. The samples had been exposed to the dry condition of the laboratory for 300 days. The results indicate that the cathodic current requirements decreased substantially when the potential of the steel was controlled by Mo/MoO_3 instead of $Cu/CuSO_4$.

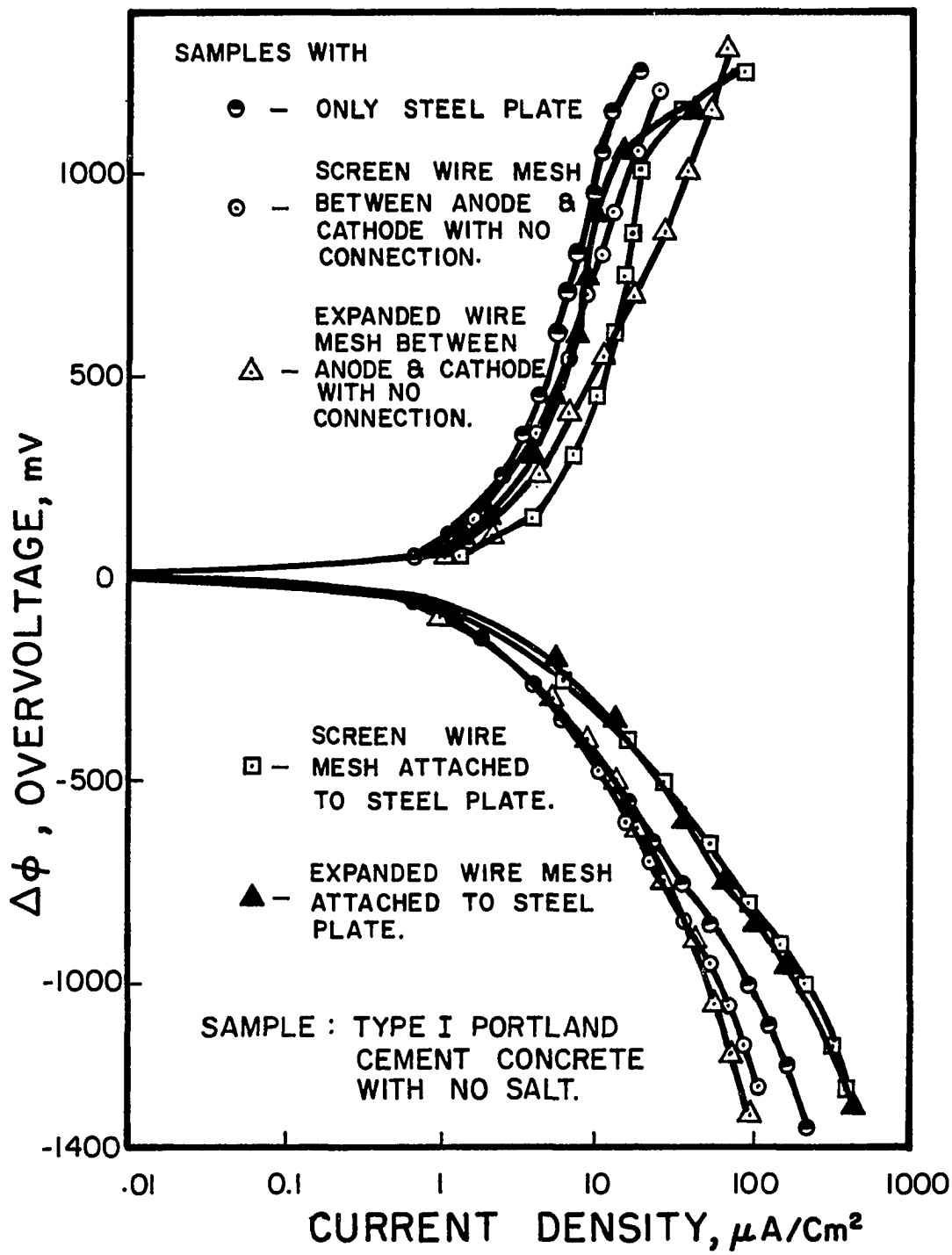

FIG. 42. ANODIC AND CATHODIC POLARIZATION OF STEEL PLATE IN PRESENCE OF WIRE MESH IN TYPE I PORTLAND CEMENT CONCRETE. SAMPLES WERE EXPOSED TO DISTILLED WATER FOR 4 MONTHS.

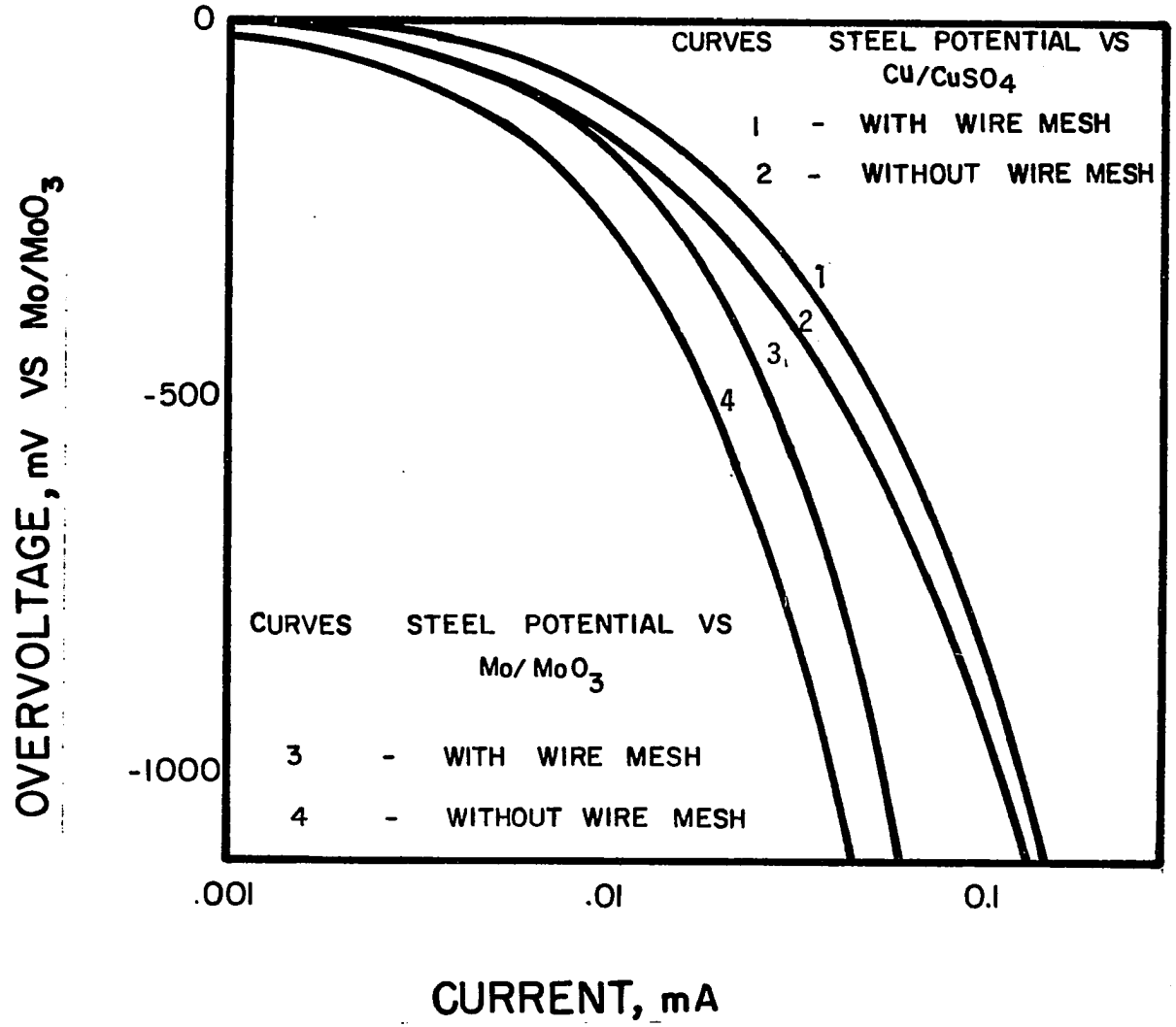

FIG. 43. POTENTIODYNAMIC CATHODIC POLARIZATION OF STEEL PLATE IN CONCRETE WITH RESPECT TO EXTERNAL ($Cu/CuSO_4$) AND EMBEDDED (Mo/MoO_3) REFERENCE ELECTRODES WITH AND WITHOUT PRESENCE OF WIRE MESH. SAMPLES WERE IN DRY CONDITION OF LABORATORY FOR 120 DAYS. [SWEEP RATE = 1 MV/SEC.]

(Compare curves 1 and 3 in Figure 43.) The data also indicates that the location of wire mesh between the steel plate and $Cu/CuSO_4$ electrode interferes with the potential and consequently with the current requirements. (See curves 2 and 4 in Figure 43.)

4.5.2 Potential Shift of the Wire Mesh Because of the Passage of Current (The Wire Mesh was Between the Anode and Cathode with no Connection.) Figures 44 and 45 present the potential shift of the wire mesh compared to Mo/MoO_3 and $Cu/CuSO_4$ reference electrodes as a result of anodic and cathodic currents for the steel plate. The potential shift of the wire mesh is toward the more positive direction as a result of the cathodic current and toward a more negative value because of the anodic current required for the steel plate. Figure 45 also indicates that the potential of the wire mesh will not change because of the cathodic current required for steel plate if the wire mesh is placed outside the electric field which exists between anode and cathode. (A cell assembly for a concrete slab used in this test is shown in Figure 46.)

4.5.3 Potential Shift of the Wire Mesh as a Function of Distance from the Cathode Because of the Passage of Current (The Wire Meshes were Between the Anode and Cathode with no Connection.) Figure 47 indicates the shift in potential of the wire mesh as a result of a change in its distance from the plate during the flow of anodic and cathodic current. A cell assembly for a concrete slab used in this test is shown in Figure 5. The data indicates that the shift in wire mesh potential increases as the distance of wire mesh from the steel plate increases. Figure 48 shows that the shift in wire mesh potential as a function of distance from the cathode is not linear. The shift in potential of the

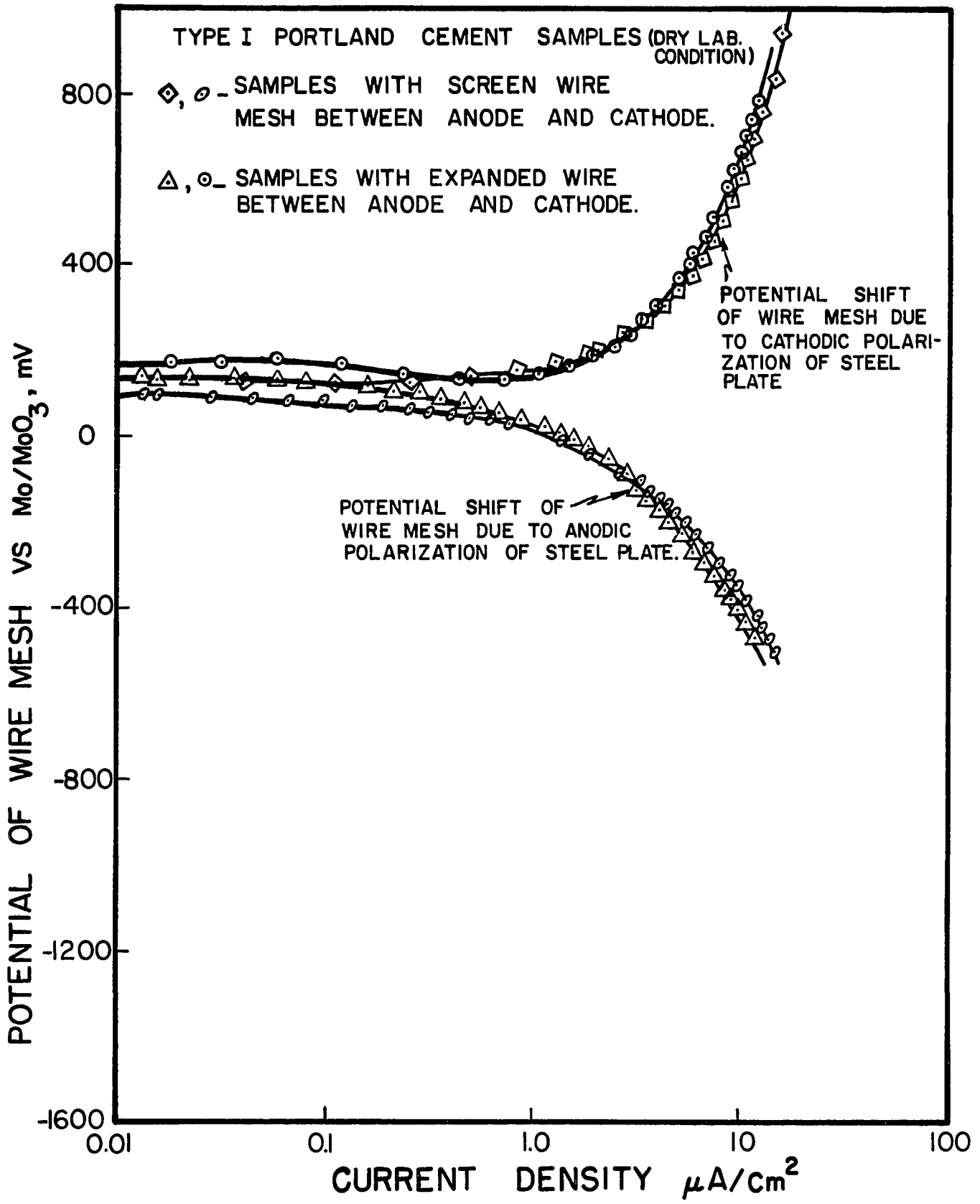

FIG. 44. POTENTIAL SHIFT OF WIRE MESH IN TYPE I PORTLAND CEMENT CONCRETE DURING ANODIC AND CATHODIC POLARIZATION OF STEEL PLATE.

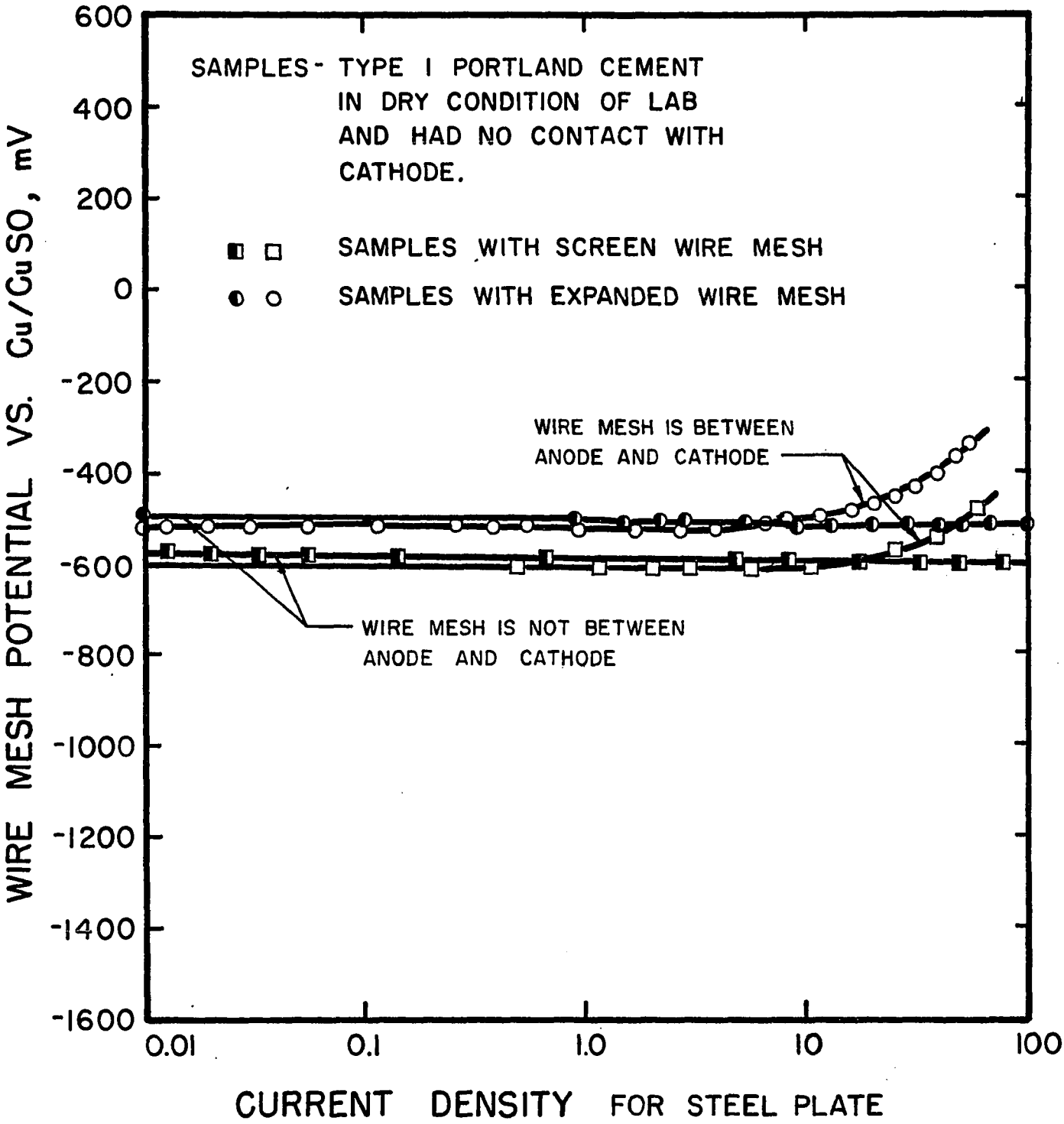

FIG. 45. POTENTIAL SHIFT OF WIRE MESH IN TYPE I PORTLAND CEMENT CONCRETE DURING CATHODIC POLARIZATION OF STEEL PLATE.

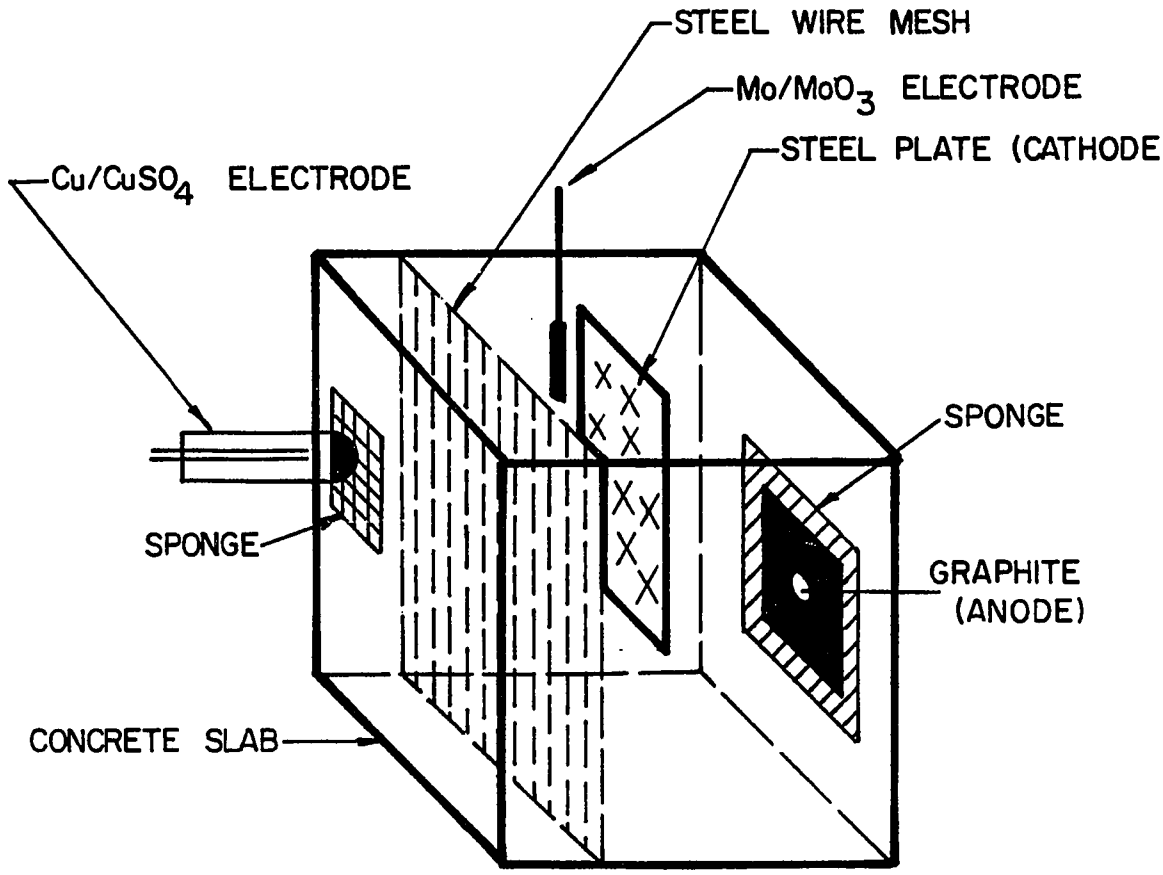

FIG. 46. CELL ASSEMBLY FOR CONCRETE SLAB WITH WIRE MESH OUTSIDE OF ELECTRIC FIELD BETWEEN ANODE AND CATHODE.

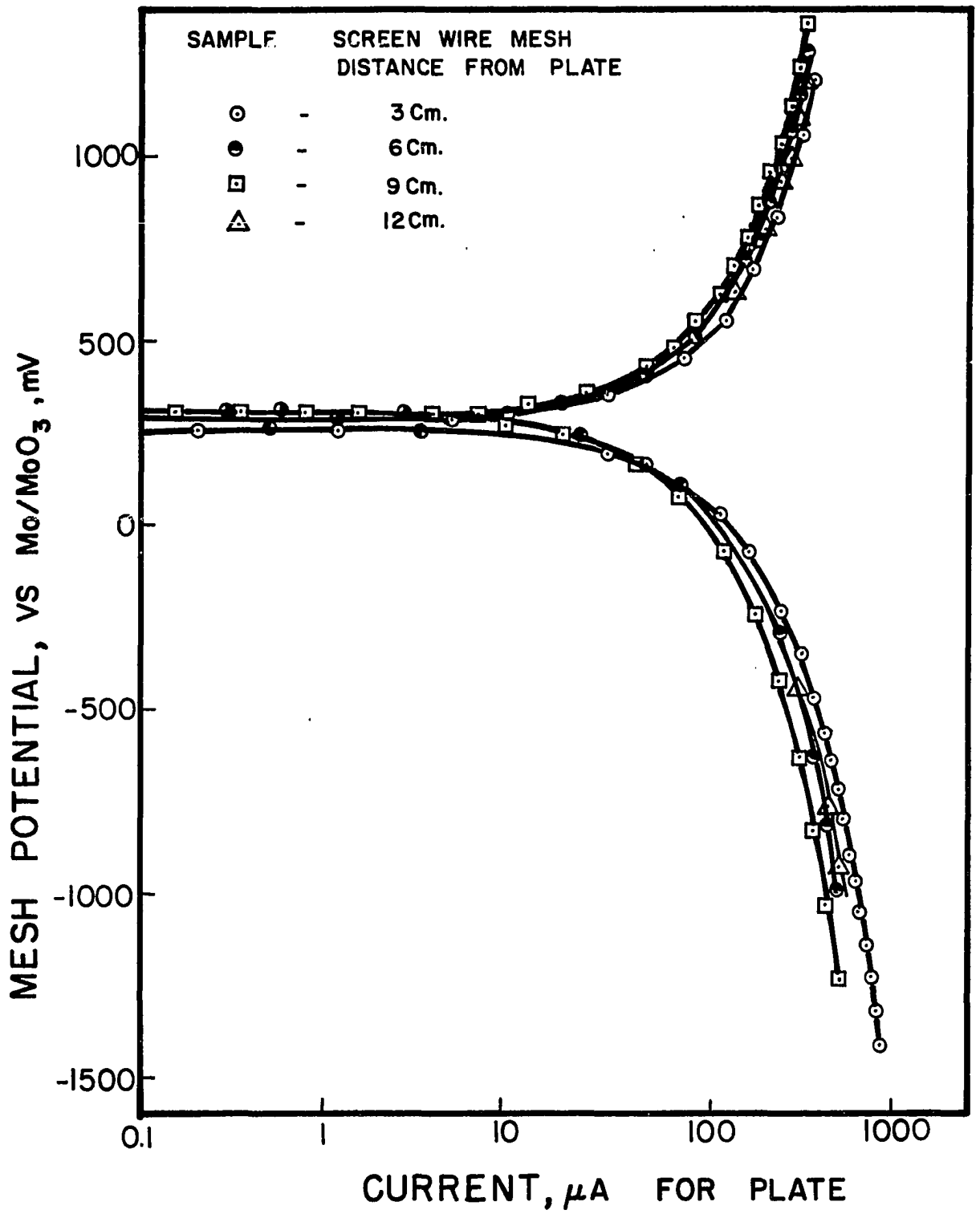

FIG. 47. POTENTIAL VARIATION OF SCREEN WIRE MESH AT VARIOUS DISTANCES FROM THE PLATE AS A RESULT OF ANODIC AND CATHODIC POLARIZATION OF STEEL PLATE IN TYPE I PORTLAND CEMENT CONCRETE.

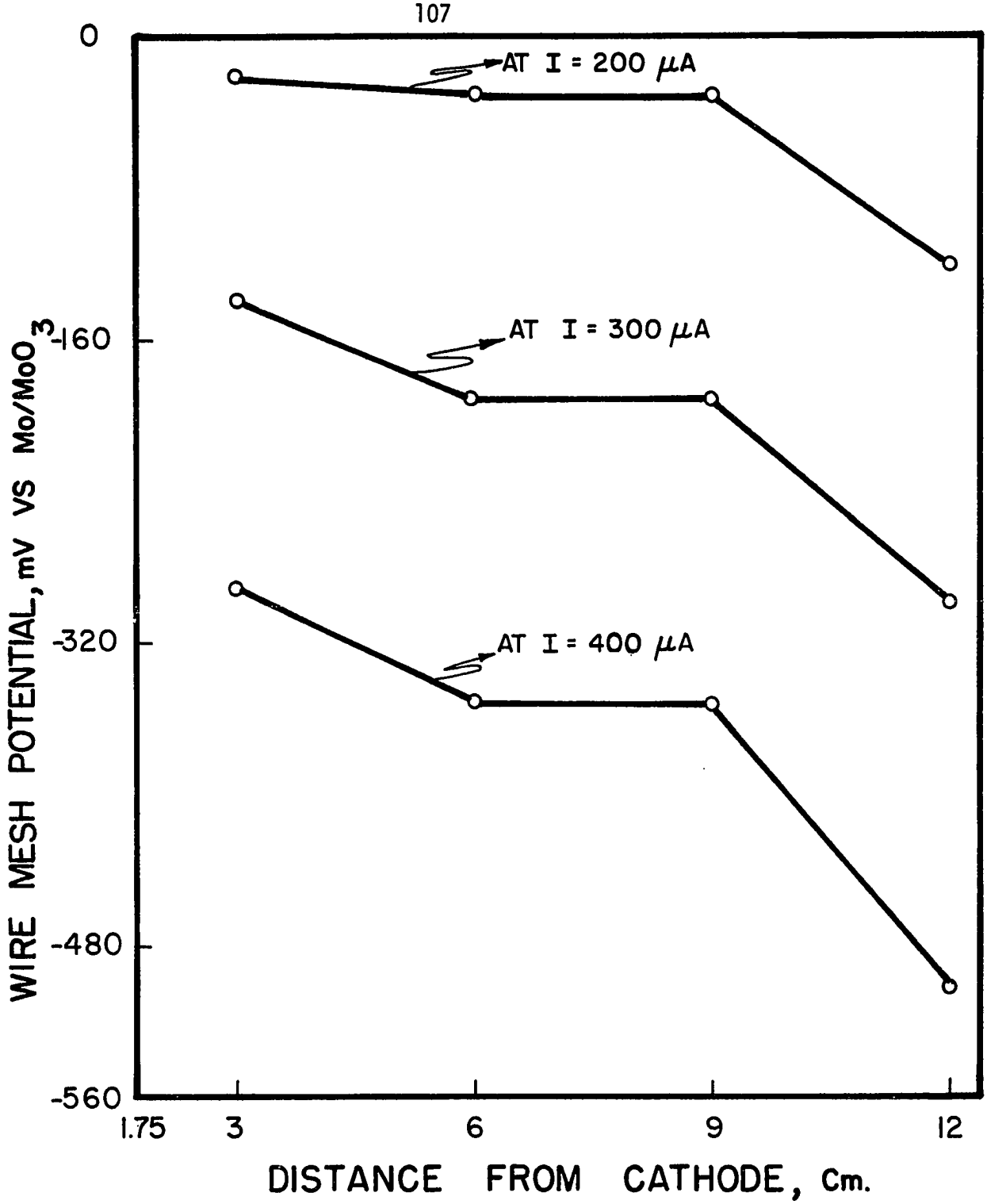

FIG. 48. POTENTIAL SHIFT OF STEEL WIRE MESH AS A FUNCTION OF DISTANCE AT THREE LEVELS OF CATHODE CURRENT FOR POLARIZATION OF STEEL PLATE IN TYPE I PORTLAND CEMENT CONCRETE.

wire mesh was also observed when an external $Cu/CuSO_4$ electrode was used (see Figure 49).

In the concrete slab shown in Figure 5, the potential shift of all wire meshes was compared only to the Mo/MoO_3 electrode placed in the position 4 ($Mo/MoO_3(4)$). In the cathodic polarization of the steel plate, the potential of the wire meshes placed at the right hand side of the Mo/MoO_3 electrode shifted toward more positive values and toward more negative values for the wire meshes placed at the left hand side of the Mo/MoO_3 electrode (see Figures 50 and 51). This result was repeated in the data presented in Figure 52.

The anodic polarization of the steel plate in the concrete sample shown in Figure 5 indicates that the potential of the wire meshes varied with anodic current. The potential of the meshes measured versus the Mo/MoO_3 electrodes placed at the left hand side of those meshes shifted towards more negative values. The opposite effect was observed when the potential of the meshes was measured versus the Mo/MoO_3 electrodes placed at the right hand side of those meshes (see Figures 53, 54, 55). The shift in the potential of the wire meshes decreased as the distance of the mesh from the reference electrodes decreased. This finding was observed in all the data.

Figure 56 presents the potential variation of the Mo/MoO_3 reference electrodes compared to an external $Cu/CuSO_4$ electrode placed in the position 1 during the cathodic polarization of the steel plate. The cell assembly and the electrode positions for this test are shown in Figure 57. The results indicate that the potential of the Mo/MoO_3 electrodes placed at the right hand side of the $Cu/CuSO_4$ electrode

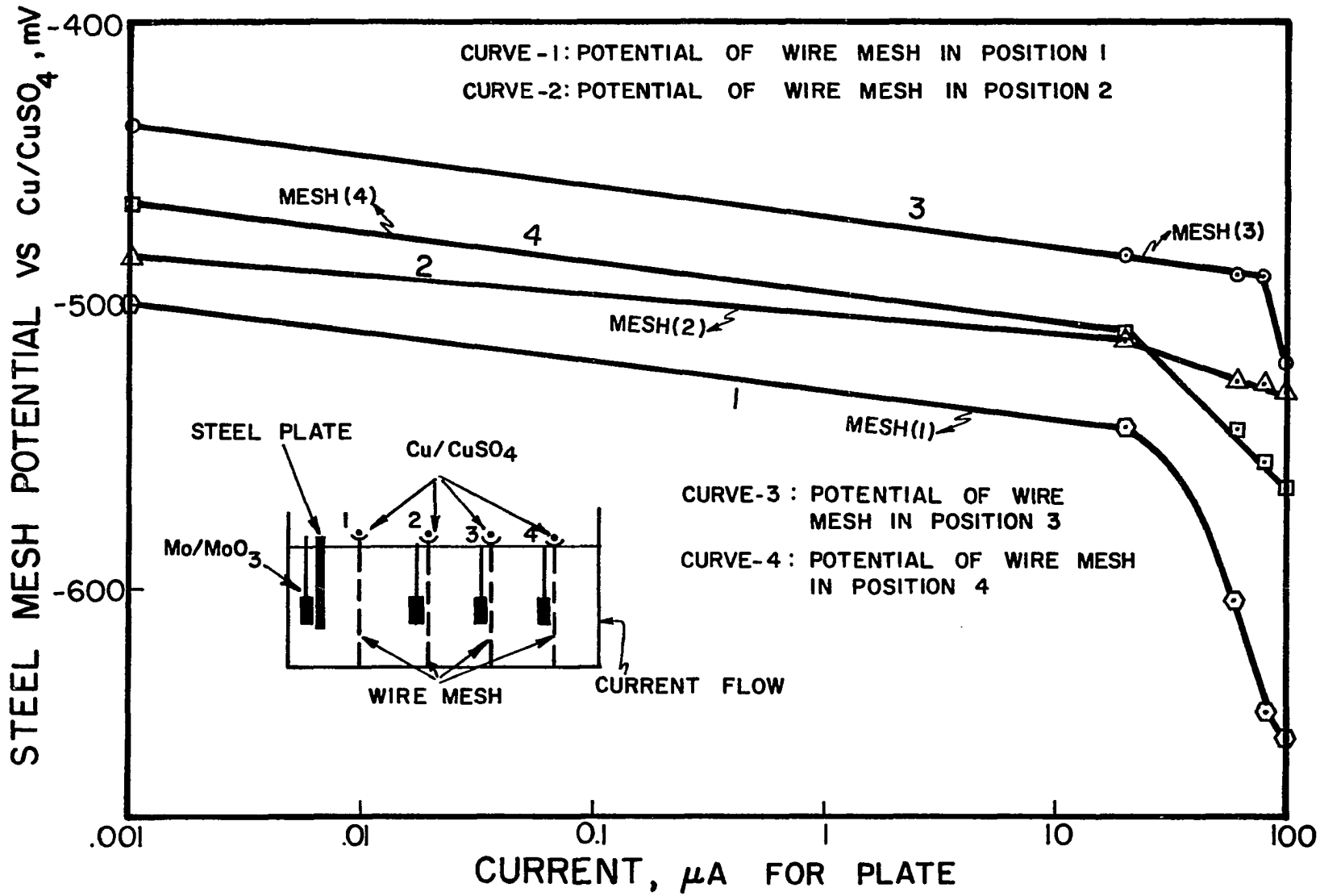

FIG. 49. POTENTIAL SHIFT OF WIRE MESH COMPARED TO $Cu/CuSO_4$ AS A RESULT OF CATHODIC POLARIZATION OF STEEL PLATE.

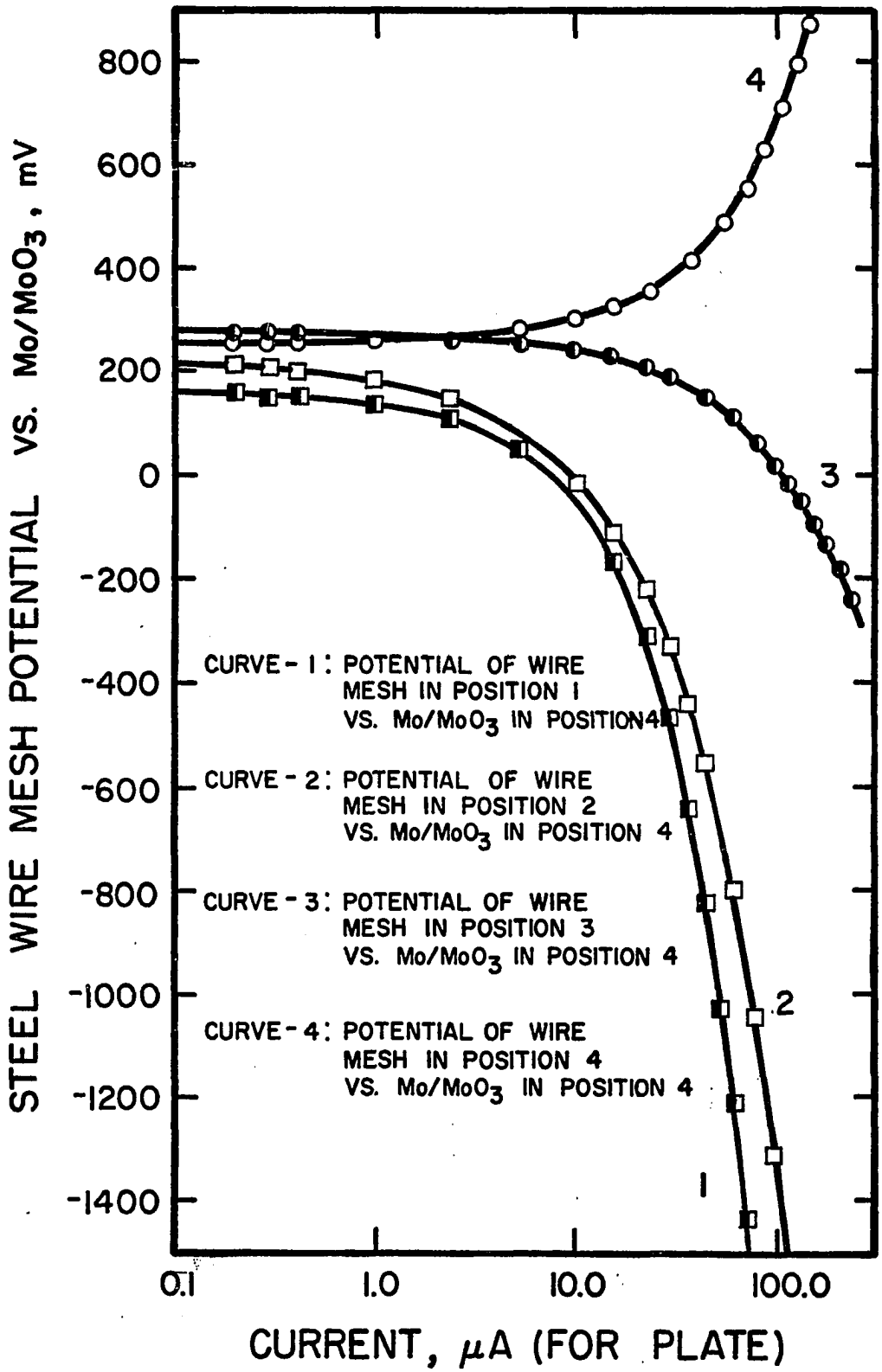

FIG. 50. SHIFT IN STEEL WIRE MESH POTENTIAL AS A FUNCTION OF CURRENT REQUIRED FOR CATHODIC POLARIZATION OF STEEL PLATE.

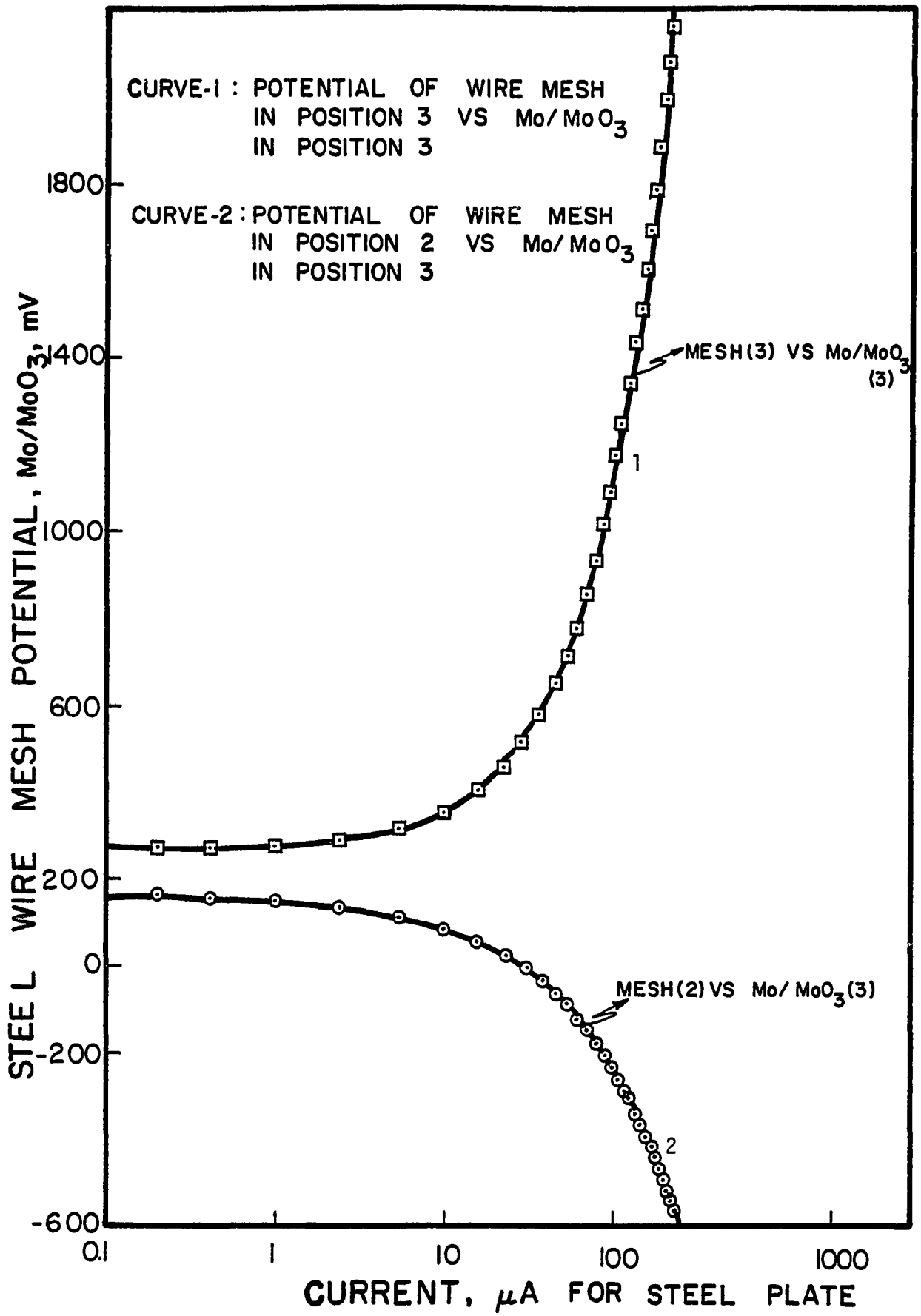

FIG. 51. SHIFT IN WIRE MESH POTENTIAL AS AS A FUNCTION OF CURRENT REQUIRED FOR CATHODIC POLARIZATION OF STEEL PLATE.

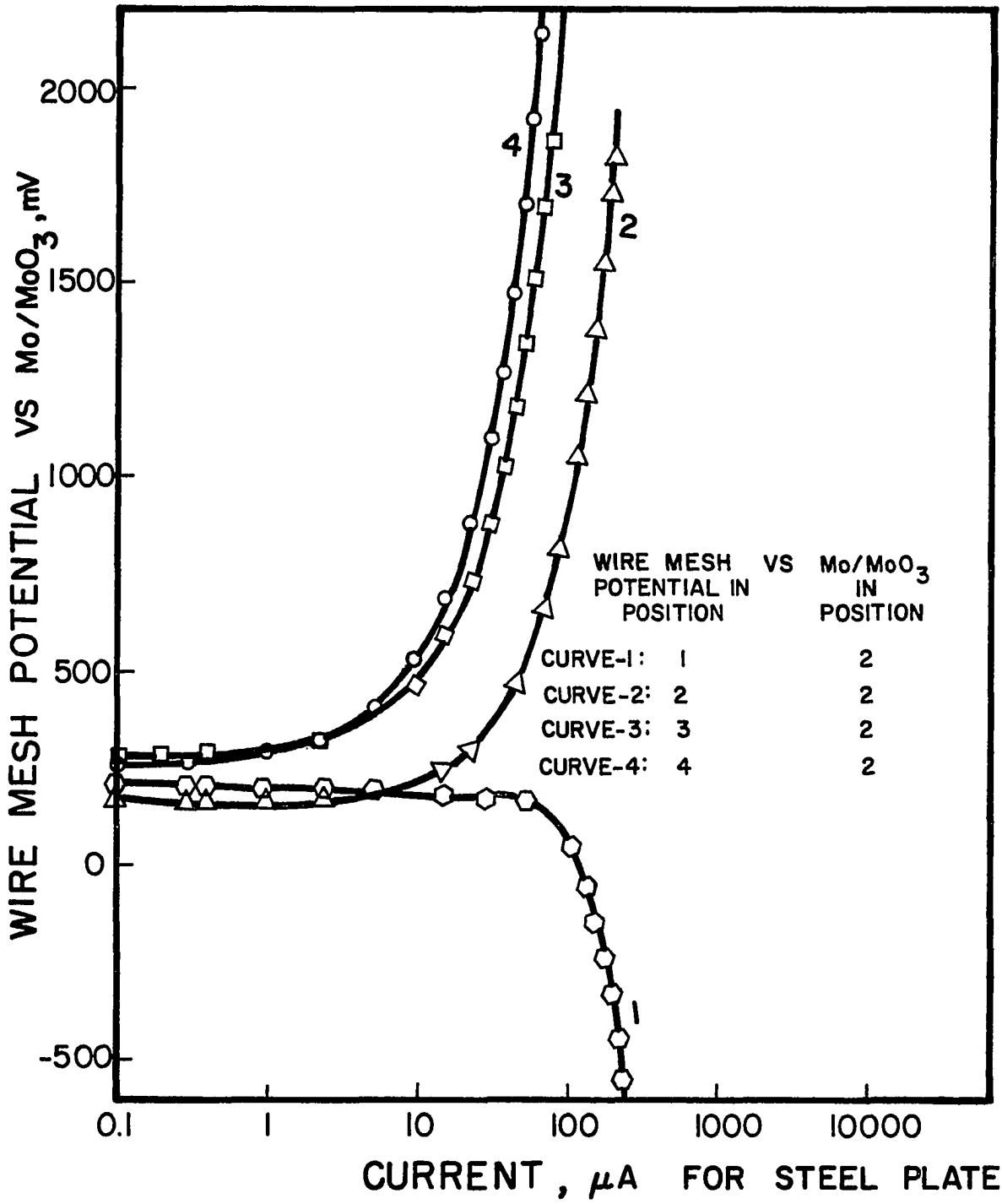

FIG. 52. SHIFT IN STEEL WIRE MESH POTENTIAL AS A FUNCTION OF CURRENT REQUIRED FOR CATHODIC POLARIZATION OF STEEL PLATE.

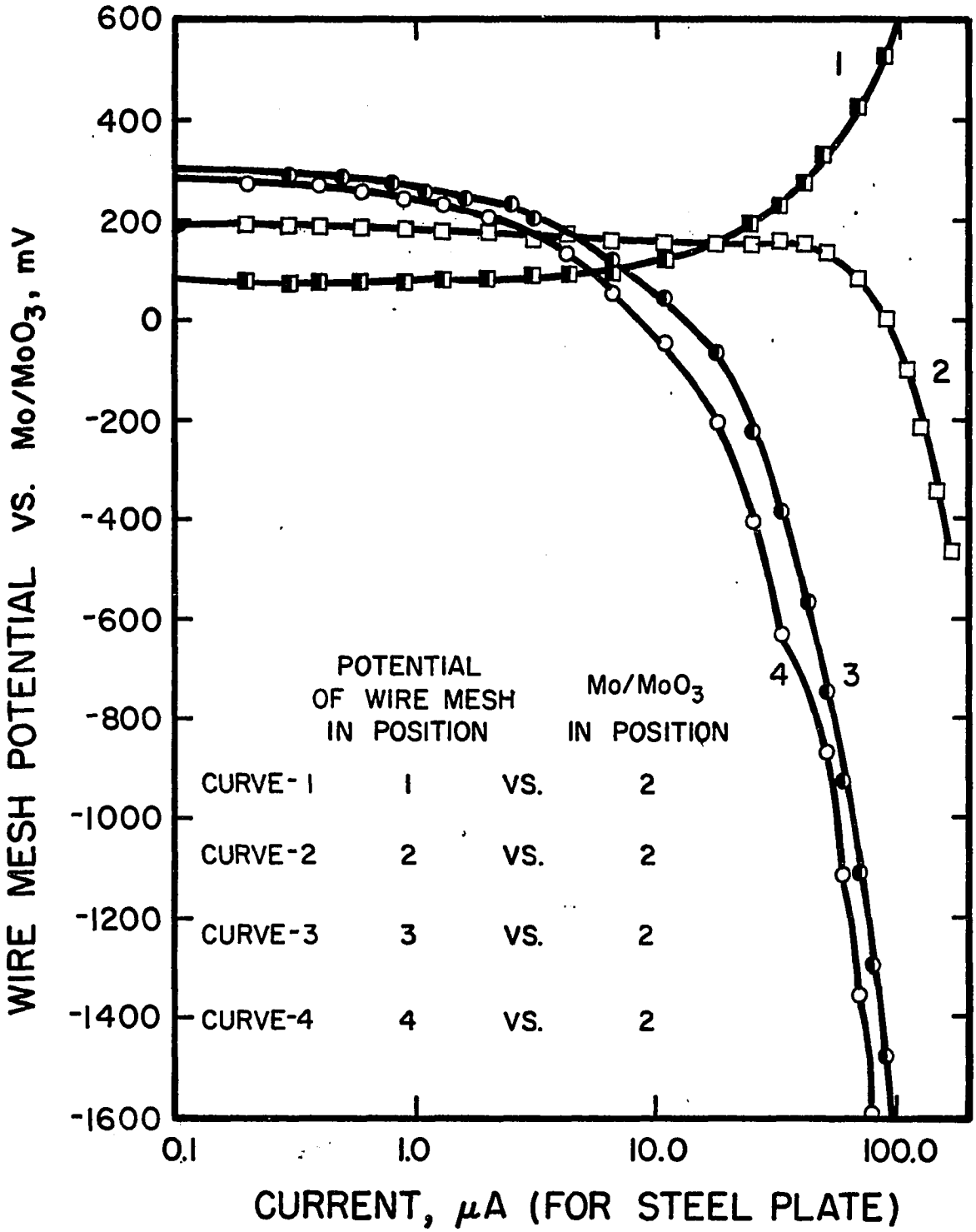

FIG. 53. SHIFT IN WIRE MESH POTENTIAL AS A FUNCTION OF CURRENT REQUIRED FOR ANODIC POLARIZATION OF STEEL PLATE.

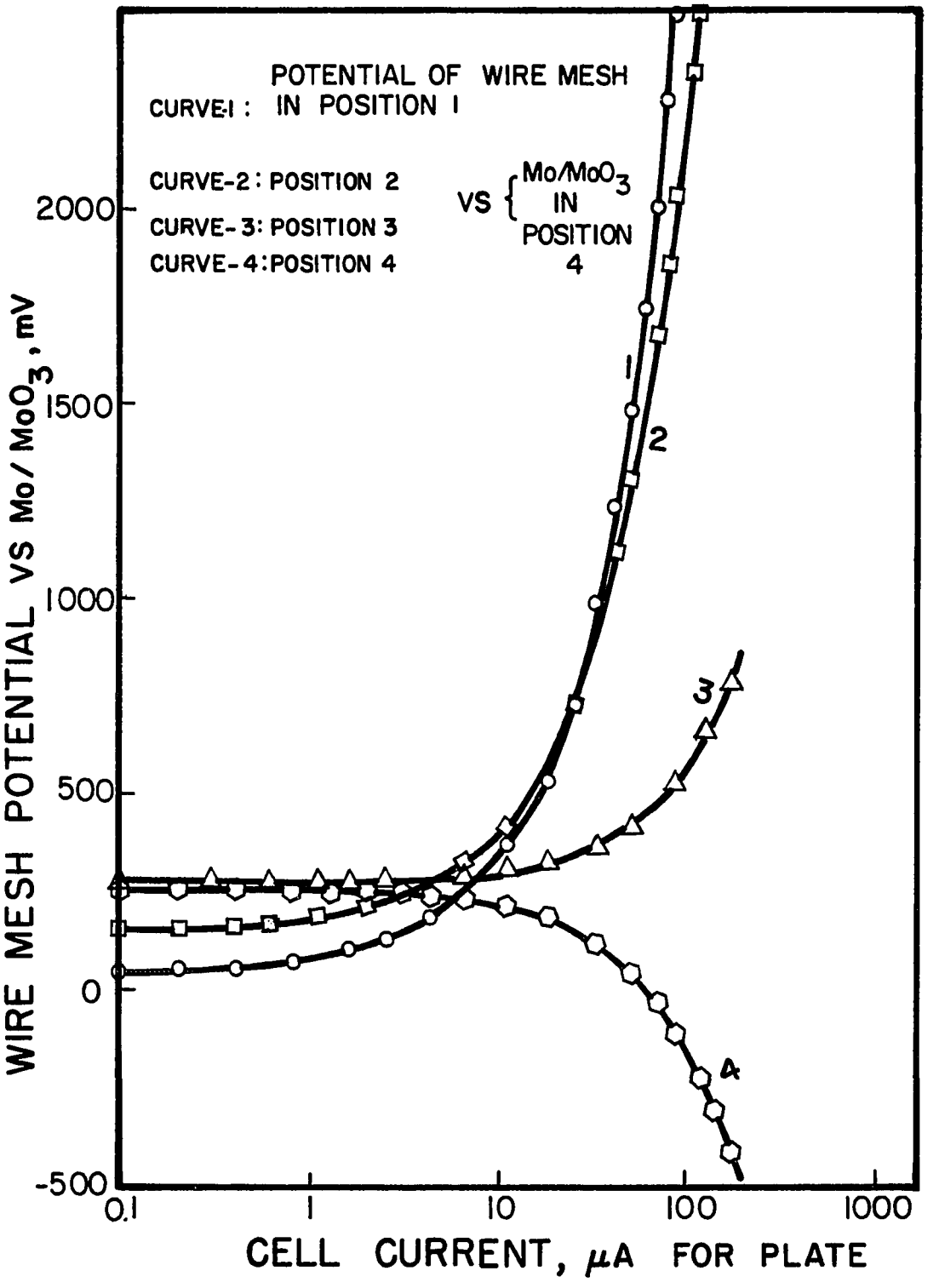

FIG. 54. SHIFT IN WIRE MESH POTENTIAL AS A FUNCTION OF CURRENT REQUIRED FOR ANODIC POLARIZATION OF STEEL PLATE.

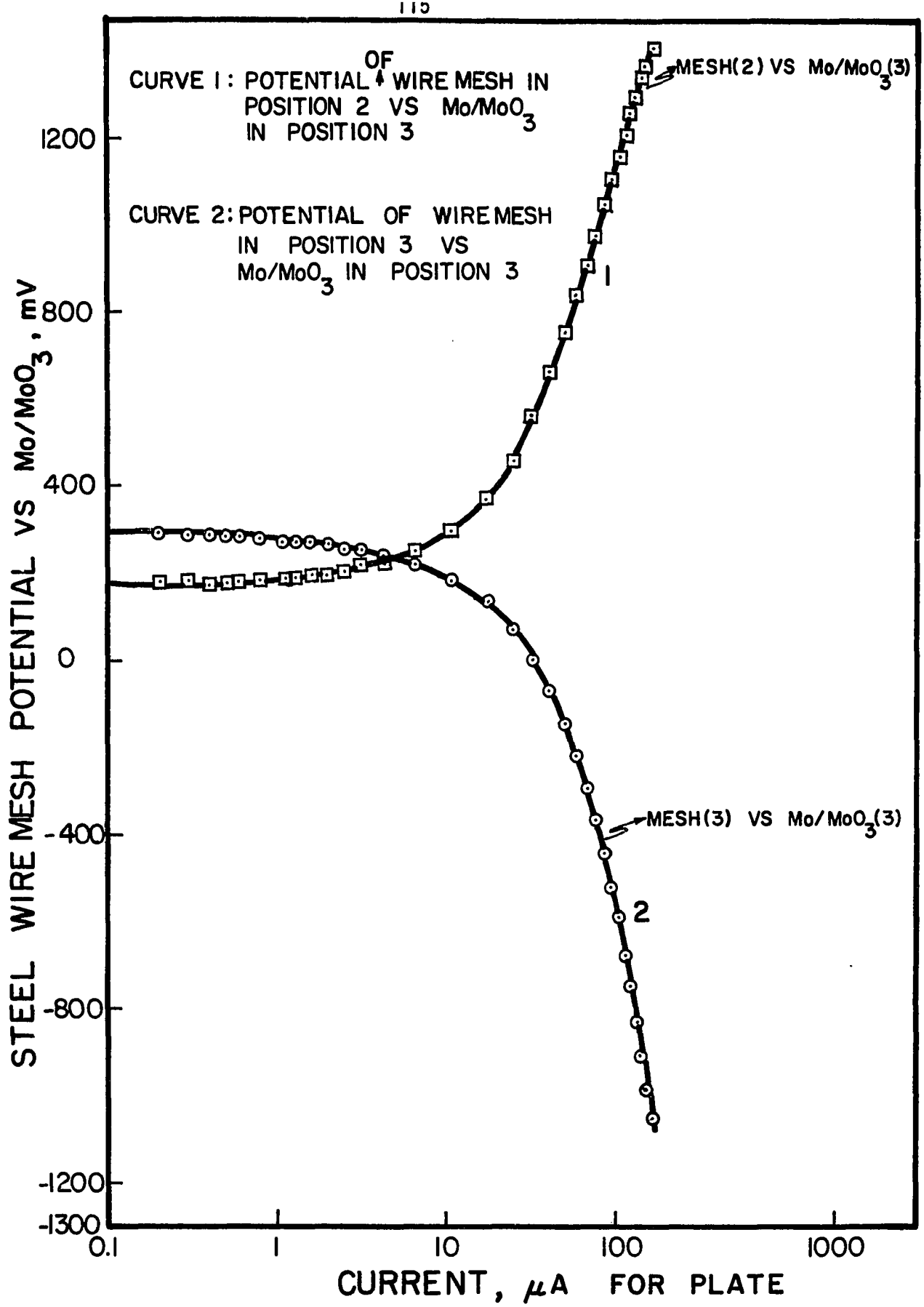

FIG. 55. SHIFT IN WIREMESH POTENTIAL AS A FUNCTION OF CURRENT REQUIRED FOR ANODIC POLARIZATION OF STEEL PLATE

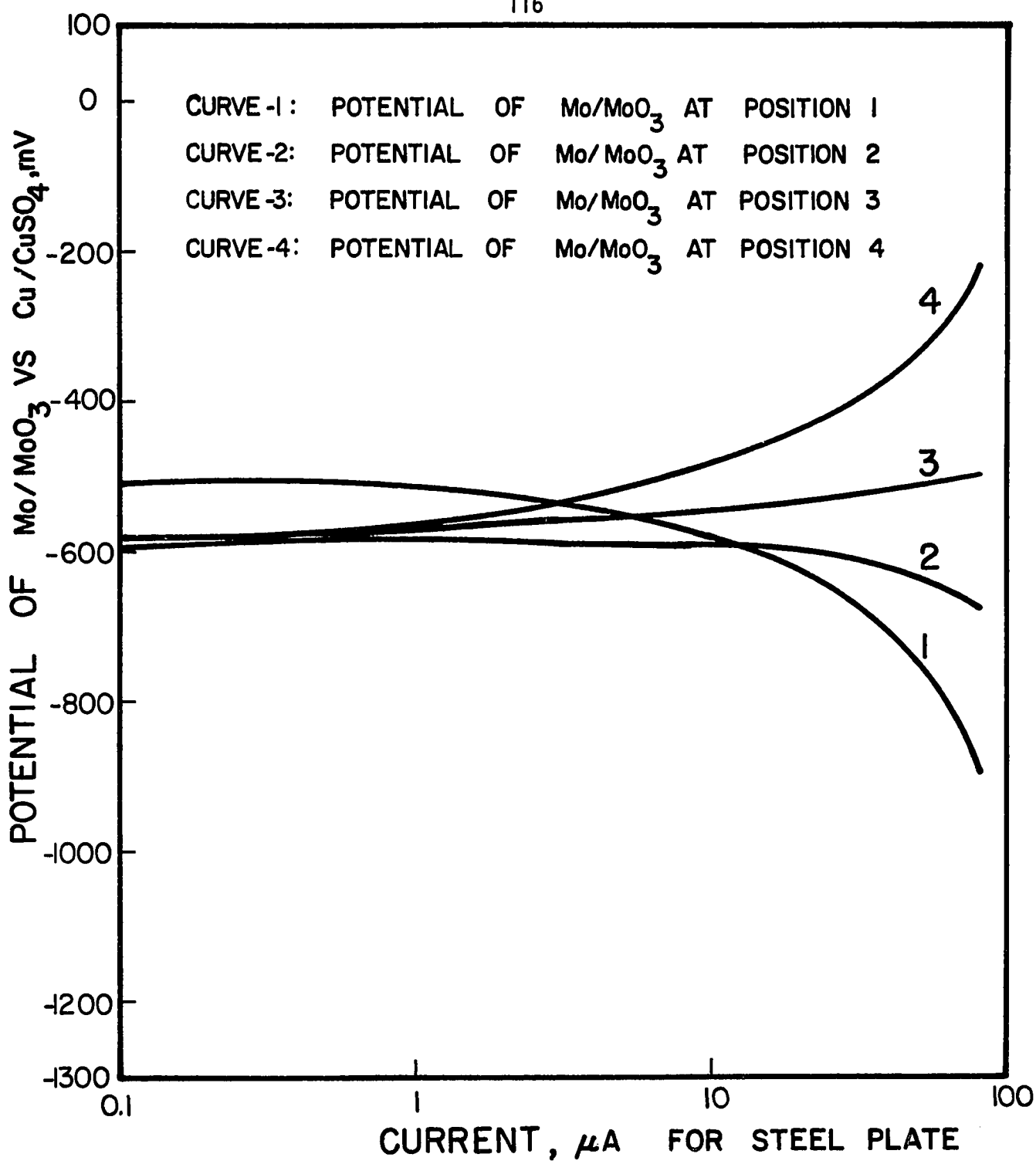

FIG. 56. POTENTIAL SHIFT OF Mo/MoO_3 ELECTRODES VS $Cu/CuSO_4$ AS A FUNCTION OF CATHODIC CURRENT FOR STEEL PLATE

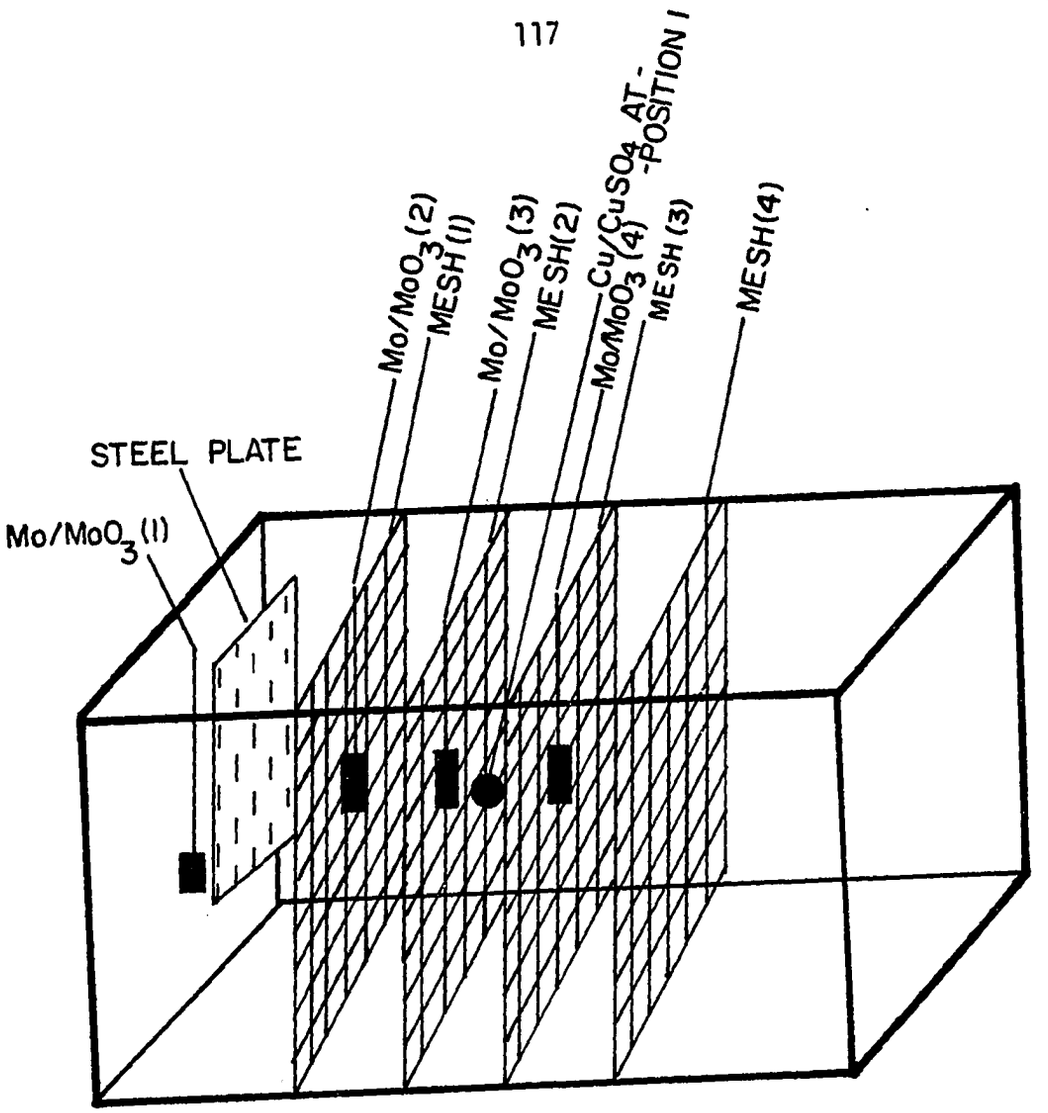

FIG. 57. CONCRETE SAMPLE WITH ONE STEEL PLATE AND FOUR STEEL WIRE MESHES AND FOUR Mo/MoO_3 ELECTRODES ADJACENT TO PLATE AND WIRE MESHES. WIRE MESHES ARE 4 Cm. APART FROM ONE ANOTHER AND EMBEDDED BETWEEN ANODE AND CATHODE.

shifted toward a more positive value while the potential of those placed at the left hand side shifted toward a more negative value. This result was similar to those obtained for the wire mesh.

4.5.4 Potential Shift of the Platinum Plate as a Function of Distance from the Cathode. (Platinum Plates were Between the Anode and the Cathode with no Connection.) Figure 58 presents the shift in potential of four platinum plates which had been placed between the anode and the cathode during anodic current flow. (The cell assembly and electrode arrangement in this test are shown in Figure 6.) The potential of each platinum plate was measured with respect to the Mo/MoO_3 electrode placed adjacent to the edge of that platinum plate. The results indicate that the potential of the platinum plates shifted toward more positive values because of anodic current flow. The shift in potential was higher as the platinum plate was moved farther from the anode.

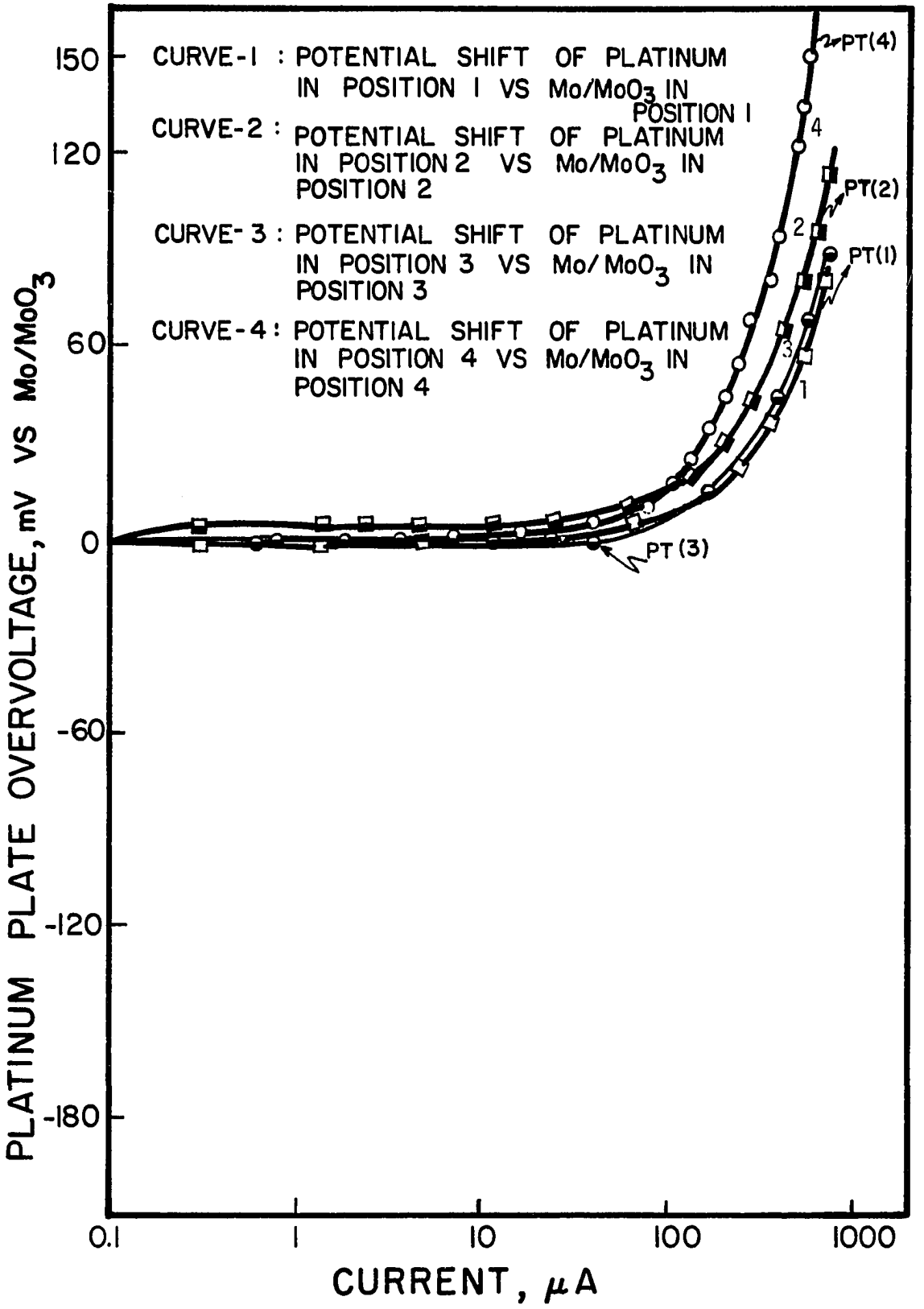

FIG. 58. POTENTIAL SHIFT OF PLATINUM PLATES AS A FUNCTION OF DISTANCE BETWEEN ANODE AND CATHODE AS A RESULT OF ANODIC POLARIZATION IN TYPE I PORTLAND CEMENT CONCRETE.

CHAPTER V

DISCUSSION OF RESULTS

The Electrochemical Behavior of Steel in Salt-Contaminated Concrete

The interpretation of results and the proposed corrosion mechanism are presented below.

5.1 Samples Exposed to the Dry Conditions of the Laboratory

The anodic and cathodic polarization curves for steel in Types I and V Portland cement exposed to the dry conditions of the laboratory for 200 days indicate that the samples with no salt requires higher current density than the samples with salt content. (See Figures 11 and 13.) This result was confirmed by the potentiodynamic anodic polarization curves for the samples exposed to the dry conditions of the laboratory for 300 days. (See Figures 12 and 14.) The current density requirements also decreased as the salt content increased.

This result may be due to the fact that the concrete samples with higher salt content retain more water than the samples with zero or lower salt content. This fact was supported by visual observation tests where the concrete samples with higher salt content absorbed less water than those with lower salt content. In other words, the samples with higher salt content retain more water when they dry than those with lower salt

content. Therefore, the moisture is uniformly distributed along the steel plate in the samples with higher salt content and the possibility of a set-up for an electrochemical cell is low. However, in the samples with low salt content, an electrochemical cell may be set up along the steel plate, because of a moisture gradient along the steel. The regions with higher moisture then become anodic and those with low water content become cathodic. As a result, a local action current will flow between these two parts. These results are confirmed by Stratfull [85]: "Highly water absorptive concrete dries more rapidly than a low absorption concrete, and the former sustains a lower electrical resistivity for a longer period than would be suspected by a comparative weight loss of water. Therefore, a highly water absorptive concrete could result in a rapid corrosion of the embedded steel." This result may be due to the deliquescent property of salt, which absorbs moisture.

The open circuit potential of steel in Types I and V Portland cement concrete samples exposed to dry conditions indicates that the steel potential for the samples with no salt is in the range of 500 - 520 mv compared to a $Cu/CuSO_4$ electrode. (See Figure 15.) These potentials indicate that the steel in this concrete is in a corrosive state, according to the findings of some investigators who say that steel in concrete will corrode if the potential is more negative than -300 to -350 millivolts with respect to $Cu/CuSO_4$ [86,87,88,89]. These investigators have also found that reinforcing steel with potentials more positive than -100 to -300 mv with respect to a $Cu/CuSO_4$ electrode was not corroded in simulated concrete environments.

The steel potential in Type V Portland cement was more positive

than Type I Portland cement for the samples with and without salt content, except for the sample with 0.5% salt. The potential of steel in Type I Portland cement was about the same for the samples with salt content up to 1%, but the potential shited a little toward a more positive direction for the 2% salt content sample. The steel potential in Type V Portland cement shifted significantly toward a more positive value compared to the samples with lower salt content. This result may be due to scattered data caused by measurement uncertainities.

Potentiodynamic anodic polarization curves for steel in concrete samples with various salt contents showed some differences in current requirements at the cathodic parts of the polarization curves. (See Figures 12 and 14.) This fact is probably due to the different oxygen concentration for different concrete samples. These variations in oxygen concentration may be caused by differences in moisture content or porosity, or even by cracks in these concrete samples.

However, in the presence of oxygen, a cathodic reaction at steel surface occurs, as follows:

$$\frac{1}{2} O_2 + H_2O + 2e^- \rightleftarrows 2OH^- \qquad (2a)$$

The rate of reaction (2a) varies with the different oxygen concentrations at the steel-concrete interface. As a consequence, the cathodic current varies too. This variation can be better explained by considering the relationship between current and the concentration of oxygen at the steel surface:

$$I = k \{[O_2]_{bulk} - [O_2]_{surface}\} \qquad (10)$$

where k is a constant.

As can be seen, the current varies with the shift in oxygen concentration at the steel surface. In the absence of oxygen at the steel surface, the current remains constant, the reaction (2a) does not take place and the steel will be polarized without any change in current density.

5.2 Samples Exposed to Distilled Water

The anodic and cathodic polarization curves for steel in Types I and V Portland cement samples with various salt contents (the samples were exposed to distilled water for 90 and 170 days) indicate that the current density of steel increases as salt content of the samples increases. (See Figures 16, 17, 18, and 20.) This result can be explained by the breakdown in the passive film because of chloride attack.

Foley [90] has derived five theories to explain this chloride attack:

1. Chloride penetration into the oxide film, which is otherwise protective.
2. Preferential adsorption of Cl^- rather than a passivating species.
3. The field effect of absorbed Cl^- ions pulling Fe^{++} ions out of the metal.
4. Catalysis of the corrosion reaction by the bridging structure.
5. A complex formation between Cl^- ions and some form of iron.

The attack of chloride by any of the above means may cause an increase in current density. This statement is supported by the work of D.L. Pirou, E.P. Koutsoukos, and Kon Nobe [91] on the corrosion behavior of nickel-200 and Inconnel-600 in solution. Their results indicate that

the passivation potential and current density increase with an increase in the concentration of chloride ions. Similar results were found by Oladis Rincon [92] and Traubenberg [93], who indicated that anodic and cathodic current density of iron in sulfuric acid with a pH of 3 increased as the concentration of chloride ions in the solution increased.

A comparison of the anodic and cathodic polarization curves for steel in Types I and V Portland cement with various salt contents (the samples were exposed to distilled water for 90 to 170 days) indicates that, in general, current density requirements for steel in Type I Portland cement are higher than for Type V. (See Figures 16, 17, 18, and 20.)

The potentiodynamic anodic polarization curves for steel in Types I and V Portland cement samples with various salt contents (the samples were soaked in distilled water for 300 days) indicate that the steel plate will passivate in Type I Portland cement samples with a salt content up to 0.1%, but steel maintains its passivity in the samples of Type V up to 0.5% salt content. (See Figures 19 and 21.)

The differences in the electrochemical behavior of steel in Types I and V Portland cement may be due to the pH differences which exist between these two types of cement. This change in pH for these two types of cement may be caused by physical damage such as cracks created by the curing process. As mentioned in the Theory Section, Type I Portland cement contains more C_3A than Type V, which produces a higher heat of hydration. Therefore, the inside temperature of the concrete is higher than the outside, which may cause a crack. The carbon dioxide and salt can then penetrate freely into the concrete and lower the pore solution

pH around the steel. However, the low C_3A in Type V Portland cement produces a low heat of hydration and therefore the possibility of the cracks in the concrete is less than in Type I. As a consequence, Type V Portland cement may maintain a higher pH than Type I.

These differences in pH affect the rate of anodic and cathodic reaction and, therefore, the current density requirements. The differences in pH may even affect the formation of the passive film. This fact can be explained by considering reactions (1) and (2b) mentioned in the Theory Section and also given below:

$$Fe \rightleftarrows Fe^{++} + 2e^- \qquad (1) \quad \text{(anodic reaction)}$$

$$\frac{1}{2} O_2 + H_2O + 2e^- \rightleftarrows 2OH^- \qquad (2a) \quad \text{(cathodic reaction)}$$

The overall reaction can be written as:

$$Fe + \frac{1}{2} O_2 + H_2O \rightarrow Fe(OH)_2 \qquad (11)$$

The ferrous hydroxide produced by equation (11) is insoluble and unstable in the presence of oxygen. Therefore, this hydroxide will be converted to $Fe(OH)_3$ (ferric hydroxide) which is less soluble than $Fe(OH)_2$. The final product is rust, Fe_2O_3.

This protective oxide film (Fe_2O_3) is stable in the presence of a high alkalinity (pH $\sim$ 12) of the pore solution within the concrete. However, the introduction of chloride ions into the concrete breaks down this protective film and therefore, increases the rate of anodic reaction. (See equation 1.) Thus, in a less alkaline concrete (one with a lower pH) and in the presence of chloride ions, the $Fe(OH)_2$ may not be converted to $Fe(OH)_3$, which is more stable and less soluble in water. Thus,

it may be assumed that the differences in pH for these two types of cement (Type I and V) may cause a different rate of reaction which, in turn, would create different current densities for the polarization of steel in concrete.

Gouda and Mourad [94] have studied the effect of pH on the polarization of steel in two different cells containing sodium hydroxide with a pH of 7 and 8. They indicated that the anodic and cathodic current density requirements for steel in the cell with a pH of 7 is higher than that for the cell with a pH of 8. The results of their studies also indicate that the rate of anodic reaction of steel in the cell with a pH of 7 is higher than that for the cell with a pH of 8. The addition of the same amount of salt into these two cells also resulted in an increase in the current density requirement, but this increase was higher for the cell with the lower pH than for that with the higher pH.

The open circuit potential of steel in the Type I Portland cement sample with no salt content was more negative (more active) than for Type V Portland cement. Similar results were found for the samples with salt content. (See Figure 23.) Gouda's work also indicated that the open circuit potential of steel in the cell with the pH of 7 is more negative than for the cell with the pH of 8. The addition of the same amount of salt into these two cells caused the steel potential to shift to more negative values for the cell with pH 7 than for the cell with pH 8. This result is similar to the data obtained for Types I and V Portland cement. Therefore, from the Gouda's study, it may be concluded that the differences in the electrochemical behavior of steel in concrete of Types I and V Portland cement may be caused by differences in PH, which indicates

that the pH of the pore solution adjacent to steel for Type I may be lower than for Type V Portland cement.

A comparison of Figures 15 and 23 indicates that the open circuit potential of steel in dry conditions for Types I and V Portland cement shifted toward a more positive value (less active) or remained constant as the salt content of the concrete increased. The opposite behavior was found for steel in Types I and V Portland cement with various salt contents, exposed to distilled water. This result indicates that the attack of chloride ions on the passive film is severe in the concrete with a higher moisture content, because the higher moisture content increases the ionic conductivity of the concrete. As a consequence, the steel corrodes because of lower resistivity ($10^3 - 10^4$ ohm-cm). In dry concrete, the resisitivity is high ($10^8 - 10^{11}$ ohm-cm). Therefore, the flow of local action current between the anode and cathode is low and corrosion of the steel is reduced.

A break at potentials of about 500 - 600 mv for anodic and -500 to -700 mv with respect to a Mo/MoO_3 electrode for cathodic polarization of steel was observed in some of the concrete samples of Types I and V Portland cement with the salt content. These samples were exposed to distilled water for 90 to 170 days. A break at approximately the same potentials mentioned above was also observed for the anodic and cathodic polarization of the platinum plate in Types I and V Portland cement with various salt contents exposed to distilled water. (See Figure 22.) This break was caused by the electrochemical reactions which take place because of the electroactive species in the concrete.

Concrete contains about 2 to 3% Fe_2O_3, which, in the presence of

moisture and chloride ions, reacts with water and forms $Fe(OH)_2$. Then the $Fe(OH)_2$ at potentials of about +600 mv (calculated by Nernst equation, see Appendix A) with respect to the Mo/MoO_3 electrode and at a pH of about 12 to 13 (this is about the same as concrete pH) will be converted to γ - FeOOH. The anodic reaction which may take place at the break potential of about 500 to 600 mv with respect to the Mo/MoO_3 electrode is presented as

$$Fe(OH)_2 \rightleftarrows \gamma - FeOOH + H^+ + e^- \qquad (12)$$

A break also occurred at potentials of about -500 to -700 mv with respect to the Mo/MoO_3 electrode for cathodic polarization of steel and the platinum plate in concrete. This result indicates that the reaction at the steel surface is only due to the electrochemical reactions associated with the electroactive species in concrete. The Fe_2O_3 in concrete reacts with oxygen at the cathode and forms Fe_3O_4. This product (Fe_3O_4), in the presence of high OH^- produced by the reduction of oxygen at the cathode, remains stable, but Fe_3O_4 will be converted to $Fe(OH)_2$ or Fe at a pH of about 12 to 13 (this is about the pH of concrete) and in the presence of moisture and chloride ions. These reactions can be written as

$$Fe_3O_4 + 2H_2O + 2H^+ + 2e^- \rightleftarrows 3Fe(OH)_2 \qquad (13)$$

or

$$Fe_3O_4 + 8H^+ + 8e^- \rightleftarrows 3Fe + 4H_2O \qquad (14)$$

These reactions occur at the potential of -650 mv with the respect to Mo/MoO_3 at a pH of 12 to 13. This was at the range of break potential, and was calculated by Nernst equation (see Appendix A). Therefore,

the reaction at the cathodic break potential is reaction (13) or (14). An analysis of the oxide film at the break potential would be necessary to determine which one of these two reactions is predominant.

5.3 Samples Exposed to Salt Solutions

The data presented in Figures 24, 25, 26, 27, 28, 29, and 30 shows that for the samples of Types I and V Portland cement with no salt content, exposed to salt solutions for 90 and 170 days, the anodic and cathodic current density increase as the salt concentration of the solution increases. This result indicates that salt penetrates at a much faster rate for the samples exposed to a solution with a higher salt concentration than for ones exposed to a solution with a lower salt content.

Figure 31 presents the differential anodic current density at the potential of 800 mv (with respect to a Mo/MoO_3 electrode) as a function of the salt-concentrated solution. The differential anodic current density was determined by subtracting the anodic current density requirement at +800 mv for the samples of Types I and V Portland cement concrete exposed to distilled water from the current density requirement for the samples of Types I and V exposed to solutions with various salt concentrations at the same potential. Figure 31 also presents the current, calculated by the diffusion process, using the Cottrel equation: $I = nFAD^{\frac{1}{2}}C_b/\pi^{\frac{1}{2}}t^{\frac{1}{2}}$ (15). In this equation, n is the number of electrons involved per molecule or ion of electroactive species, F is a Faraday's number (96500 Coulomb), A is the surface area of the electrode, D is the diffusivity coefficient, C_b is the electroactive concentration in the bulk

solution, π is a constant, and t is the exposure time to the solution.

The calculated chloride diffusivity coefficient, obtained from the diffusion process equation mentioned above, indicates that in order to calculate the same differential anodic current density obtained in Figure 31, the diffusivity coefficient of concrete must be in the range of $10^{-1} cm^2/sec$. This is about 4 to 5 orders of magnitude higher than the true concrete diffusivity coefficient, because concrete is a porous media and the diffusivity coefficient of a porous media is about the same as that of an aqueous solution (i.e., $10^{-5} cm^2/sec$) or lower. Therefore, the differential anodic current density of steel caused by the chloride ions for the concrete samples of Types I and V Portland cement exposed to solutions with various salt contents is not a diffusion-related process. Instead, it may be due to more complex reactions which may take place in the presence of chloride ions.

The open-circuit potential of steel in Types I and V Portland cement samples exposed to salt solution shifted toward more negative values (more active potential) as the salt content of the solution increased. (See Figure 32.) This data is in agreement with that obtained for the anodic and cathodic polarization of steel in these samples. The results of both data indicate that the steel is in a more active state for the samples exposed to solutions with a higher salt content.

The potentiodynamic anodic polarization curves presented in Figures 27 and 28 indicate that the steel will depassivate in the samples of Types I and V Portland cement exposed to solutions with various salt concentrations ranging from 0.1 to 3.5% salt content. The open-circuit potential of steel in Types I and V Portland cement exposed to salt

solutions also confirms that steel has a potential more negative than -350 mv with respect to the $Cu/CuSO_4$ electrode. This fact is an indication that the steel is in a corrosive state.

A comparison of the results presented in Figures 24, 25, 26, and 28 indicates that the current density requirement for the polarization of steel in Types I and V Portland cement samples increases as the exposure time to the salt solution increases. This effect was more pronounced in Type I than in Type V Portland cement. (See also Figure 30.) This result indicates that the intrusion of chloride ions into concrete increases as the exposure time to the salt solution increases. Similar results were found by Gjorv and Vennesland [95,96] who showed that even for a 0.4 water-cement ratio (high quality concrete) mortar, the depth of penetration of the chloride ions increased progressively with exposure time to the salt solution.

The results obtained for Types I and V Portland cement samples with various salt contents exposed to distilled water and those with no salt content exposed to a salt solution show that some of the chloride ions mixed with the concrete may react effectively with concrete compounds, but the reaction may not occur with chloride ions added externally, or if it does occur, it is on a very small scale. Therefore, the corrosion of steel may be more severe for that type of chloride which diffuses from the salt solution into the concrete than for the type of chloride which is mixed with the concrete.

The results in this study indicate that the pitting breakdown of the oxide film on the steel surface is a kinetic process which strongly depends on the existence of non-equilibrium solution conditions created

by the chloride ion concentration and depressed hydroxyl ion concentration around the pits. The transport rates of chloride and hydroxide ions, which can be maintained near the pits, depend not only on the bulk activities in solution of the two ions but also on the composition and pore structure of the solid phases deposited adjacent to the metal.

The data presented in Figure 33 indicates that the electronic IR drop compensation has no significant effect on the polarization of steel in concrete compared to that without any IR drop compensation, when steel potential is controlled by an Mo/MoO_3 electrode. The Tafel slope for IR compensated and uncompensated steel was the same. (See curves 1 and 2 in Figure 33.) The electronic IR drop compensation of steel in concrete, when the steel potential was controlled with respect to $Cu/CuSO_4$, also indicated no significant change in Tafel slope compared to the uncompensated IR drop, but a small shift in the current requirement for cathodic polarization was observed. (See Figure 34.)

It should be noted that the Tafel slope ($d\eta/d \log i$) of the polarization curves for steel in concrete with and without IR drop compensation is very high (at the range of 1200 to 1600 mv). This high Tafel slope can be explained by considering the Butler-Volmer equation

$$i = i_o [e^{(1-\beta)\eta F/RT} - e^{-\beta\eta F/RT}] \qquad (16)$$

This equation shows that the current density across a metal-electrolyte interface depends on the difference between the actual non-equilibrium and equilibrium potential differences (η). In the above equation, β ($0 < \beta < 1$) is a symmetry factor associated with the rate of charge-transfer reaction, i is the current density, η is over voltage, F is the

Faraday's number (96500 Coulomb), R is the gas constant, and T is the temperature (25°C). A small change in η makes a large increase in i, only when β is small in the range of 0.5. This situation occurs when the charge transfer for the ions and electrons at the metal-electrolyte interface proceeds quickly which indicates that the diffusion of the ions to or from the electrolyte is taking place fast. This has been observed for the solution electrolyte where the movement of the ions is freely taking place in the electrolyte. Therefore, the Tafel slope ($d\eta/d \log i$) is small. However, when β is large, the change in η makes a small change in i. Therefore, the Tafel slope (d /d log i) becomes large. (See equation 17.) The large β may be created by concentration polarization because the electrochemical reactions on the steel surface are caused by the combination of activation and concentration polarization. In the case of concentration polarization, the electrochemical reactions are controlled by the diffusion in the electrolyte. The diffusion rate of reducible species in concrete, such as oxygen from the bulk concrete to the steel-concrete interface, will be reduced because of low conductivity of concrete. Therefore, the reaction rate increases and the current approaches to diffusion limiting-current resulting in high β and in turn, causes the high Tafel slope.

The high value of β for concrete was calculated from the equation below, which was obtained from the Butler-Volmer equation:

$$\text{Tafel slope} = \frac{d\eta}{d \log i} = \frac{RT}{F} \cdot \frac{1}{1-\beta} \qquad (17)$$

The β was determined to be in the range of 0.978 for the Tafel slope of 1200 mv. Therefore, the high Tafel slope in concrete is not mainly due

to the IR drop potential but rather to the rate of the charge transfer reaction, which in turn, depends on the diffusion rate of ions into or from the concrete.

However, there was a difference in the Tafel slope of the polarization curves because of the IR drop when the steel potential was controlled with an Mo/MoO_3 electrode, compared to that when the steel potential was measured with an external $Cu/CuSO_4$ electrode. The Tafel slope was about -1200 mv/decade when the steel potential was measured with an Mo/MoO_3 electrode but was in the range of -1650 mv/decade when the steel potential was measured with a $Cu/CuSO_4$ electrode. Therefore, there was a reduction of 450 mv/decade in IR drop when the steel potential was measured with respect to an Mo/MoO_3 electrode rather than a $Cu/CuSO_4$ electrode.

Effect of Wire Mesh on Current and Potential

5.4 Solution

Current density requirements and the shape of anodic and cathodic polarization curves for steel in a saturated $Ca(OH)_2$ solution did not vary when a wire mesh was placed between the anode and the cathode with no connection. (See Figure 35.) Various wire mesh sizes were used but these made no differences in the current density requirement. Therefore, the presence of a wire mesh between the anode and the cathode with no connection does not shield the current requirement for the cathodic protection of steel in a saturated $Ca(OH)_2$ solution.

The data in Figure 36 indicates no significant variation in cathodic current density for the steel with the wire mesh connected to

to the top and bottom of the steel plate compared to the steel without any wire mesh. However, in anodic polarization curves, the region of passivity for the samples with a wire mesh connected to the top and bottom of the steel plate was reduced compared to the samples with only a steel plate. This fact may be due to metallurgical factors such as heterogeneity, which may exist between the steel plate and the steel wire mesh. This heterogeneity may set up an electrochemical cell, which may lower the region of passivity as a result of local action current flow.

The results in Figure 37 indicate that the cathodic current density for samples with the wire mesh lying on the plate did not vary compared to the sample with only a steel plate. The mesh hole sizes also did not affect the current density, but in the anodic polarization curves, the region of passivity for the samples with the wire mesh lying on the steel plate a little were lower compared to the sample without the wire mesh. This result was again due to metallurgical factors associated with the steel plate and the wire mesh due to the heterogeneity which may exist between the steel plate and the wire mesh. A comparison of Figures 36 and 37 indicates that in the anodic polarization curves, the region of passivity for the samples with the wire mesh attached to the top and bottom of the plate was much lower than for the sample with no wire mesh. In addition, the passive current density for the samples with the wire mesh attached to the top and bottom of the plate was lower than for the sample without any wire mesh. These effects for the samples with the wire mesh lying on the plate were much smaller than for the previous samples, and even the passive current density for the samples with the wire mesh lying on the plate was about the same as that for the sample without any wire

mesh. This difference may be due to non-uniformity of the current distribution along the steel plate for the samples with the wire mesh attached to the top and bottom of the plate and raised in an arc of about one inch, compared to the samples with the wire mesh lying on the plate. This non-uniformity in turn may cause a potential shielding along the plate.

The data in Figure 38 indicate that the potential of the wire mesh (the mesh was placed between the anode and the cathode with no connection) during anodic and cathodic polarization shifted toward more negative and positive values respectively. This result may be due to the IR drop which exists between the wire mesh and the reference electrode at the electric field in the anode and cathode. This IR drop causes the potential of the wire mesh to increase as the current increases. This shift in wire mesh potential was higher at higher currents, which again confirms the fact that even a small resistance between the reference electrode and the wire mesh at high currents can cause this shift to occur.

The results in Figure 39 indicate that the potential of the platinum plates placed between anode and cathode in a 3% salt solution shifted toward more negative values as the cathodic current increased. The potential shift was toward more negative values as the distance of the platinum from the cathode decreased. The data presented in Figure 40 indicate the same. This potential shift may be due to the potential gradient caused by the IR drop in the electric field between the anode and the cathode.

5.5 Concrete

In Figure 41, the current density for the steel in the anodic and cathodic polarization curves of the samples (with a wire mesh between anode and cathode) decreased compared to the sample with no wire mesh, but the cathodic current density for the steel with the wire mesh connected to it increased compared to the sample without any wire mesh (the samples were in dry conditions of a laboratory for 20 to 30 days after curing).

Figure 42 indicates results for the same samples tested in Figure 41 when exposed to distilled water for four months. There was no significant shift in cathodic current density for the samples with the wire mesh placed between the anode and cathode compared to the sample without any wire mesh, but a little increase in anodic and cathodic current density occurred for the samples with the wire mesh connected to the steel plate. This result may be due to the metallurgical factors mentioned before to the under-estimating the wire mesh surface areas, because the current density for the samples with the wire mesh connected to the plate was calculated as the cell current divided by the total surface area of the mesh and the plate. The differences in current density observed for the samples with the wire mesh between the anode and the cathode compared to the steel with no wire mesh when the samples were exposed to dry conditions is probably due to the moisture content of concrete. The moisture in the different concrete samples may not have been distributed uniformly, which would cause the variation in current density. Figure 42 confirms this statement. It indicates that a little difference in current density was observed for the same samples exposed to distilled water. This result may be due to the fact that moisture

was uniformly distributed after the samples were exposed to distilled water.

Curves 2 and 3 in Figure 43 indicate the differences in Tafel slopes and current requirement for cathodic polarization of the steel plate when the potential was measured with respect to a $Cu/CuSO_4$ electrode external to the mesh compared to the potential measured at the steel-concrete interface. At a constant current level of 0.03 mA, a potential shift of -775 mv was obtained when the steel potential was measured with a $Cu/CuSO_4$ electrode external to the wire mesh, but at the same level of current, a potential shift of -400 mv was obtained when the potential of the steel plate was measured at the concrete-steel interface with an Mo/MoO_3 electrode. Therefore, there is an error in potential measurements, due to the IR drop which exists when the steel potential is measured with a reference electrode external to the wire mesh. It should be mentioned that the electronic IR drop compensation for the samples used for the electrochemical study of steel did not show a significant difference in Tafel slope when the steel in these samples was polarized with and without electronic IR drop compensation. This fact may be due to the sample size, since the concrete cover on the steel for these samples was about 1/2 inch thick. Therefore, IR drop did not play an important role here, but when the samples of a larger size such as the ones used in the wire mesh study were used, the IR drop did play a significant role and caused a potential measurement error. This indicates that the geometry of the sample is important in reducing IR too.

Figure 44 indicates that the potential of the wire mesh shifted toward more positive values during cathodic polarization and toward more

negative values during anodic polarization of the steel plate. This shift in wire mesh potential is due to the potential measurement error caused by the IR drop which exists between the reference electrode and the wire mesh. Because the wire mesh was placed in the electric field between the anode and cathode and because concrete has a very high resistivity, the measured potential of the wire mesh is the sum of the actual potential of the wire mesh and the IR drop associated between the reference electrode and the wire mesh. The IR drop becomes large as current flow increases and causes the mesh potential to shift. Otherwise, the actual potential of wire mesh remains constant. The above statement was substantiated when a wire mesh and reference electrode were placed outside the electric field between the anode and cathode. In this case, since there was no variation in current flow, the wire mesh potential remained constant. (See Figure 45.) The cell assembly is shown in Figure 46.

The data in Figure 47 indicate that the wire mesh potential shifted when the location of the wire mesh was changed. This wire mesh potential shift was increased by increasing the distance of the wire mesh from the cathode, which indicates that a potential gradient exists in the electric field between the anode and cathode. The work of Stammen and Townsend [97] also indicates that a potential gradient will be created between the anode and cathode because of the flow of impressed current into the chemical solution. This result agrees with those obtained in this study.

The data presented in Figure 48 also confirm the fact that the wire mesh potentials shift as the location of the wire mesh between the

anode and cathode varies. A similar result was obtained when the wire mesh potential was measured with respect to an external $Cu/CuSO_4$ electrode instead of an embeddable Mo/MoO_3 electrode. (See Figure 49.) Therefore, all of these results confirm that a potential gradient exists between the anode and cathode, caused by the IR drop, which in turn causes the wire mesh potential to shift.

However, it is possible to correlate a relationship between the IR drop and variables such as current, concrete geometry, and moisture content of concrete. This relationship in its simplest form can be expressed as

$$\text{IR drop} = k \frac{I \cdot C}{M} \qquad (18)$$

In this relationship, k is a constant, I is the current flow between anode and cathode, C is the concrete thickness between the steel and the reference electrode, and M is the moisture content of the concrete. The above relation for the IR drop calculation is supported by the data presented in Figures 50 through 56. The results in these figures indicate that the shift in wire mesh potential increases as the distance of the wire mesh from the reference electrode increases and the shift in the potential increases when the current flow is increased. Therefore, it can be concluded that the current flow and geometry of concrete are two of the major factors affecting the IR drop. The third factor is the moisture content of the concrete. The ionic mobility of concrete increases as the moisture content increases, which in turn decreases the resistivity of concrete and, as a result, the IR drop.

Therefore, the factor of the IR drop must be taken into account

in the potential measurement of the steel structures in concrete, and a correction must be made to determine the true potential of the steel-concrete interface.

The results in Figure 50 indicate that the potential of the wire mesh (the mesh was placed between the anode and cathode with no connection) shifted toward more positive values when the wire mesh potential was measured with respect to the Mo/MoO_3 electrode placed at the left hand side of the wire mesh. This shift was toward more negative values when the potential was measured with respect to the Mo/MoO_3 electrode placed at the right hand side of the mesh. Similar results were obtained when different reference electrodes were tested. (See Figures 51, 52, 53, 54, 55, and 56.) This fact is probably due to the additive and subtractive properties of IR drop.

The results in Figure 58 indicate that the potential of the platinum plate shifted when it was placed between the anode and cathode. This platinum plate potential shift was increased by decreasing the distance of the platinum from the cathode, which indicates that the potential shift of wire mesh is not due to the reaction which may take place on the wire mesh surface, but it is because of a potential gradient which exists in the electric field between the anode and cathode.

The results presented in this section indicate that the presence of a wire mesh between the anode and cathode does not affect the potential measurement of the structure, but that the major error in potential measurement is due to the IR drop associated with the high resistivity of concrete. This potential measurement error, in turn, may cause an underestimation of the correct potential of reinforced structures which are

cathodically protected. Therefore, the corrosion of the reinforced structure may not be sufficiently reduced and failure of the structure occurs.

CHAPTER VI

CONCLUSION

1. The open-circuit potential of steel in concrete (Types I and V Portland cement) is dependent on the salt concentration. The potential shifted from the passive region to a value indicating corrosive conditions when the concrete was exposed to distilled water. The opposite effect was observed for concrete exposed to dry conditions.
2. The open-circuit potential values shift with moisture content. This is caused by increased concrete conductivity which in turn, causes an increase in ion mobility.
3. The open-circuit potential of steel is in the less active (corrosive condition) potential for Type V Portland cement than for Type I Portland cement concrete.
4. Steel is passivated in Type I Portland cement with a salt content up to 0.1%, but the passivation of steel is maintained in Type V Portland cement with a salt content up to 0.5% (the concrete samples were exposed to distilled water).
5. The current requirements increase as the salt content of concrete increases. This occurred when samples were exposed to distilled water, but the opposite effect was observed when samples were exposed to dry conditions.
6. Generally, the current requirements for steel in Type I Portland

cement are higher than for Type V Portland cement.

7. Current requirements for steel in Types I and V Portland cement (with no salt content) increase as the concrete is exposed to solutions with a higher salt concentration. In other words, the penetration of chloride ions into concrete is higher for concrete exposed to solutions with a higher salt concentration than it is for concrete exposed to solutions with a lower salt content.
8. The penetration of chloride ions into concrete increases as the exposure time to salt solutions increases. The penetration of chloride ions into the concrete is higher for Type I than for Type V Portland cement.
9. The increase in current requirements for the concrete with no salt exposed to solutions with various salt concentrations is not a diffusion related process but is due to more complex reactions which may take place at the presence of chloride ions.
10. It seems that the chloride ions added externally to cured concrete do not react with concrete compounds or, if they do react, it is on a small scale compared to the chloride ions which are mixed with fresh concrete.
11. A break occurs for the anodic polarization curves at potentials of about +500 to 600 mv with respect to an Mo/MoO_3 electrode and at potentials of -500 to -700 mv for the cathodic polarization curves. These breaks were observed for the concrete with salt content exposed to distilled water or with no salt content, but exposed to salt solutions. The breaks were postulated to be due to the following reactions:

$$Fe(OH)_2 \rightleftarrows \gamma\text{-}FeOOH + H^+ + e^- \quad (13) \text{ (anodic reaction)}$$

$$Fe_3O_4 + 2H_2O + 2H^+ + 2e^- \rightleftarrows 3Fe(OH)_2 \quad (15) \text{(cathodic reaction)}$$

or

$$Fe_3O_4 + 8H^+ + 8e^- \rightleftarrows 3Fe + 4H_2O \quad (16) \text{(cathodic reaction)}$$

12. The wire mesh with various hole sizes does not shield the current flow with or without connection to the steel plate when the wire mesh is placed between anode and cathode.
13. The variation in the wire mesh potential is caused by the potential measurement error which in turn is caused by the IR drop associated with the high resistivity of concrete. The IR drop is dependent on the current flow, geometry, and moisture content of concrete.
14. The IR drop in the concrete can be reduced significantly when the potential is measured at the steel-concrete interface, compared to that measured externally.
15. The high Tafel slope for anodic and cathodic polarization of steel in concrete is mainly due to the slow charge transfer reaction caused by the slow rate of ion diffusion.

CHAPTER VII

RECOMMENDATION

Many unanswered questions about the electrochemistry of steel in concrete still exist. Further work, as recommended below, is required to obtain answers to these questions.

1. Polarization curves similar to the ones used in this study must be obtained in the absence of oxygen for dry and moist concrete.
2. The composition and pH of the pore solution adjacent to the steel-concrete interface must be determined for both types of Portland cement (Types I and V).
3. The study of the diffusion of chloride ions into concrete must be repeated with salt solutions different from the one (NaCl) used in this study.
4. A study of the diffusion of chloride through a light-weight concrete must be carried out, to compare results with those obtained in this study.
5. The corrosion product on the steel surface after exposure for a period of six months to potentials of about 500 to 700 mv vs. Mo/MoO_3 electrode must be analyzed.
6. The physical properties of moist and dry concrete such as cracks and voids must be carefully examined.

7. The reaction products of concrete compounds of Types I and V Portland cement where salt has been mixed with the fresh concrete must be determined for two different conditions: (1) after six months of exposure to distilled water and (2) after six months of exposure to the dry conditions of the laboratory.
8. The moisture content in the concrete (Types I and V Portland cement) with various salt contents after six months of exposure to the dry conditions of the laboratory must be determined.
9. Steel with a composition different from the one used in this study must be employed. Polarization curves similar to those in this study must be obtained.
10. The corrosion products on the steel surface must be analyzed to check differences which may exist in the reactions for the steel with a different chemical composition. The corrosion product at the steel surface when the steel is embedded in Types I and V Portland cement must also be determined.
11. The cathodic polarization curves for steel in concrete must be obtained when the steel reaction is controlled by: (1) activation polarization and (2) concentration polarization. The results of these two tests will elucidate the effect of ions diffusion on the tafel slope.

REFERENCES

1. D.A. Hausmann, "Steel Corrosion in Concrete," Materials Protection, Nov. 1967, pp. 19-23.

2. T.J. Larsen, W.H. McDaniel, Jr., R.P. Brown, and J.L. Rosa, "Corrosion Inhibiting Properties of Portland and Portland Pozzolan Cement Concrete," Status Report Florida Dept. of Transportation, Office of Materials and Research (1975) January.

3. B. Tremper, J.L. Beaton, and R.F. Stratfull, Bulletin, Highway Research Board, p. 18 (1958).

4. D.L. Spellman and R.F. Stratfull, "Concrete Variables and Corrosion Testing," California Dept. of Public Works, Division of Highways, Materials and Research Dept., Report No. 635116-6 (1972) January.

5. S. Halstead and L.A. Woodworth, Trans. S. African Institute of Civil Engineering (1955) April.

6. D.A. Lewis and W.J. Copenhagen, S. African Ind. Chemist, Vol. 11, p. 10 (1955).

7. P.D. Cady, "Chloride Corrosion of Steel in Concrete," STP 629, ASTM, Philadelphia, 1977, pp. 3-11.

8. G.N. Scott, "The Corrosion Inhibitive Properties of Cement Mortar Coating," A Paper Presented at the 18th Annual Conference of National Assocation of Corrosion Engineers, March, 19-23, 1962 (unpublished).

9. T.C. Power and T.L. Brownyard, "Physical Properties of Hardened Portland Cement Paste," Bulletin 22, The Portland Cement Association, Research Laboratories.

10. G.J. Verbeck, "Hardened Concrete - Pore Structure," ASTM SP Tech., Publication, No. 169, pp. 136-142 (1955).

11. T.C. Powers, "Structure and Physical Properties of Hardened Portland Cement Paste," J. Am. Ceramic Soc., 41, pp. 1-6 (Jan. 1958).

12. D.A. Hausmann, "The Electrochemical Behavior of Steel Encased in Concrete," American Pipe and Construction Co. (1962) December.

13. "Electrolysis in Reinforced Concrete," Engineer, p. 453 (1948) November.

14. E. Hammond and T.D. Robson, "Comparison of Electrical Properties of Various Cements and Concretes," The Engineer (London), Vol. 199, pp. 78-80, Jan. 1955.

15. G.E. Monfore, "The Electrical Resistivity of Concrete," Journal, PCA Research and Development Laboratories, Vol. 10, No. 2, pp. 35-48, May 1968.

16. R.L. Henry, "Water Vapor Transmission and Electrical Resistivity of Concrete," Final Report, U.S. Naval Civil Engineering Laboratory, Technical Report R-314, June 1964.

17. C.E. Locke and D.A. Ismaila, "Polymer Impregnated Concrete and Polymer Concrete Overlays," Final Report, Vol. 1, Presented to Oklahoma Department of Transportation, April 1980.

18. C.M. Hsue, "The Measurement of Polymer Depth in Partially Polymer Impregnated Concrete," Master Thesis, University of Oklahoma, 1979.

19. P. Impraseit, D.W. Fowler, and D.R. Paul, "Durability, Strength and Method of Application of Polymer Impregnated - Concrete for Slabs," Jan. 1979.

20. Temperature and Concrete, Publication SP-25, American Concrete Institute, Detroit, 1968.

21. A.M. Neville, "Role of Cement in Creep of Mortar," J. Am. Concrete Inst., 55, pp. 263-284 (March 1959).

22. W. Czervin Zementchemie für Bauingenieure (Bauverlag G.M.B.H., Wiesbaden - Berlin, 1960).

23. J.C. Witt, "Portland Cement Technology," Chemical Publishing, New York, 1947.

24. R.W. Carlson, "Development of Low Heat Cement for Mass Concrete," Eng. News Record, Vol. 109 (1932), pp. 461-463.

25. T.C. Powers and T.L. Brownyard, "Studies of the Physical Properties of Hardened Portland Cement Paste (Nine Parts)," J. Am. Concrete Inst., 43 (Oct. 1946 to April 1947).

26. R.H. Bogue, "Chemistry of Portland Cement," New York, Reinhold, 1955.

27. J.J. Shideler, "Calcium Chloride in Concrete," J. Am. Concrete Inst., 48, pp. 537-559 (March 1952).

28. U.R. Evans, An Introduction to Metallic Corrosion, Edward Arnold Publishers Ltd., London, 1948, p. 200.

29. I. Cornet, "A Short Course in Corrosion," National Association of Corrosion Engineers, University of California, Berkeley, 1953, p. 119.

30. F.N. Speller, Corrosion - Causes and Prevention, McGraw-Hill Book Co., New York, 3rd Edition, 1951.

31. C.W. Borgman, "Basic Principals of Metallic Corrosion," Corrosion of Metals (Series of Lectures on Corrosion Presented at the 27th National Metal Congress and Exposition), American Society of Metals, Cleveland, Feb. 1946, pp. 1-29.

32. Alan A. Pollitt, The Causes and Prevention of Corrosion, Ernest Benn Ltd., London, 1923, p. 222.

33. H.A. Berman, "Determination of Chloride in Hardened Portland Cement Paste, Mortar and Concrete," Report No. FHWA-RD-72-12, Federal Highway Administration, Sept. 1972.

34. D.G. Moore, D.T. Klodt, and R.J. Hensen, "Protection of Steel in Prestressed Concrete Bridges," National Cooperative Highway Research Program Report 90, 1970.

35. H.H. Uhlig, Corrosion and Corrosion Control, 2nd Edition, John Wiley and Sons, Inc., New York, 1971.

36. R. Shalon and M. Raphael, "Influence of Sea Water on Corrosion of Reinforcement," Proc. Am. Concrete Inst., Vol. 55, No. 12, pp. 1251-1268, June 1959.

37. J.L. Beaton and R.F. Stratfull, "Environment Influence on the Corrosion of Steel in Concrete Bridge Structure," State of California Division of Highways, Sacramento, Jan. 1968.

38. T. Tokuda and M.B. Ives, Corrosion Sci., 11, pp. 297-306 (1971).

39. G. Okamoto, Corrosion Sci., 13, pp. 471-489 (1973).

40. R. Kondo, M. Satake, and H. Ushiyama, "Diffusion of Various Irons in Hardened Portland Cement," Japan Review of the 28th General Meeting - Technical Session, pp. 41-43, May 1974.

41. M. Collepardi, A. Marcials, and R. Turiziani, "The Kinetics of Penetration of Chloride Ion into the Concrete," Journal of the American Ceramic Society, 55, No. 10, pp. 534-535, 1972.

42. C.A.L. De Bruyn, "Cracks in Concrete and Corrosion of Steel Reinforcing Bars," Proceedings, Symposium on Bond and Crack Formation in Reinforced Concrete (Stockholm, 1957).

43. D.A. Lewis and W.J. Copenhagen, "Corrosion of Reinforcing Steel in Marine Atmospheres," Corrosion, Vol. 15, No. 7, July 1959, p. 3821.

44. F.L. Laque, Marine Corrosion, Wiley-Interscience, New York, 1975.

45. R.F. Stratfull, "Knowledge and Needs in the Field of Impressed Current Cathodic Protection; System Control and Monitoring," Paper Presented at the FHWA Federally Coordinated Research Program of Highway, Williamsburg, VA, Dec. 1979.

46. U.S. Bureau of Reclamation, Concrete Manual, 5th Edition (Denver, CO, 1949).

47. G.E. Monfore and G.J. Verbeck, "Corrosion of Prestressed Wire in Concrete," Proceedings, Am. Concret Inst., Vol. 57, 1960, pp. 491-515.

48. M.H. Roberts, "Effect of Calcium Chloride on the Durability of Pre-Tension Wire in Prestressed Concrete," Magazine of Concrete Research, Vol. 14, Nov. 1962, pp. 143-154.

49. A. Baumel, Beton Herstellung - Verwendung, 10 (16), 256-259 (1960).

50. G. Pickett, J.A.C.I. Proc. 44, pp. 1149-1175 (1948).

51. R.L. Blaine, et al., "Interrelations Between Cement and Concrete Properties," NBS Building Science Series 2, Part 1, Sec. 2 (1965).

52. H.H. Stinour, "Influence of the Cement on the Corrosion Behavior of Steel in Concrete," Research Department Bulletin No. 168, Portland Cement Association, 1964.

53. F.M. Lea, The Chemistry of Cement and Concrete, Arnold, London, 3rd Edition, 1970, p. 232.

54. M.H. Roberts, "Effect of Calcium Chloride on the Durability of Pre-Tensioned Wire in Prestressed Concrete," Concrete Research, Vol. 14, No. 42, pp. 143-154, March 1962.

55. M. Rogourd, "The Action of Sea Water on Cements," Annales de L'Inst. Tech. du Batiment et des Travaux Publiques, No. 329, pp. 86-102 (1975).

56. J.L. Ratiff and D.W. Norman, "Corrosion Behavior of Reinforcing Steel in Concrete and Automated Monitoring Systems for Corrosion Detection and Corrosion Control," Report Submitted to Florida Department of Transportation Office of Materials and Research, April 1975.

57. H.A. Berman, "Effect of Sodium Chloride on the Corrosion of Concrete Reinforcing Steel and on the PH of Calcium Hydroxide Solution," FHWA-RD-74-1, Jan. 1974.

58. M. Metzger, "The Pourbaix Diagram and its use in Corrosion Control," Fourth Biennial Short Course on Corrosion Control, University of Illinois, Urbana, Dec. 1959.

59. J.E.O. Mayene, J.W. Menter, and M.J. Proyor, "Mechanism and Inhibition of the Corrosion of Iron by Sodium Hydroxide Solution, Part 1," Journal of the Chemical Society (London), Nov. 1960, pp. 3229-3235.

60. R.F. Stratfull, "The Corrosion of Steel in a Reinforced Concrete Bridge," Corrosion, Vol. 13, No. 3, Mar. 1957, pp. 173t-178t.

61. ACI Committee 201, "Durability of Concrete in Service," ACI Journal Proceedings, Vol. 59, No. 12, Dec. 1962, pp. 1796-1801.

62. C.M. Wakeman, et al., "Use of Concrete in Marine Environments," ACI Journal Proceedings, Vol. 54, No. 10, Apr. 1958, pp. 841-856.

63. A.M. Neville, "Behavior of Concrete in Saturated and Weak Solutions of Magnesium Sulphate and Calcium Chloride," J. Mat., ASTM, 4, No. 4, pp. 781-816 (Dec. 1969).

64. U.R. Evans, The Corrosion and Oxidation of Metals; Scientific Principles and Practical Applications, Edward Arnold, Ltd. London, 1960, p. 307.

65. W.P. Kinneman, "Discussion of use of Concrete in Marine Environments," C.M. Wakeman et al., Proceedings, A.M. Concrete Inst., Vol. 54, 1958, pp. 1325-1327.

66. R. Friedland, "Influence of Quality of Concrete and Mortar upon Corrosion of Reinforcement," Proceedings, A.M. Concrete Inst., Vol. 47, 1950, pp. 125-140.

67. I.L. Tyler, "Long-Time Study of Cement Performance in Concrete; Chapter 12, Concrete Exposed to Sea Water and Fresh Water," ACI Journal, Proceedings, Vol. 56, No. 9, Mar. 1960, pp. 825-836.

68. D.H. Pletta, E.F. Massie, and H.S. Robins, "Corrosion Protection of Thin Precast Concrete Sections," ACI Journal, Proceedings, Vol. 46. No. 7, Mar. 1950, pp. 513-528.

69. J.P. Hoar, Corrosion Sci., 5, p. 279 (1965).

70. G. Bianchi, A. Cerguetti, F. Mazza, S. Torchio, and V.R. Evans, International Conference on Localized Corrosion, Preprints, 29 (1971).

71. G. Kortum and J. Bockris, Textbook of Electrochemistry, Amsterdam, Elservier Publiching Co.

72. J. Seijka, C. Cherki, and J. Yahalom, 119, 8, p. 991 (1972).

73. K.J. Vetter, Electrochem. Acta, 16, p. 1923 (1941).

74. M. Pour Baix, et al., Corrosion Sci., 3, p. 239 (1963).

75. B. Kabanov, R. Burstein, and A. Frumkin, Discussions Faraday Soc., 1, p. 259 (1947).

76. C.E. Locke and C. Dehghanian, "An Embeddable Reference Electrodes for Salt Contaminated Concrete," Materials Performance, Vol. 18, No. 2, Feb. 1979.

77. C. Dehghanian, "The Evaluation of Molybdenum/Molybdenum Oxide and Silver/Silver Chloride as Reference Electrodes in Chloride Contaminated Concrete," Master Thesis, University of Oklahoma, 1977.

78. J.M. Stanmen and C.R. Townsend, "Cathode Effect in Anodic Protection," Corrosion, Nov. 1967, pp. 343-348.

79. J.N. Agar and T.P. Hoar, Discussion Faraday Soc. 1, pp. 158-162 (1947).

80. C. Kasper, Trans. Electrochem. Soc., 78, p. 131 (1940).

81. G.L. Booman and W.B. Holbrook, Anal. Chem., 35, p. 1793 (1963).

82. F.A. Scott, J.C. Stouffer, and R.L. Richardson, Document No. HW 80365, Handford Atomic Products Operation, Richland, Wash., 1964.

83. T.R. Mueller, U.S. Atomic Energy Comm. Report ORNL-3750, p. 5 (1965).

84. R.W. Stelzer, M.T. Kelley, and D.J. Fisher, U.S. Atomic Energy Comm. Report ORNL-3537, pp. 9-12 (1964).

85. R.F. Stratfull, "How Chloride Affects Concrete used with Reinforcing Steel," Material Protection, March 1968, pp. 29-34.

86. I. Cornet, T. Ishikawa, and B. Brosler, Material Protection, 7 (3), p. 45 (1968).

87. D.A. Hausmann, Material Protection, 6 (11), p. 19 (1967).

88. R.C. Robinson, "Concrete for Corrosion Control of Steel," Proceedings of 2nd Western States Corrosion Seminar, May 1968, pp. 108-120.

89. D.A. Hausmann, "Steel Corrosion in Concrete," Material Protection, 6 (11), Nov. 1967, pp. 19-23.

90. R.T. Foley, Corrosion, 26, No. 2, February 1970, pp. 58-70.

91. D.L. Piron, E.P. Koutsoukos, and K. Nobe, Corrosion, 25, p. 156 (1969).

92. O. Rincon, "Effect of Chloride Ion on the Passive Film on Nickel-200 and Inconel X-750," Master's Thesis, University of Oklahoma, 1975.

93. S.E. Traubenberg and R.T. Foley, J., Electrochem. Soc., 118, No. 7, July 1971, pp. 1066-1070.

94. V.K. Gouda and H.M. Mourad, Corrosion Science, 14, pp. 681-690 (1974).

95. O.E. Gjorv and O. Vennesland, "Diffusion of Chloride Ions from Seawater into Concrete," Cement and Concrete Research, 9, pp. 229-238 (1979).

96. O.E. Gjorv, "Durability of Reinforced Concrete Wharves in Norwegian Harbours," Ingenior for Laget, Oslo, p. 153 (1968).

97. J.M. Stammen and C.R. Townsend, "Cathode Effects in Anodic Protection," Corrosion, pp. 343-348, November 1967.

APPENDICES

APPENDIX A

CALCULATION OF THE ELECTROMOTIVE FORCES FOR THE FOLLOWING REACTION USING NERNST EQUATION

(Anodic Reaction)

$$Fe(OH)_2 \rightleftarrows \gamma\text{-}FeOOH + H^+ + e^- \quad E^o = -.247v$$

$$E = E^o - \frac{.0592}{1} \log \frac{a_{H^+} \cdot a_{\gamma\text{-}FeOOH}}{a_{Fe(OH)_2}}$$

$$a_{\gamma\text{-}FeOOH} = a_{Fe(OH)_2} = 1$$

therefore,

$$E = -.247 - .0592 \log a_{H^+}.$$

$$a_{H^+} = -\log[H^+] = PH$$

therefore,

$$E = -.247 + .0592 \log PH$$

at pH = 12 $\rightleftarrows$ E = 0.463 volt = 463 mv

at pH = 13 $\rightleftarrows$ E = 0.522 volt = 522 mv.

By the similar calculation E for the two following cathodic reactions can be expressed as:

$$Fe_3O_4 + 8H^+ + 8e^- \rightleftarrows 3Fe + 4H_2O \quad E^o = -.085v$$

$$E = 0.085 - .0592\ PH$$

at pH = 12 $\rightleftarrows$ E = - 0.795 volt = - 795 mv

at pH = 13 $\rightleftarrows$ E = - 0.855 volt = - 855 mv

$$Fe_3O_4 + 2H_2O + 2H^+ + 2e^- \rightleftarrows 3Fe(OH)_2 \quad E^0 = -.026 \text{ volt}$$

$$E = -0.026 - 0.0592\ PH$$

at $pH = 12 \rightleftarrows E = -.735 \text{ volt} = -735 \text{ mv}$

at $pH = 13 \rightleftarrows E = -.795 \text{ volt} = -795 \text{ mv}.$

APPENDIX B

CALCULATION OF DIFFUSION CURRENT USING DIFFUSION PROCESS EQUATION KNOWN AS COTTREL EQUATION

$$I_t = \frac{nFAD^{\frac{1}{2}}C_b}{\pi^{\frac{1}{2}} t^{\frac{1}{2}}}$$

A = surface area, cm^2

I = diffusion current, ampere

D = diffusion coefficient, cm^2/sec

C_b = electroactive species concentration in bulk solution, mole/ml

t = exposure time, sec

For the concrete sample exposed to the salt solution of concentration of 0.1%, the diffusion current for the chloride ion can be calculated as:

Assuming $D = 10^{-8}$ cm^2/sec

$$I = \frac{2 \times 9600 \times 38.709 \times (10^{-8})^{\frac{1}{2}} \times 1.709 \times 10^{-5}}{(3.14)^{\frac{1}{2}} (90 \times 24 \times 3600)^{\frac{1}{2}}} = 2.571 \times 10^{-11} A = 2.57 \times 10^{-5} \mu A$$

The diffusion current density for the other salt concentration solutions was calculated by the same method.